Liquid Crystalline Silsesquioxanes

Richard Booth

MSc in Chemistry by Research

University of York

Department of Chemistry

December 2013

Abstract

In order to study the effects of calamitic mesogenic units on the self-assembly of liquid crystalline phases in silsesquioxane supermolecules, various di- and tri-substituted silsesquioxane supermolecules have been prepared. They contain incompletely condensed silsesquioxanes substituted with a variety of alkyl chains. These moieties contain various calamitic mesogenic units including two-ring and three-ring terminally appended mesogenic units as well as laterally appended mesogenic units. These mesogenic units were prepared using hydrosilylation chemistry and the properties of these new compounds were elucidated using polarized optical microscopy, differential scanning calorimetry and single crystal X-ray diffraction techniques.

A novel octasilsesquioxane core has been prepared with two distinct moieties covalently bonded to it in order to study the effect of a non-mesogenic chiral entity along with a calamitic mesogenic group on the self-assembly of this mesogenic moiety in the liquid crystalline phase. This compound has been prepared using standard hydrosilylation techniques and its properties have been elucidated using polarized optical microscopy and differential scanning calorimetry.

Table of Contents

vi

List of Figures

List of Schemes

List of Tables

Acknowledgments

I would like to thank my supervisor Dr Isabel M. Saez for her patience and guidance along this project and for her support throughout.

My acknowledgements should also be directed towards Dr Adrian Whitwood whose extraordinary efforts provided an X-ray crystal structure for this project and towards Dr Graeme McAllister who made extraordinary efforts to complete the elemental analysis as quickly as possible.

I would also like to thank Professor John Goodby FRS, Dr Stephen Cowling, Dr Richard Mandle and Dr Edward Davis and the rest of the York liquid crystal group for their helpful advice and support along the way.

Authors Declaration

I, Richard Booth, hereby certify that this MSc by research thesis has been written by myself, is the product of work carried out at the University of York between October 2012 and December 2013 and has not been submitted in any previous application for a higher research degree.

Chapter One:

Introduction

1. Introduction

1.1. Introduction to Liquid Crystals

Liquid crystals are partially ordered fluid systems that are intermediate in symmetry and structure between that of the crystalline solid and the isotropic liquid. The order in a crystalline solid is usually both positional and orientational, in that the constituent molecules are constrained to occupy distinct sites in a three-dimensional lattice and to point their molecular axis in specific directions, giving a structure with long-range positional and orientational order in all directions.[1] Conversely, the molecules in an isotropic liquid are able to rotate and flow freely with no positional or orientational ordering. Liquid crystals are often viewed as an intermediate state of matter between these two systems, having a degree of positional or orientational order and yet retaining some degree of fluidity. A number of different liquid crystal phases exist; these phases are known as mesophases (derived from the greek word *mesos* which means between or intermediate). Liquid crystals can roughly be divided into two distinct categories depending on how the mesophase arrises. These are lyotropic liquid crystals and thermotropic liquid crystals. Lyotropic liquid crystals are formed through interactions between a solvent system and a material that is amphiphilic in nature such as a surfactant. Upon the addition of a suitable solvent, these amphiphilic molecules self-organize in order to give a liquid-crystalline phase.[2] Thus, the mesophase behaviour of a lyotropic material is dependent both on the concentration and on the temperature of the solution. Conversely, thermotropic liquid crystals are formed from either heating the crystalline solid or cooling the isotropic liquid and so the formation of the mesophases are temperature dependent and in the absence of solvent. Thermotropic liquid crystals will be discussed in more detail later in this chapter.

1.2. Thermotropic Liquid Crystals

When a solid is heated there reaches a point where the molecules lose their translational order and can now rotate and move freely. This point is known as the melting point, and, in most cases, this is the point where the crystalline solid changes to the isotropic liquid. However, with materials that exhibit thermotropic liquid-crystalline behaviour this process is more complicated. In these materials there is a step-wise decay of order where the molecules gradually lose their positional and orientational order. The stages of this stepwise decay are temperature dependent, with each step being a transition from one thermodynamically stable mesophase to another, and eventually to the isotropic liquid. Thermotropic liquid crystals are usually formed by materials that are endowed with specific structural and molecular criteria; these materials are usually dichotomous in nature, in as much as they have two portions of their molecular structure that have contrasting structural or chemical properties,[3] *e.g.* a rigid anisotropic biphenyl group with a flexible peripheral alkyl chain. The anisotropic character of a material such as this is the origin of the step-wise decay of order, and although mesogens that are not anisotropic in shape do exist, they tend to form plastic crystals rather than true liquid-crystalline phases.[4][5] Thermotropic mesophases are stabilised by the anisometric intermolecular forces (van der Waals, hydrogen bonding, *etc*) that are a result of the anisotropic character of the material. The two most common shapes for a mesogenic material to possess are rod-like (calamitic) and disk-like (discotic), although a wide range of molecular shapes have been shown to support liquid-crystalline behaviour, *e.g.* bent rods, pyramidal-shaped molecules *etc*. A rod-like mesogen is longer than it is broad and so possess one, unique, long axis. A discotic mesogen is disc-shaped, *i.e.* flat, and has one, unique, short axis. Example structures of a rod-like, a disc-shaped and a bent-core mesogen can be seen in Figure 1.1.
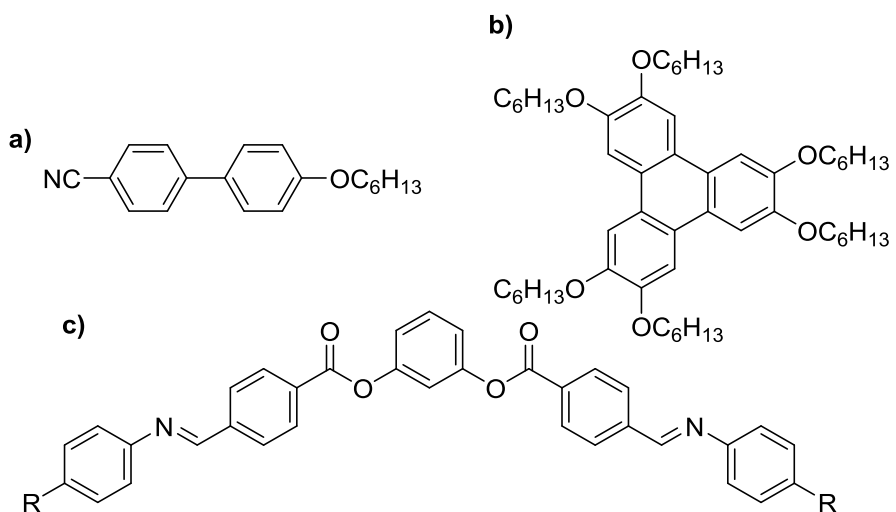
Figure 1.1: A representative example of (a) rod-shaped mesogen; (b) disc-shaped mesogen and (c) bent core mesogen.

Although rod, disk-like and bent core mesogens are three of the most common shapes for mesogenic materials, a wide range of other shapes do exist and these systems include bowl-shaped and ABC triblock copolymers.[6][7]

1.3. The Structure of Rod-Like Mesogens

In general, rod-like mesogenic materials consist of a single semi-rigid core attached to which are one, or two, terminal alkyl chains. It is usually the anisotropic interactions between the cores, often consisting of phenyl rings bridged through short unsaturated groups that give rise to the liquid-crystalline behaviour. The terminal alkyl chains tend to lower the melting point of the material in order to allow the observation of liquid-crystalline phases. In Figure 1.2 is the structure of an example mesogenic entity namely, 5CB. The structure of 5CB consists of a cyanobiphenyl unit and a five-carbon alkyl chain. As noted above it is the interactions between these two distinct entities that produces liquid-crystalline behaviour, 5CB exhibits a nematic mesophase.
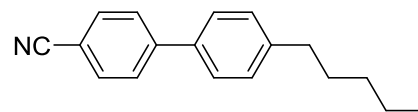
Figure 1.2: Structure of a common rod-like mesogen known as 5CB (4′-pentyl-4-cyanobiphenyl), consisting of a core made up of two phenyl rings and a terminal pentyl chain.

The different types of molecular structure *i.e.* the semi-rigid, polarisable core and the flexible alkyl chains lead to a dichotomous nature to the structure. This means when molecules of this type self-organise, they generally do so with the semi-rigid cores tending to pack together and their flexible alkyl chains tending to orient in the same direction, this leads to the system becoming nanophase segregated.[3] Of course, a large number of variations of this structural scaffold are possible, *e.g.* replacement of the phenyl rings with cyclohexane rings, insertion of an ester linking group between the two rings, replacement of the alkyl chain for a fluorocarbon *etc*, all of which will impact upon the relative stability and physical properties of the resulting mesophases.

1.4. The Mesophases of Rod-Like Thermotropic Liquid Crystals

As noted previously, a material is defined as a crystalline solid when it possesses long-range positional order in three-dimensions. As this material is heated it will gain energy and the constituent molecules will eventually gain enough energy to break free of their lattice sites, thereby resulting in a transition to an isotropic liquid. In non-liquid crystalline materials this is a one-step process (T1 in Figure 1.3) but in liquid-crystalline compounds this is a stepwise process. In the first step a smectic-like crystal phase is formed (T2 in Figure 1.3). This is not a liquid-crystalline phase but merely a crystalline solid where the molecules are able to oscillate and rotate about their axis, *i.e.* they have gained some rotational freedom but still have long-range positional order. As more and more energy is put into the system, at a defined temperature, the molecules lose their long-range positional order and form a fluid, smectic liquid-

5

crystalline mesophase where the molecules are arranged in diffuse layers but still flow like a liquid (T3 in Figure 1.3). The step from the so-called plastic crystal to the fluid liquid crystal in general happens due to the anisotropic nature of the rod-like mesogen, the lateral intermolecular forces are stronger than the terminal intermolecular forces meaning the terminal forces break first leading to a lamellar arrangement of the molecules.[1] In the next step of the process the molecules lose their short-range positional order leaving them only with orientational order and the nematic mesophase, which possesses only an orientational ordering of the constituent molecules, (T4 in Figure 1.3). Finally in the last step of the process the molecules lose all order entirely and this is the isotropic liquid (T5). It should be noted that a material will not necessarily exhibit each of these distinct phases, for example, 5CB (Figure 1.2) exhibits only a nematic phase.

Crystalline solid
Long-range order

T2

Smectic-like crystal phase
Long-range order
Can rotate about it's axis

T1

T3

Isotropic liquid
No long/short range order
No orientational ordering

T5

T4

Nematic mesophase
No short-range order
Orientational ordering

Smectic mesophase
No long-range order
Diffuse layer ordering
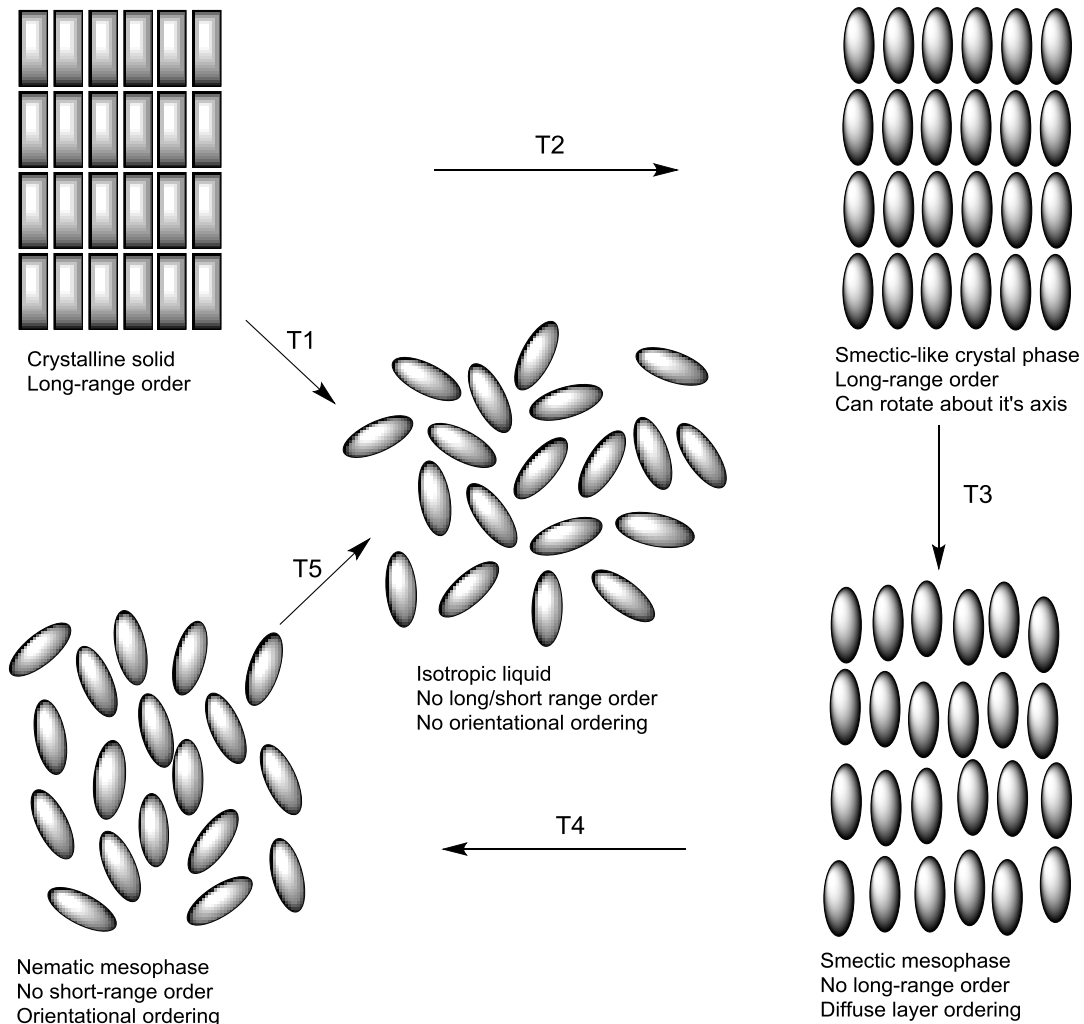
Figure 1.3: Possible melting sequences for a liquid-crystalline material.

Thus, in a broad sense there are only two groups of mesophase that rod-like mesogens form, these are the smectic and the nematic mesophases. The nematic phase is the least ordered and the most fluid of the mesophases where the molecules don't have short or long-range order but do possess orientational order *i.e.* the long axis of the rod-like mesogen statistically points in a preferred direction, this is known as the director. Nematic materials can be designed so that their orientation switches in response to an applied electric or magnetic field; the different optical properties of these different orientations combined with the fluidity enables these materials to be used in display applications.[1] A diagram of the nematic phase is show below in Figure 1.4.
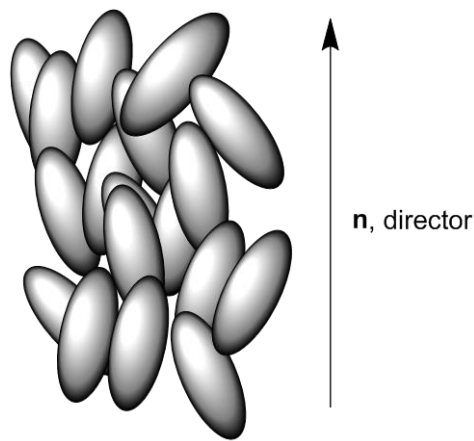
Figure 1.4: Illustration showing the nematic phase, with the director labelled **n**.

The simplest nematic phase is the uniaxial nematic, named so as it is optically uniaxial, possessing one degree of orientational order and no positional order.[8] An important quantity that is associated with the nematic phase and other liquid crystalline phases for that matter is the order parameter, which is given the symbol S and is shown in equation 1.

$$S = \frac{1}{2}\left(3\cos^2 q - 1\right)$$

(1)

In equation 1, θ is defined as the angle between the long molecular axis of individual molecules and the director, usually labelled **n**. When S is one the equation describes a crystalline solid, when S is zero the equation describes the

isotropic liquid. For the simplest nematic phase i.e. the unixaial nematic S usually takes a value between 0.35 and 0.70.[8]

Smectic mesophases have a lamellar (layered) structure and are more ordered than the nematic mesophase. Smectic materials also exhibit mesophase polymorphism *i.e.* there are different types of smectic mesophase, defined mainly by the orientation of the molecules with respect to the layer planes and the degree of in-plane positional ordering of the system. The true smectic mesophases consist of equidistant molecular layers and are characterised by the orientation of the molecules within the layers but with no in-plane, long-range positional order.[9] The smectic phases can be categorised by the orientation of the molecules with respect to the layers and by the degree of order in the system. In smectic A (SmA) and smectic B (SmB) phases the molecules are parallel to the layer normal and are true liquid crystals in that they have no long-range order.[10] The smectic B phase differs from the smectic A in that its molecules occupy nodes of a 2D hexagonal lattice and has increased short-range order.[9] In the smectic C (SmC) phase the molecules are tilted slightly with respect to the layers but this is still a true liquid crystal phase, as it has no long-range order. Analogous to it, the molecules in the smectic I (SmI) and smectic F (SmF) phase are also tilted with respect to the layers but like the smectic B phase the molecules occupy nodes of a 2D hexagonal lattice, with the molecules tilted toward a vertex in the smectic I and toward an edge in the smectic F phase. The smectic B, F and I phases (known as hexatics) are also characterised by the higher degree of order in the system but only have repeat positional order over ~1500-6000 nm.[1] The smectic C, F and I phases also have anticlinic versions, where alternating layers are tilted in opposite directions. The '*soft crystalline*' phases can be derived from the smectics and are also hexagonally ordered but unlike the smectic B, F and I phases the hexagonal lattice positions are predictable over a long range in three dimensions. The crystal B, J and G phases are analogous of the smectic B, I and F phases but with long-range ordering of the hexagonal lattice.[11] The crystal E, K and H phases

are also analogous with the smectic B, I and F phases but have lost rotational freedom.[2]
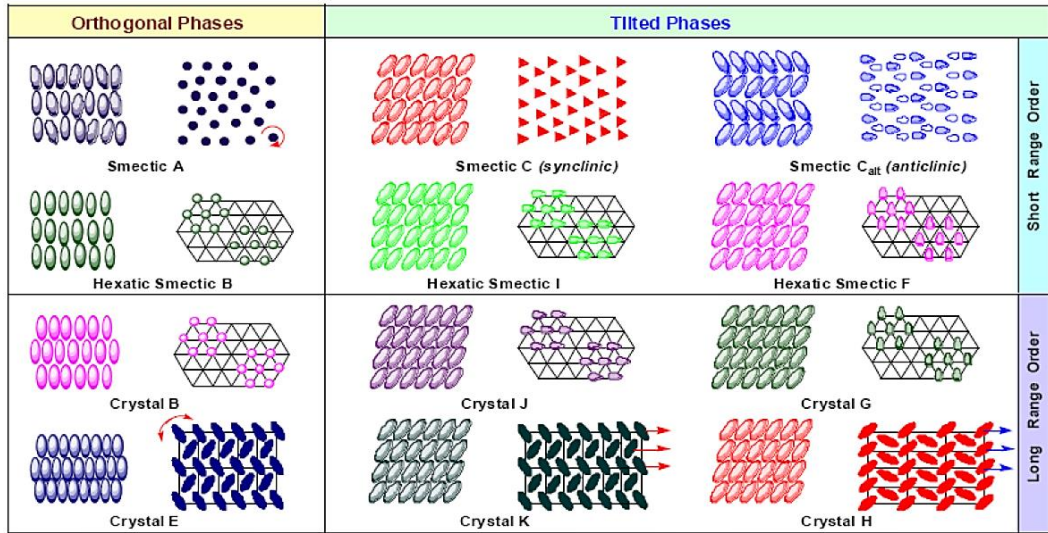
Figure 1.5: Illustration showing the structure of the different smectic phases.[11]

Not all materials will exhibit all the phases outlined above; most compounds only exhibit certain phases and will skip others entirely. Some materials only exhibit liquid-crystalline phases on supercooling, *i.e.* below the melting point. These are said to be metastable and the transitions are termed monotropic. Materials that form liquid-crystalline phases on cooling and on heating are said to be thermodynamically stable and the transitions are said to be enantiotropic.

1.5. The Smectic A phase

The smectic A phase is the least ordered of all the smectic phases, with the molecules having their overall long axis perpendicular to the layer plane. The structure of the smectic A phase is presented in Figure 1.6.
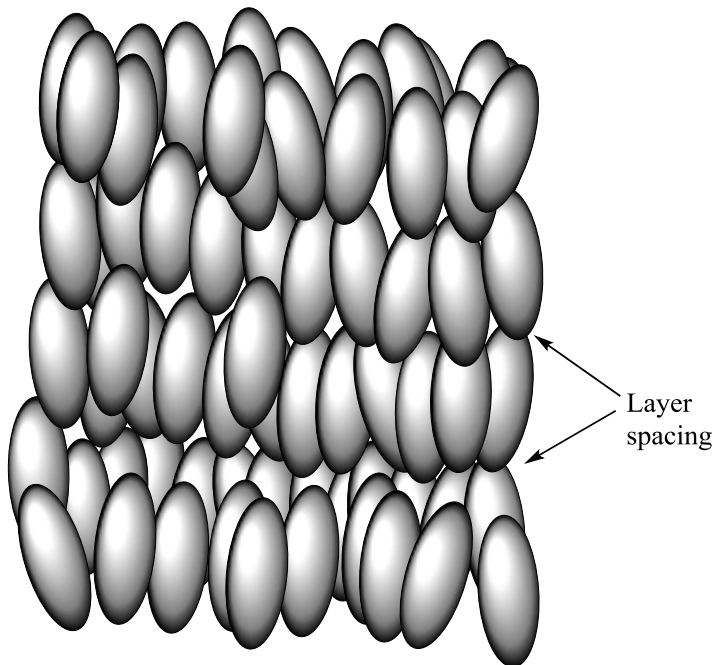
Figure 1.6: A representation of the structure of the smectic A phase.

The smectic A phase is a fluid smectic phase and so the molecules have some rotational degrees of freedom, this can cause there to be a time-dependent tilting of the molecules with respect to the layer plane.[12] The molecular ordering of the layers typically exists over small distances in the order of 15-25 Å.[15] Thus, this phase is characterised by its $D_{\infty h}$ symmetry and is optically uniaxial.

1.6. The Hexatic Smectic B Phase

The hexatic smectic B phase is characterised by the molecules occupying nodes of a 2D hexagonal lattice structure. It is a true liquid crystal phase as it possesses no long-range order, and thus is fluid. The molecules are packed into what is formally short-range positional order however, the correlation length is of the order of 100 Å which is an order of magnitude larger than the correlation length in the smectic A phase.[2] The local structure of the smectic B phase is presented in Figure 1.7.
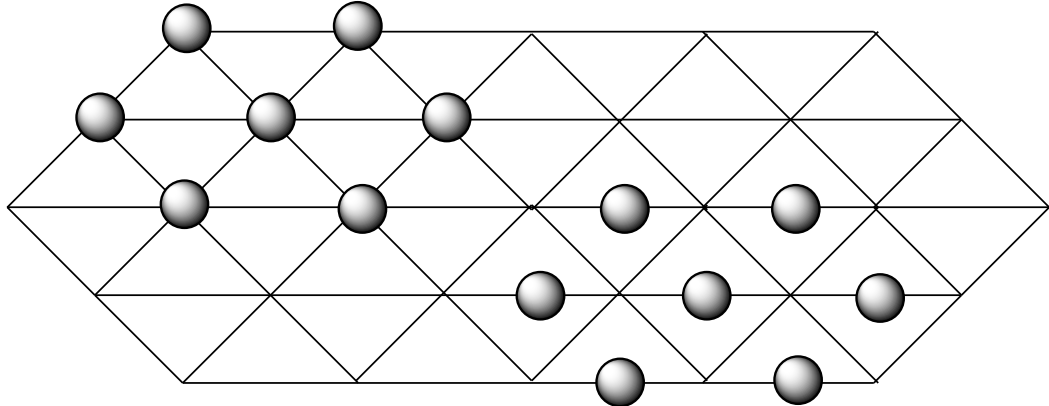
Figure 1.7: Illustration showing the local structure of the hexatic smectic B phase.

The phase is optically uniaxial and possesses true hexagonal symmetry, as the molecules lie parallel to the director and perpendicular to the layer normal as in the smectic A phase. Consequently, it can be difficult to tell the difference between the two phases by polarized optical microscopy.[13]

1.7. The Smectic C Phase

The smectic C phase is similar in structure to the smectic A phase as it also has a layered structure and no long-range order. However, it differs from the smectic A phase in that the molecules possess a net average tilt with respect to the layer normal. There are several different variations of the smectic C phase, two of which are presented in Figure 1.8.
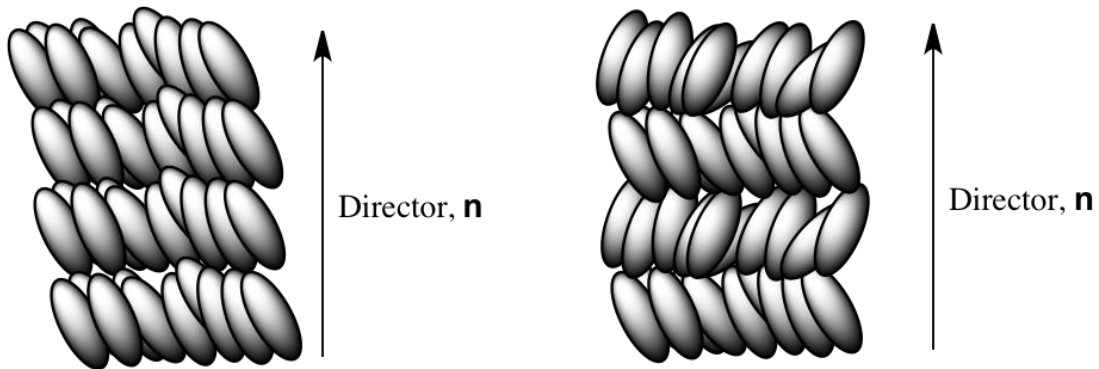
Figure 1.8: Local structure of the synclinic smectic C phase on the left and the anticlinic smectic C phase on the right.

The correlation length within the layers of the smectic C phase is around 15 Å, which is comparable with the smectic A phase but just less than an order of magnitude less than the smectic B phase.[11] Although the correlation between the layers is small, the tilt direction is on average the same between successive layers and so extends over a comparatively large distance. This means that overall the smectic C phase is C_{2h} symmetric and is weakly optically biaxial.[14]

1.8. Chirality in Liquid Crystals

A molecule is said to be chiral when it is not super-imposable on its mirror image. Conversely, if a molecule is super-imposable on its mirror image it is called achiral. Chirality usually arises from four different substituents being present on the same carbon atom. The non-superimposable mirror images are called enantiomers and are distinguished in name by the *(S)-* and the *(R)-* prefixes which denote the way in which the substituents are arranged when they are assigned according to their relative priorities. The *(R)-* prefix denotes a rotation to the right the *(S)-* prefix denotes a rotation to the left.
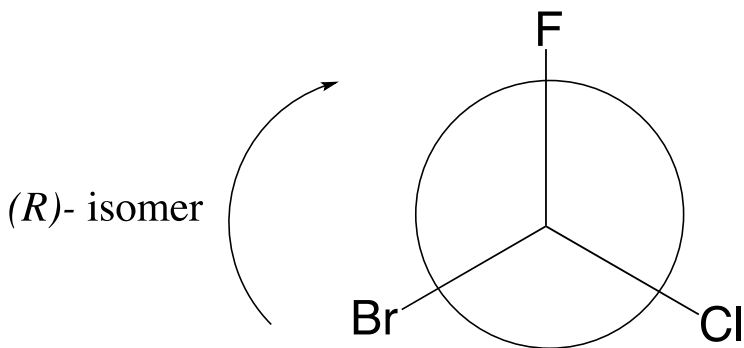
Figure 1.9: Newman projection of the hypothetical bromochlorofluoroiodomethane looking down the axis of the highest priority constituent molecule *i.e.* iodine. This molecule is an *(R)-* isomer due to the rotation of priority being to the right.

There are two main ways of introducing chirality into a liquid crystal system; the first way is to incorporate a stereocentre into some part of the molecule

during the synthesis. The second is by doping a chiral dopant into the system *i.e.* doping a chiral material into a liquid crystalline host that is achiral, thereby introducing chirality into the system.

1.9. The Chiral Nematic Phase

The chiral nematic phase is very similar to the nematic phase as the chiral nematic phase also has no long-range positional order, it does however have a twist in its local structure in the form of a helix, which is due to the incorporation of chirlaity into the system. This phase is also sometimes known as the cholesteric phase due to the first molecules known to possess this phase being derivatives of cholesterol.[15] The local structure of the chiral nematic phase is shown in Figure 1.10.
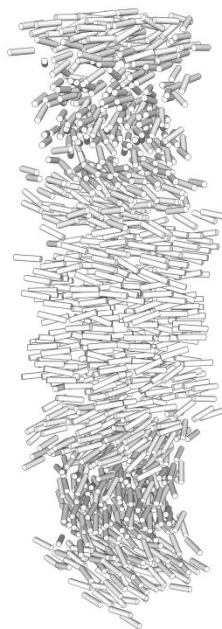
Figure 1.10: An illustration of the helix in the chiral nematic phase.

As noted previously, in the chiral nematic phase the asymmetry of the system results in the director precessing around an axis, giving a helical macrostructure. This helix has a temperature-dependent pitch, which is

described in equation 2, where p_0 is the pitch and q_0 is the helical wave number, the sign of the helical wave number signifies the rotation of the helix.[15]

$$p_0 = 2\pi/q_0 \qquad (2)$$

The length of the pitch of the helix is defined as the distance between two points where the angle of twist has made a complete 360° rotation. As well as the pitch, the director can also be described mathematically as is shown in equation 3, where the helical axis is the z-axis.[16]

$$n_x = \cos(q_0 z + \phi) \qquad (3)$$
$$n_y = \sin(q_0 z + \phi)$$
$$n_z = 0$$

The helical axis, termed (z) and the value of ϕ are both arbitrary, the states, **n** and **−n** are equivalent, which means that the structure is periodic along the z axis.[16]

1.10. The Chiral Smectic C Phase

Due to the asymmetric nature of having a non super-imposable mirror image, the macrostructure of the smectic C phase has a tilt that rotates around an axis that is perpendicular to the layer planes. Hence, the phase is helical. However, in contrast to the structure of the helix in the chiral nematic phase, the pitch length of the twist *i.e.* the distance between two points where there has been a 360° rotation is typically in the order of micrometres in the chiral smectic C phase.[14]
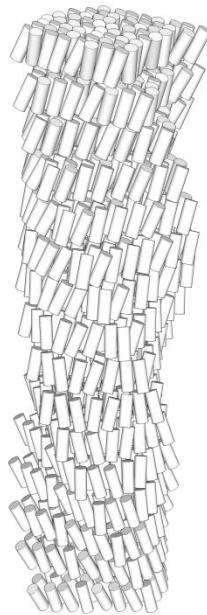
Figure 1.11: An Illustration of the helix in a chiral smectic C phase.

The chiral smectic C phase has taken on increased importance in liquid crystal research in recent times. This is due to work carried out by Meyer *et. al.* in the 1970s who showed that, from symmetry considerations, the chiral smectic C phase exhibits local spontaneous polarization.[17] If the spontaneous polarization can be reversed by application of an external magnetic field, then the material is said to be ferroelectric.[18] This was followed by the discovery of surface stabilised ferroelectric liquid crystals by Clark and Lagerwall that shows the promise that ferroelectric materials have in fast-switching, large viewing angle displays. Chiral modifications of the other tilted phases, such as the hexagonal smectic I and F phases, can also show ferroelectric properties but these are studied less frequently due to their relatively high viscosities.[13]

1.11. Supermolecular Liquid Crystals

For many years liquid crystal research has been dominated by low-molecular weight materials, which consist of a single monogenic unit. This is due in large part to the industrial success of materials such as those in devices such as

displays. Supermolecular molecular entities are defined as giant molecules made up of many covalently bonded smaller units, in the case of supermolecular liquid crystals the unit is usually a mesogenic entity. There are many different topologies that can give rise to a wide range of supermolecular liquid crystal entities. These include, linear systems such as dimesogens,[19] bimesogens[20] and trimesogens[21] as well as other more complex systems such dimeric,[22] cage-like[23] and dendritic.[24]

1.12. Linear and Laterally Appended Supermolecules

The simplest forms of supermolecular liquid crystal are the linear systems and the simplest of these is the bimesogen. A bimesogen is made up of two identical mesogenic entities that have been covalently bonded together; this differs from the dimesogen as this is made up of two different mesogenic units that can be either similar or dissimilar. A higher order than this is the trimesogen, which is made up of three mesogenic units covalently bonded together but of course there are higher orders than this up to the polymeric scale. In Figure 1.12 are examples of a dimesogen, a bimesogen and a trimesogen.[19][22]

Dimesogen

Bimesogen
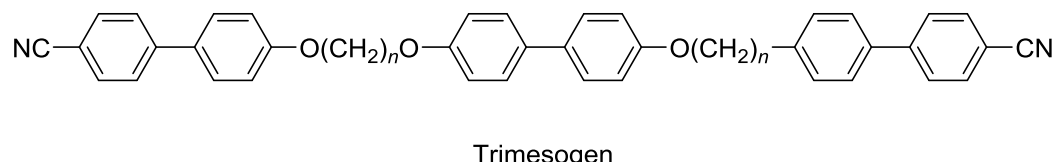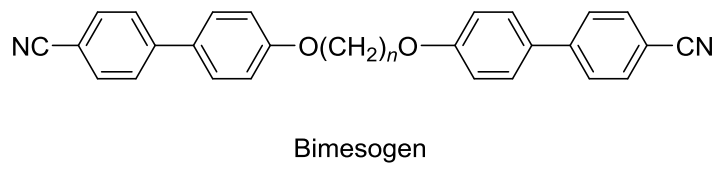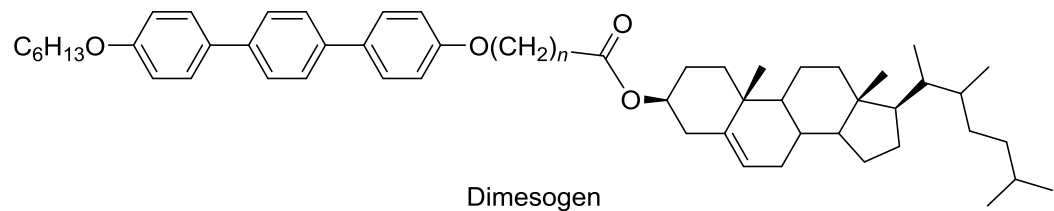
Trimesogen

Figure 1.12. Examples of a dimesogen (top), a bimesogen (middle) and a trimesogen (bottom).

It has been found by Imrie *et al.* that the symmetrical dimers usually form a smectic phase consisting either of the mesogens terminal chains interdigitated or by forming a monolayer structure.[19] A diagram of these two possibilities is shown in Figure 1.13.

(a)   (b)
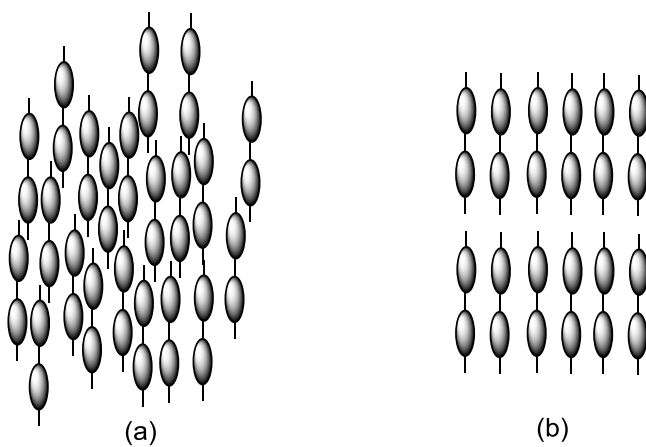
Figure 1.13: Illustration showing the possible smectic-like configurations of the liquid crystalline bimesogens.[19]

For dimesogens, as depicted in Figure 1.12, the two mesogenic units are dissimilar. If the mesogenic units are dissimilar then the properties of the mesogenic units may also be dissimilar, this causes the like-mesogens to pack together. As the dissimilar mesogenic units are covalently bonded together, they cannot move apart from one-another, this causes nano-segregation to appear in the system.[25] Two examples of dimesogens are shown in Figure 1.14 with their thermal properties and phase classification.

Cryst 116 N 217 °C Iso Liq

Cryst 112 SmC 134 SmA 199 °C Iso Liq
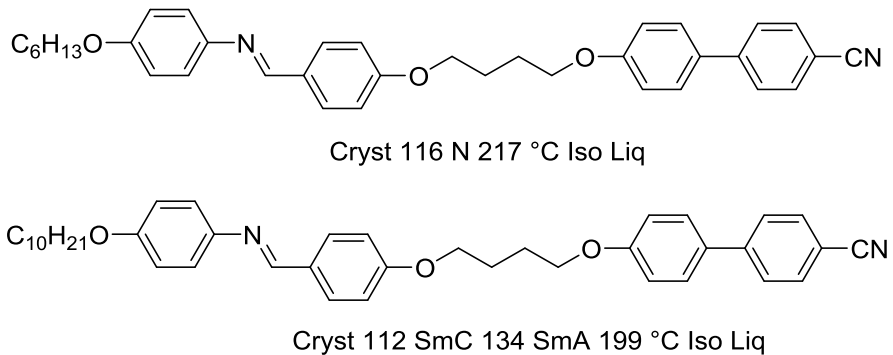
Figure 1.14. Illustration showing the structures and mesophase behaviour of dimesogens[19][26]

As can be seen from Figure 1.14, the two compounds only differ by the terminal alkyl chain on the left mesogen, but the mesophases formed by these two compounds are completely different. There have been many other examples of liquid-crystalline dimesogens, but these are out of the scope of this thesis.[27] As well as having two distinct mesogens being terminally appended, it is also possible to laterally append the mesogens [27][28] (Fig. 1.15)

18

Cr 99.5 N 149.4 °C Iso Liq
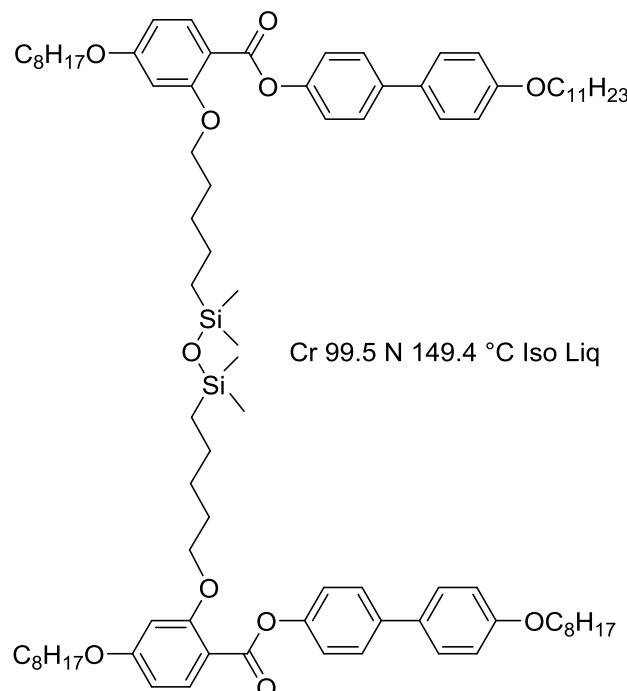
Figure 1.15. Illustration showing the structure of a laterally appended dimer and its transition temperatures and phase classification.

The compound in Figure 1.15, as well as its two parent molecules, all exhibited the nematic mesophase. This can be attributed to the disorder caused by the laterally appended group, which deceases the molecules ability to pack together in a lamellar-like formation which is what is required for the molecule to exhibit smectic-like behaviour.

1.13. Liquid-crystalline polypedes

It is clear from what has been said previously that terminally appended dimers normally exhibit smectic phases and laterally appended dimers usually form the nematic phases due to the lateral group's inability to pack together in a lamellar-like structure. As well as the point of attachment, the number density of these materials and the difference between each mesogen are also important as can be seen from the mesophases formed by dimers and higher oligomers.[22] When the mesogenic units are attached to a central core, the

length of the linking group attaching the two moieties also has to be considered. The longer the linking group the less likely the molecule will act as a supermolecule, it will instead act like two or more distinct entities, *i.e.* if the linking group is shorter in length the molecules are more likely to act as a supermolecule since the mesogenic motions are not decoupled from those of the core.[29] As well as these considerations relating to the mesogen and the point of attachment of the mesogen there are also variables relating to the core unit itself. The core can be a soft core or a rigid core *i.e.* the flexibility of the core can change, there are also considerations to make on how many points of attachment there are and whether one or more different groups are going to be attached to the same core. It could be possible to attach many groups to the same core, these groups could be very similar or very dissimilar, in this case the like groups will associate together and this causes micro-segregation in the system.[30][31] An illustrative diagram of just some of the possible combinations is shown in Figure 1.16.

Supermolecule with all groups beng the same

Dichotomous Supermolecule

Supermolecule with half laterally and half terminally appended groups
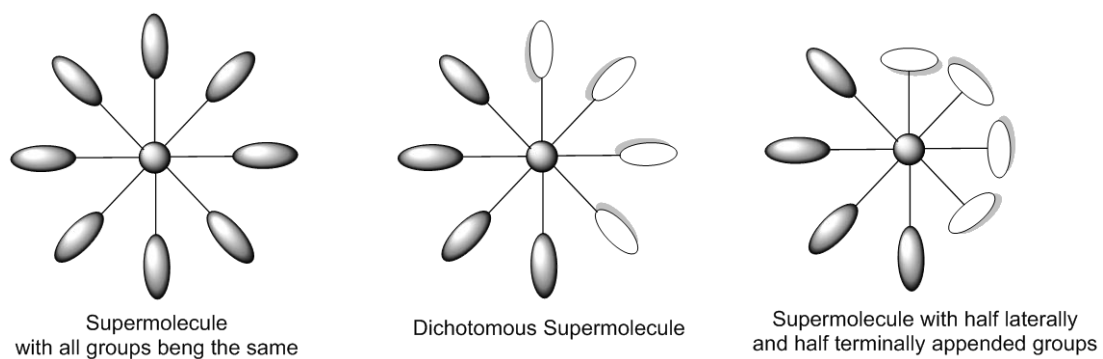
Figure 1.16: Illustration showing some of the combinations possible when attaching a mesogen to a central core.

At this point, supermolecular LCs merge into the field of side-chain LC dendrimers, in which the scaffold is made of layer upon layer of repeating branched units to which the mesogens are attached to the end of each arm. An important aspect of supermolecular LCs and LC dendrimers is that they are monodisperse entities, a difference they have with traditional LC polymers. The dendritic and supermolecular architectures offer the possibility of very precise fine-tuning of the structure, which is crucial for developing new self-assembling

20

mesomorphic materials. The discussion of LC dendrimers is outside the scope of this project and will not be developed further.

As in LC dimers, trimers, polypedes, multipedes and dendrimers the topology of the attachment of the mesogen to the core has a strong influence on the mesomorphic behaviour. In general, terminal attachment of the mesogens to the core can support smectic and nematic phases. However, side-on attachment of the mesogen to the core doesn't allow efficient packing of the mesogens in layers therefore the smectic tendency is suppressed and only the nematic phase is observed.[29] Similarly, increasing the number of mesogens on a scaffold leads to a stabilisation of the mesophase/s observed, in parallel with the behaviour observed in LC polymers.

As has been noted previously, the core of the supermolecule can either be soft or rigid *i.e.* it can be either flexible or stiff and this has a profound impact on the properties of the materials in question as it determines the ability of the molecule to either deform and act as a whole entity, or act as independent mesogenic parts.[32] An example of a dendritic molecule with a soft core is shown in Figure 1.17 below.
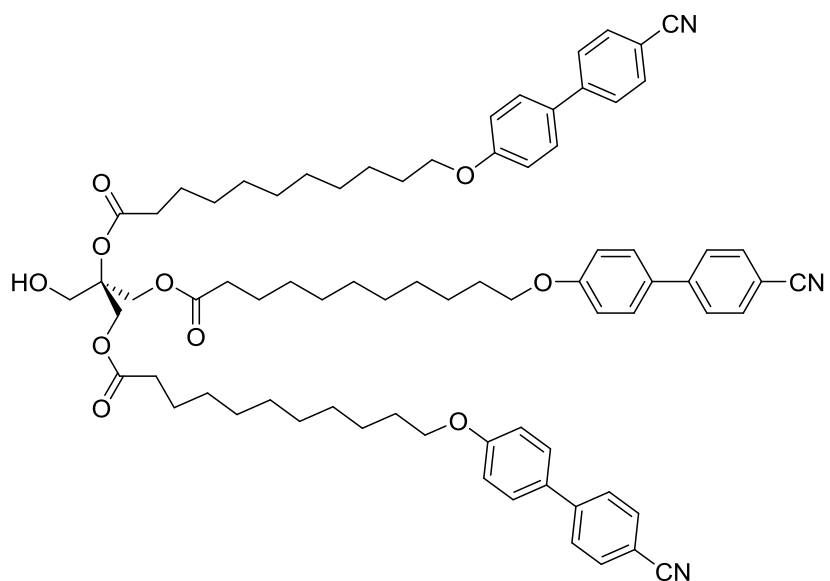
Crystal 26.2 Smectic C 43.5 Smectic A 96.2 °C Iso Liq

Figure **1.17:** Structure of a dendritic liquid crystal with a flexible core and its transition temperatures.

1.14. 'Janus' Liquid Crystal Supermolecules

Molecular self-assembly and self-organization is an important area of chemistry in terms of understanding various life processes such as protein folding. This has brought a new generation of supramolecular structures and ensembles to the fore.[33] At the height of this field are 'Janus' materials, which include Janus grains[34], Janus micelles[35] and segregated amphiphillic dendrimers.[36-37] The basic structure of a 'Janus' material is one with two distinct moieties that are attached to the same structure in a segregated manner (not randomly mixed) *i.e.* two poles. The name 'Janus' derives from the Roman god of the same name who possessed two faces looking in opposite directions. The idea of making these materials is to make a material that possesses two different groups with different properties *e.g.* a face made up of hydrocarbon moieties and a face made up of fluorocarbon moieties. Various supermolecular liquid crystalline 'Janus' materials have been prepared.[38-39] In terms of the field of liquid crystals, an ideal would be to have a 'Janus' material with two different mesogens attached to it in order to study the formation of liquid crystalline phases. Two examples of such a material are shown in Figure 1.18.
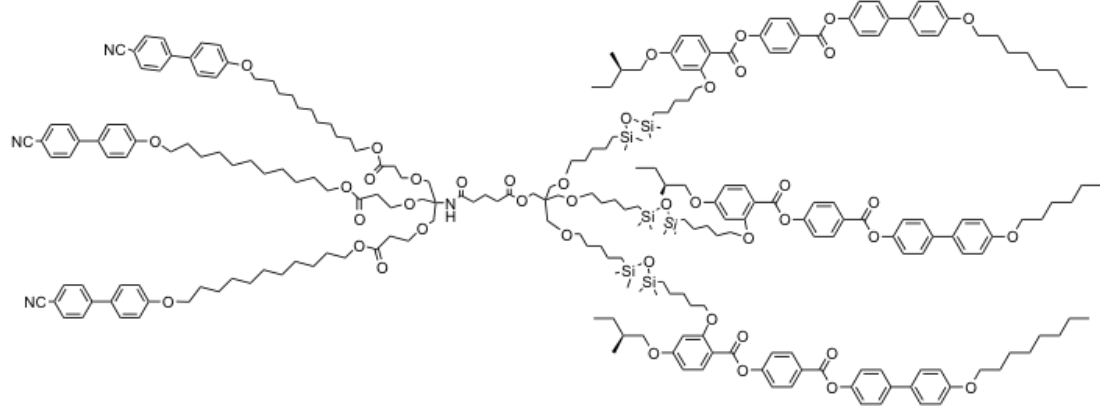
a) g -2.8 SmC 36.1 N* 60.8 °C Iso Liq
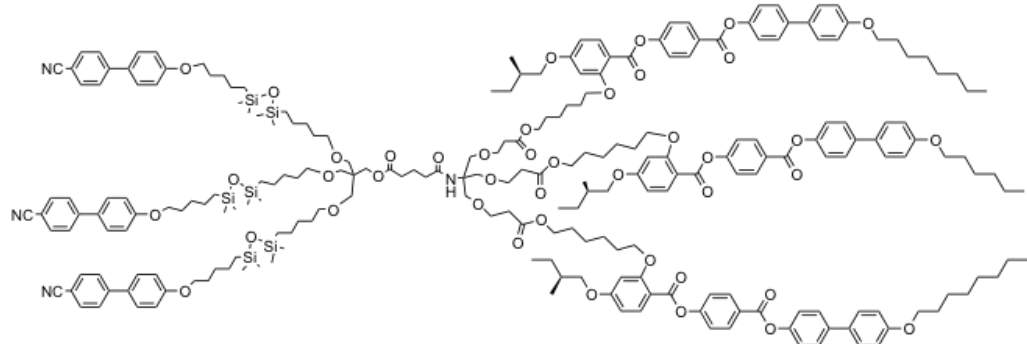
b) g -7.9 N* 38.2 °C Iso Liq

Figure 1.18: Structures and mesomorphic behaviour of two 'Janus' liquid crystal supermolecules.

The structures above contain two different mesogenic entities one of which is laterally attached. The mesomorphic behaviour is different depending on which lobe of the dendrimer carries which mesogen.

1.15. 'Hard' Core Supermolecular Liquid Crystals

As well as 'soft' core supermolecular liquid crystals, where the core is flexible, there are also 'hard' core scaffolds for supermolecular liquid crystalline entities where the core is rigid. A common 'hard' core scaffold used in supermolecular liquid crystals is the polyhedral silsesquioxane, which will be discussed in more detail later on in this thesis. As well as silsesquioxanes, other rigid core scaffolds

have been used as central building blocks for supermolecular entities; for example the hexa-adducts of fullerene can give a spherical distribution of mesogenic substituents about the central scaffold.[40-41] An example of a 'hard' core supermolecular liquid crystal based around a fullerene scaffold is shown in Figure 1.19.

g 80 SmA 133 °C Iso Liq
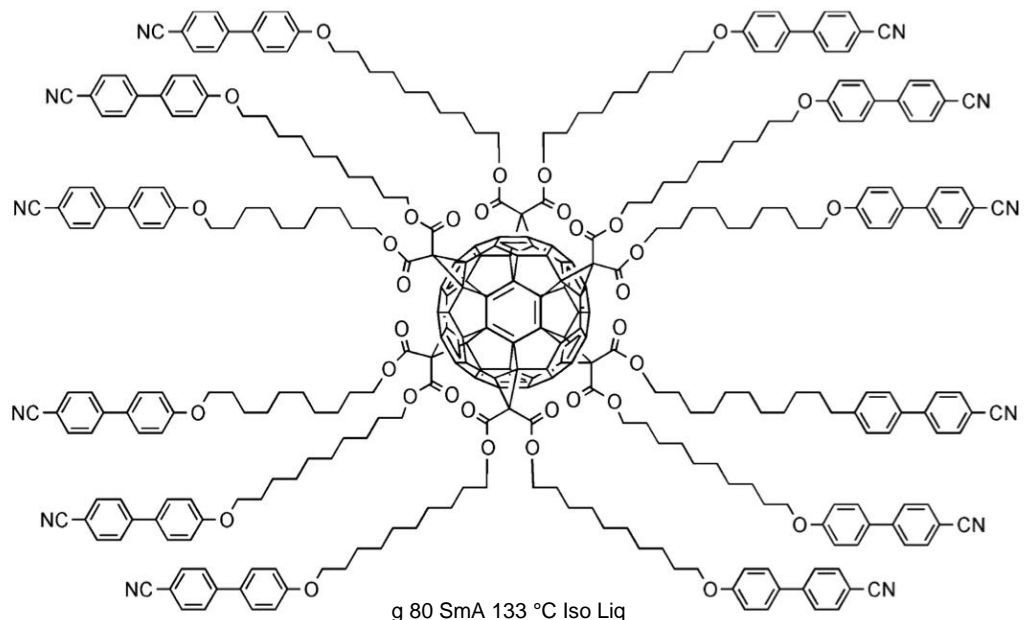
Figure 1.19: Structure and phase behaviour of a supermolecular fullerene liquid crystal.[32]

This material exhibits a smectic A phase which is common among 'hard' core supermolecular liquid crystals.[32] The effect the rigid core has on the molecule is to reduce the flexibility associated with the arms attached to the core and so it can only possess a cylindrical shape which is perfect for exhibiting a smectic A mesophase.
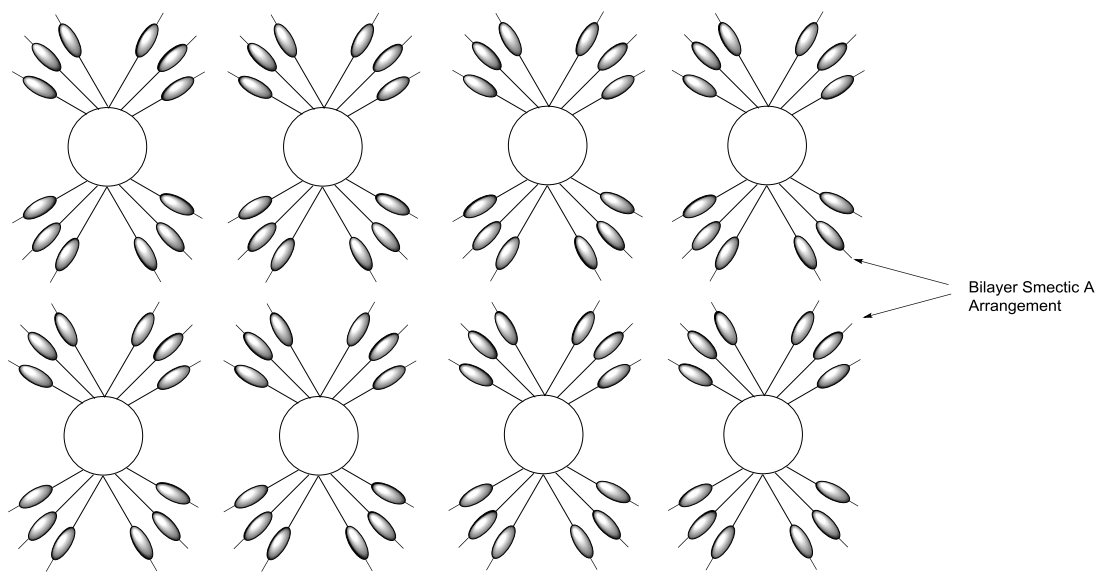
Figure 1.20: Schematic drawing showing the possible bilayer smectic A arrangement of a supermolecular liquid crystal.

Attachement of lateral mesogens on a fullerene core can lead to some interesting properties.[42] Similar to compounds mentioned previously, when a lateral mesogen is attached to a central scaffold the disorder caused by its inability to pack generally leads to nematic mesophases. An example of a fullerene supermolecule with laterally attached mesogens is shown in Figure 1.21.

g 47 N* 103 °C Iso Liq
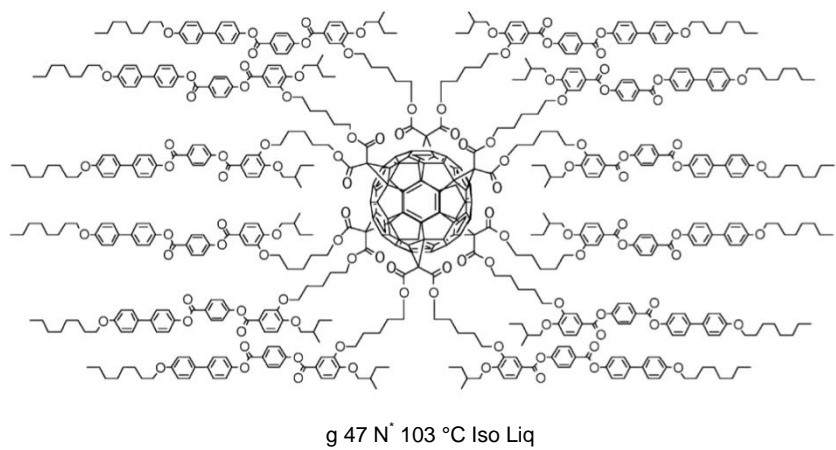
Figure 1.21: Structure and thermal properties of a fullerene supermolecule with laterally attached mesogens.[42]

The molecule in Figure 1.21 exhibits only a chiral nematic phase, as is the case for the octasilsesquioxanes substituted with the same mesogen.[23] The structure of the fullerene dendrimer depicted in Figure 1.21 was thought to be very similar to the proposed structure in Figure 1.20. However, this is not the case as the mesogenic units of the dendrimer were found to pack in an organised way both relative to the surface of the dendrimer and between dendrimer molecules. This causes a spherical shape to form, which is not as cylindrical as the structures seen in Figure 1.20.

1.16. Silsesquioxanes

Silsesquioxanes are a group of silicon and oxygen containing materials that have the general formula $RSiO_{3/2}$[43-44] with a cage-like structure where the silicon atoms are bridged by the oxygen atoms. Structurally, silsesquioxanes consist of tetrahedral units in which a silicon atom is bonded to three oxygen atoms and one R-group. The oxygen atoms can act as a bridge between two silicon atoms belonging to different tetrahedral units, or between silicon and hydrogen atoms. A unit where a silicon atom is connected to three oxygen atoms is commonly referred to as a 'T' unit, a subscript number is often used within this nomenclature to describe how many 'T' units a molecule contains *e.g.* a T_8 unit would contain eight and be in the shape of a cube. Examples of various silsesquioxanes along with their 'T' nomenclature and structural formulae are given in Figure 1.22.

T_6R_6 ($Si_6O_6R_6$) T_8R_8 ($Si_8O_8R_8$) $T_{10}R_{10}$ ($Si_{10}O_{10}R_{10}$)
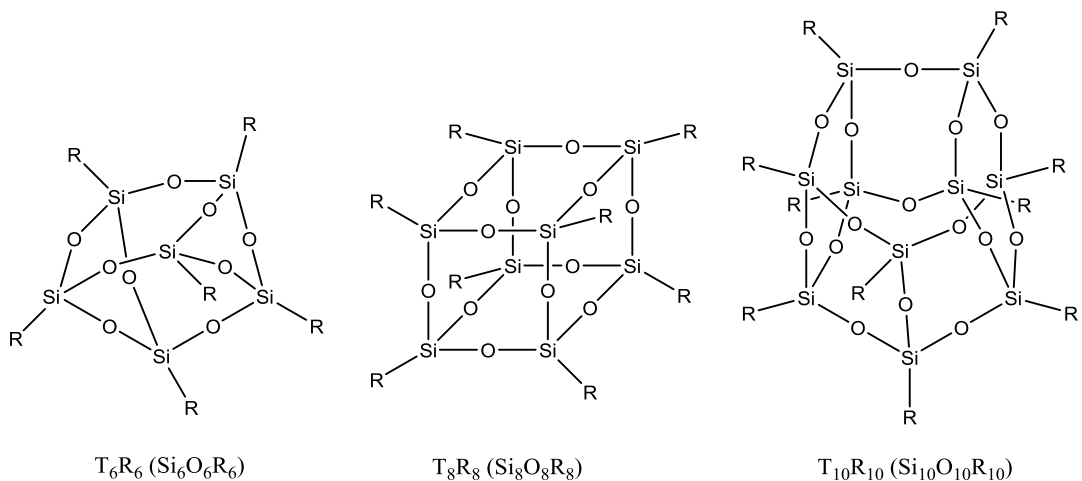
Figure 1.22: Idealised structures of various silsesquioxanes.

Silsesquioxanes can either be synthesised as discrete entities or as polymeric species. These two species have completely different properties and applications.[45] Polymeric silsesquioxanes are beyond the scope of this thesis and so discrete, also known as polyhedral silsesquioxanes, will be the focus of the discussion in the following sections.

1.17. Polyhedral Oligomeric Silsesquioxanes

There are two main forms of polyhedral oligomeric silsesquioxanes, namely completely condensed silsesquioxanes and incompletely condensed silsesquioxanes. Completely condensed silsesquioxanes can be described by the general formula of $(RSiO_{3/2})_a$ where a is number greater than two. Incompletely condensed silsesquioxanes contain silanol groups *i.e.* the Si-O-Si bridges are not all complete.

27

Trisilanol   Disilanol
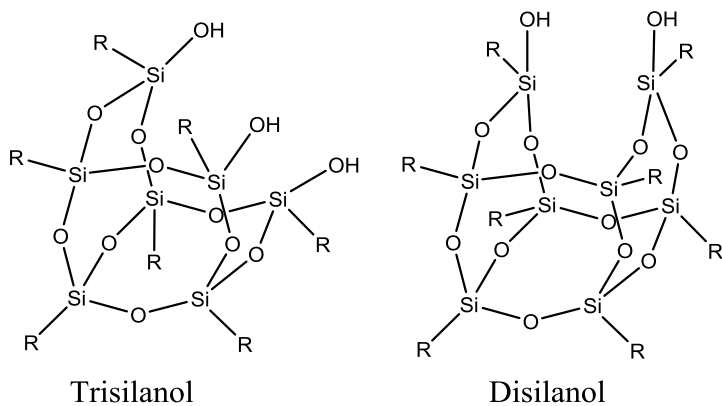
Figure 1.23: Idealized representation of two incompletely condensed silsesquioxanes.

1.18. Synthesis of Polyhedral Oligomeric Silsesquioxanes

There are two main methods of producing silsesquioxanes, namely hydrolytic condensation of an $RSiX_3$ species, where R is an unreactive species and X is a reactive species,[46-48] or by corner capping of an incompletely condensed silsesquioxane species.[49] The most common method used today is the hydrolytic condensation reaction (Figure 1.24).

$$RSiX_3 \;+\; 3H_2O \longrightarrow RSi(OH)_3 \;+\; 3HX$$

$$aRSi(OH)_3 \longrightarrow (RSiO_{1.5})_a(H_2O)_{0.5b} \;+\; (1.5a\text{-}0.5b)H_2O$$
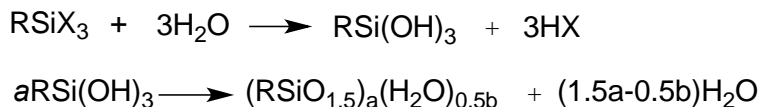
Figure 1.24: Equation for the formation of a silsesquioxane species (X = Cl, OMe, OEt...).

The first step in the reaction is the hydrolysis of $RSiX_3$ to give the corresponding trisilanol $RSi(OH)_3$, this step in the reaction is usually very fast.[50] The subsequent step in the reaction is the condensation reaction of the trisilanol into various cages, this step in the reaction is also relatively fast but there have been cases where the trisilanol species has been isolated.[51-52] This step is a multistep process going through many intermediates. Whether this condensation reaction forms one of the completely condensed species or one of the incompletely condensed species is dependent on many factors. These include the nature of the R group, the nature of the X group, solvent, pH, *etc.* For

example, bulky R groups such as cyclopentyl or cyclohexyl favour the formation of incompletely condensed species, due to steric effects.[53] Conversely, small, less bulky groups such as methyl or hydrogen are known to favour more completely condensed species, due to the lack of steric effects.[54] The R group also has a profound effect on the solubility of the compound. For example, the solubility in most organic solvents is lower for a trisilanol with a cyclopentyl R group compared with if the R group was a methyl substituent, allowing their isolation from the hydrolysis mixture.

An alternative method of making completely condensed silsesquioxane species is by corner capping of an incompletely condensed species.[49] The reaction involves reacting an incompletely condensed trisilanol species with $RSiX_3$ to 'cap' the missing corner of the species. A schematic diagram of the reaction can be seen in Figure 1.25. The advantage of this reaction is that it allows the synthesis of materials with two different R groups, if the capping reagent is different from the original $RSiX_3$.
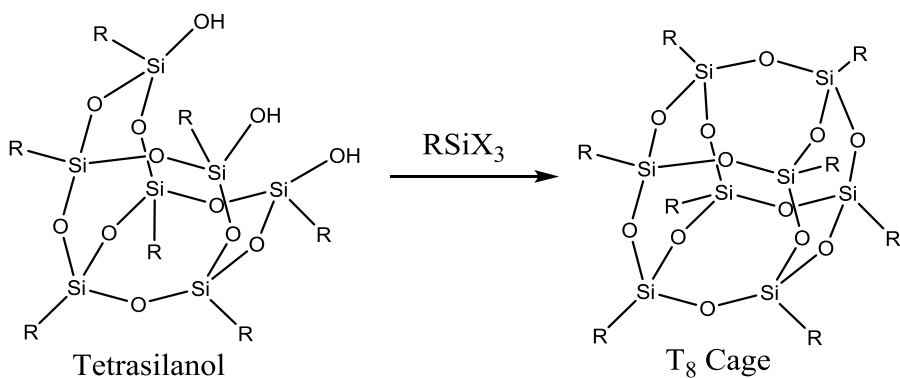
Figure 1.25: Schematic of corner capping reaction to produce completely condensed silsesquioxanes.

An alternative method of making incompletely condensed species is by cleavage of the Si-O-Si bond. This process was also pioneered by Feher *et al.* and involves either reacting the completely condensed species with either a strong acid (HBF4/BF$_3$, CF$_3$SO$_3$H) or a base (NEt$_4$OH).[55-59] Good yields have been achieved using this method, such as a yield of 47% for the cleavage of a completely condensed species with a cyclohexyl R group.[59] However, other

by-products form during the reaction such as the C_2-symmetric tetrasilanol species which was identified *via* its symmetry by ^{29}Si NMR spectroscopy. A schematic of the reaction is shown in Figure 1.26.
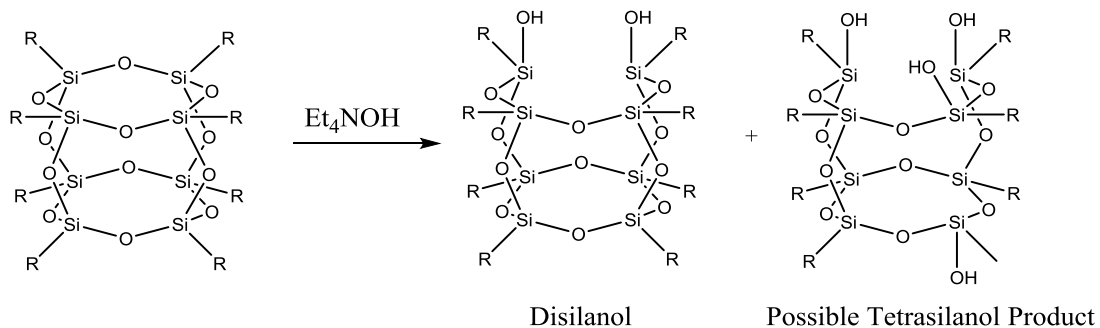
Figure 1.26: A schematic showing the reaction used to cleave the Si-O-Si bond of a completely condensed silsesquioxane species.

1.19. Characterisation of Polyhedral Oligomeric Silsesquioxanes

The main method of characterising the structure of a silsesquioxane species is by Nuclear Magnetic Resonance Spectroscopy (NMR). Silsesquioxane species have at least three NMR-active nuclei, each of which provides useful information in characterising the silsesquioxane species. However, in this case ^{13}C NMR spectroscopy is a more useful technique than ^{1}H NMR as it allows considerations regarding the symmetry of the molecule to be made. For example the resonances of the Si-*C* of the D_2 symmetric disilanol pictured in Figure 1.25 would appear in a 2:4:2 ratio. ^{29}Si NMR is also a very useful technique in characterising silsesquioxane species by the symmetry of the molecule. It has the advantage over ^{13}C NMR that the spectra are simpler to interpret, however has the disadvantage of long relaxation times of the [29]Si nuclei. Mass spectrometry is a useful technique in characterising silsesquioxane species but only when soft ionisation techniques are used.

1.20. X-ray Diffraction Studies of Polyhedral Oligomeric Silsesquioxanes

El Aziz *et al.* has reported the single crystal structure of long alkyl chain POSS compounds.[60] They proposed a number of different packing models of the octafunctionalised octasilsesquioxane, with different interdigitation arrangements (Fig 1.27 a-d) or with a columnar arrangement (Fid. 1.27 e)
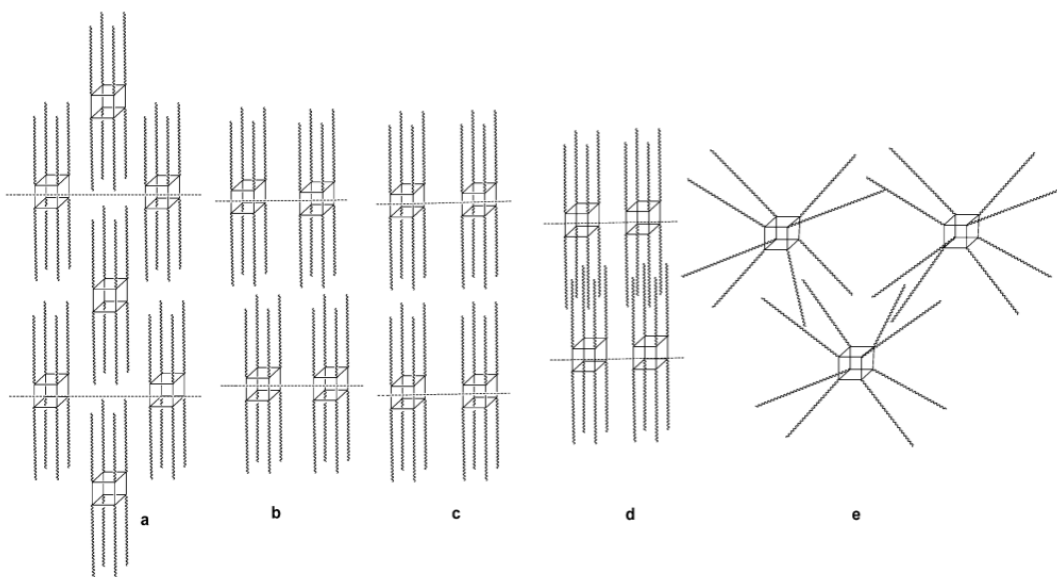
Figure 1.27: Possible octafunctionalised octasilsesquioxane packing models.[60]

$R_8Si_8O_{12}$ derivatives, for R = butyl-decyl are triclinic with the centrosymmetric *P*-1 space group, whereas heptyl and pentyl are tetragonal with the *P*4/*n* space group.[60] In all the cases the molecules possess a cylindrical shape with the *c*-axis being the longest axis and this long axis increases as a function of the length of the organic substituent's for the triclinic structures. The long alkyl chain POSS molecules were found to pack in a lamellar-like formation, drawing similarities to the way rod-like molecules pack in a smectic mesophase.[60]
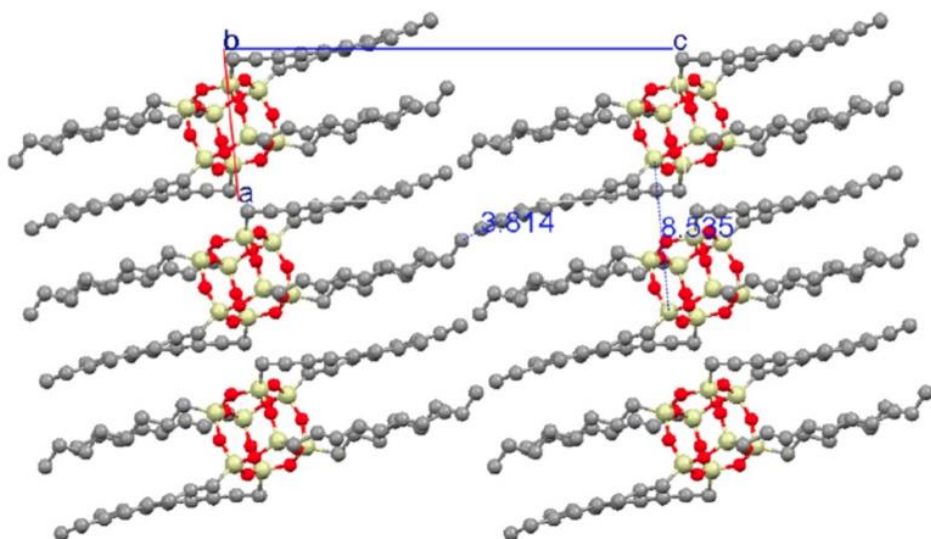
Figure 1.28: Packing diagram of T_8Octyl_8 viewed along the b-axis of the unit cell.[60]

1.21. Liquid-crystalline Silsesquioxanes

Liquid-crystallline silsesquioxanes are synthesised by the reaction of a POSS core with an appropriately functionalised mesogen. The functionalisation is almost exclusively carried out using the hydrosilylation reaction, either of a hydrido silane POSS ($Si_8O_{12}H_8$ or [$(Si_8O_{12})(SiMe_2)H_8$]) and an olefinic mesogen or by hydrosilylation of octavinyl POSS with a mesogenic hydridosilane. A number of liquid-crystalline octasilsesquioxanes functionalised with calamitic mesogenic groups have been reported, most of the mesophases exhibited by these materials have been found to be lamellar phases and these phases are usually exhibited over a much larger temperature range than the mesogenic monomer on its own due to the core suppressing crystallization. If the length of the alkyl spacer between the mesogen and the core is increased the stability of these lamellar phases has been found to increase, this is due to the longer alkyl chain enabling the supermolecule to form a more rod-like shape due to better decoupling of the core and the mesogenic unit.[61]

In addition, nematic mesophases have also been produced in octafunctionalised silsesquioxanes and these have been achieved by two methods. The first method, developed by Kreuzer *et al.,* involves the octafunctionalisation of a cubic silsesquioxane with a laterally attached calamitic mesogen.[62] The mesogenic units inability to pack in a lamellar formation increases disorder in the system and favours the formation of the nematic mesophase. The second method developed by Laine *et al.* involves the addition of a statistical distribution of terminally appended calamitic mesogens to an octasilsesquioxane, this random distribution also increases the disorder in the system and thus suppresses the formation of smectic mesophases.[63] A number of examples of specific liquid-crystalline silsesquioxanes will now be discussed in more detail.

g -12.8 Cr 4.7 Cr 39.0 SmC 74.2 SmA 102.9 °C Iso Liq
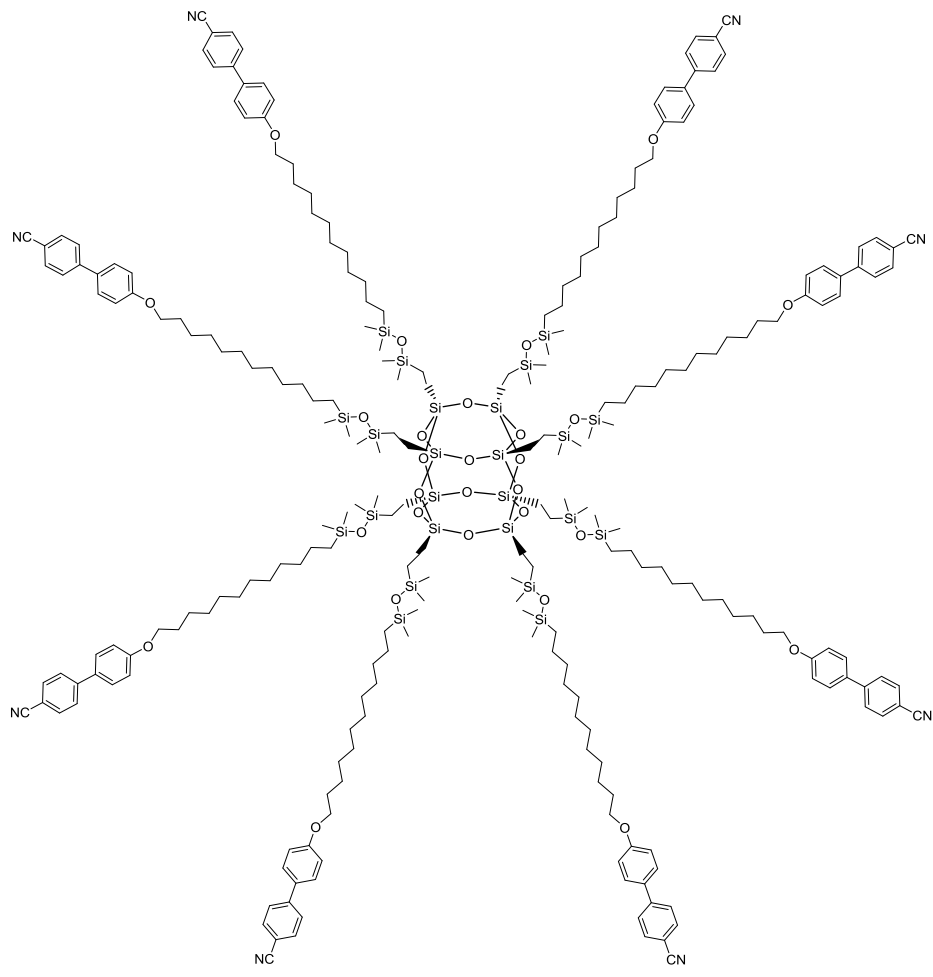
Figure 1.29: Structure of an octamer based on a T_8 silsesquioxane, along with its thermal properties.[64]

Unlike the 'hard' core dendrimer fullerenes discussed previously, the octamer supermolecule in Figure 1.29 shows smectic polymorphism, smectic C and smectic A mesophases.[64] The mesophase sequence of this molecule indicates that the structure conforms to a rod-like shape and so therefore exhibits smectic mesophases with the molecules packing in a layered structure. The smectic C phase exhibited by this molecule could have two possible structures with either the whole molecule tilting or the mesogenic units tilting as can be seen in Figure 1.30.
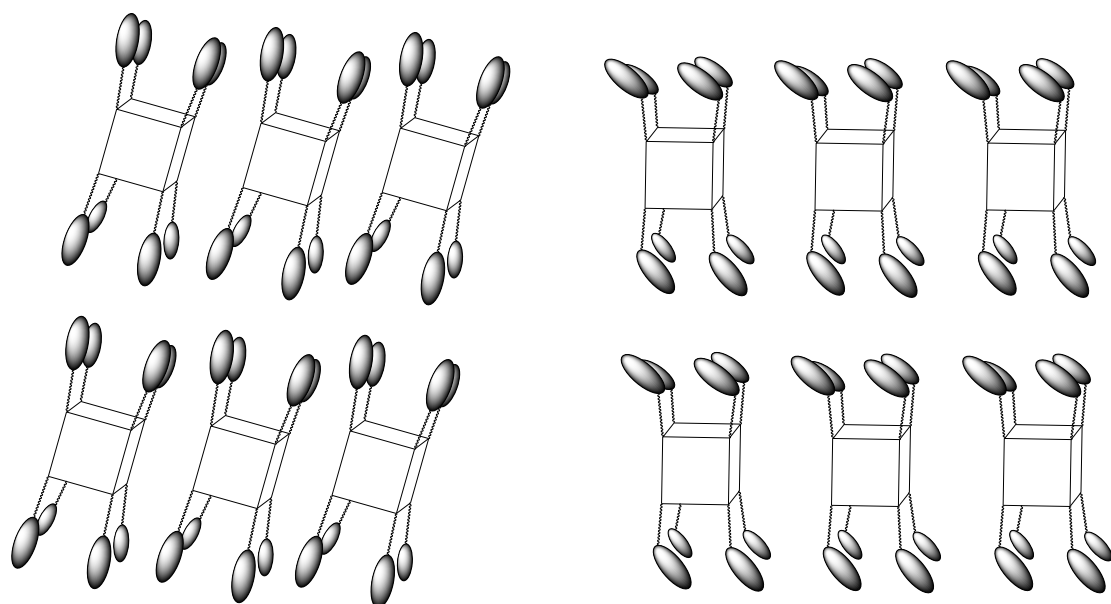
Figure 1.30: Possible molecular topologies enforced by the liquid-crystalline environment of the Smectic C phase.

It is clear from Figure 1.30 that the mesogenic arms are split into two groups with the core sandwiched between, half of them towards one side and the other half towards the opposite side and therefore the structure is microphase segregated with the mesophase having a quasi-bilayer structure with respect to the mesogen and a monolayer structure with respect to the core.[64]

In addition to terminally attached cyanobiphenyl units, laterally attached mesogens can also be used in the formation of silsesquioxane supermolecules,

two examples of such molecules are in Figure 1.31 along with their thermal properties.

a) g 11.2 N* 72.0 °C Iso Liq

b) g 5.4 Col*$_r$ 30 Col*$_h$ 102.3 N* 107.7 °C Iso Liq
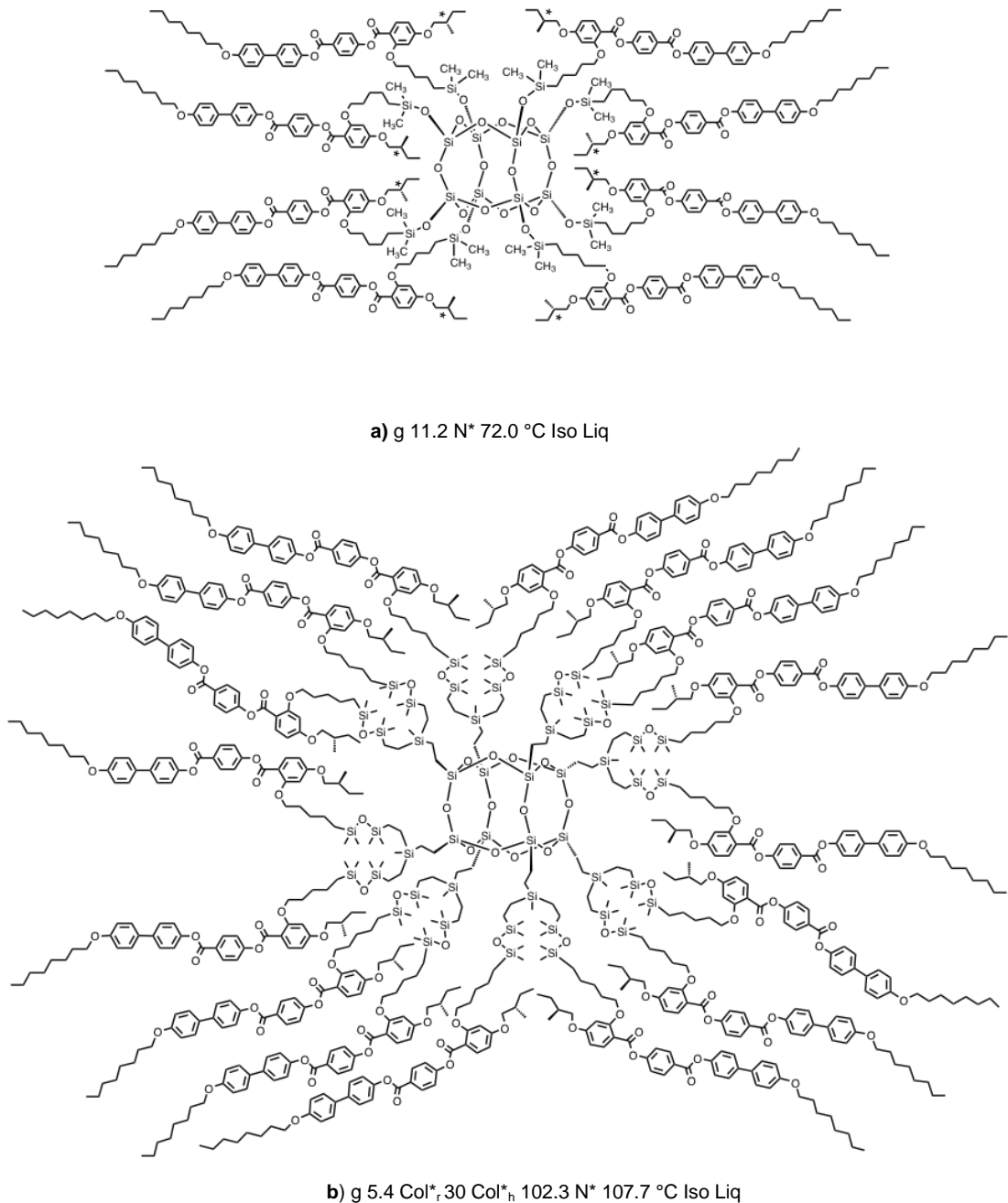
Figure 1.31: Two examples of silsesquioxane supermolecules with laterally attached mesogens along with their thermal properties and phase classification.

As noted earlier, laterally attached mesogenic units normally favour the formation of the nematic phase, or in these two cases a chiral nematic phase due to the chiral centre present in the molecule. The chiral nematic phase of

compound (a) exists over a large temperature range, a much larger temperature range than low-molar mass equivalents, this suggests supermolecular systems may provide a route to liquid crystal phases over a much larger temperature range.[23] The number of mesogenic units from compound (a) to compound (b) has doubled from 8 to 16 units, this increase in mesogenic units has altered the phases this compound exhibits to now include the hexagonal and rectangular columnar phases. The compound is thought to exhibit a cylindrical shape, with the long axes of the mesogenic units parallel to the rotational axis that is normal to the cylinder.[29] The formation of columnar phases in laterally attached mesogenic supermolecules such as compound (b) in Figure 1.31 but not in side-chain polysiloxanes, gives a good indication that the core unit is playing an important role in their formation.[65] This is possibly due to the microphase or nanophase segregation caused by the core being sandwiched in between the two sets of mesogenic units.

In addition to calamitic mesogenic units, bent-core and discotic mesogens have also been used as mesogenic moieties attached to a silsesquioxane scaffold.[66][67] The structures of an example bent-core and an example discotic mesogenic unit that have been used to form silsesquioxane supermolecules can be found in Figure 1.32 along with the thermal properties and phase classification of each compound.
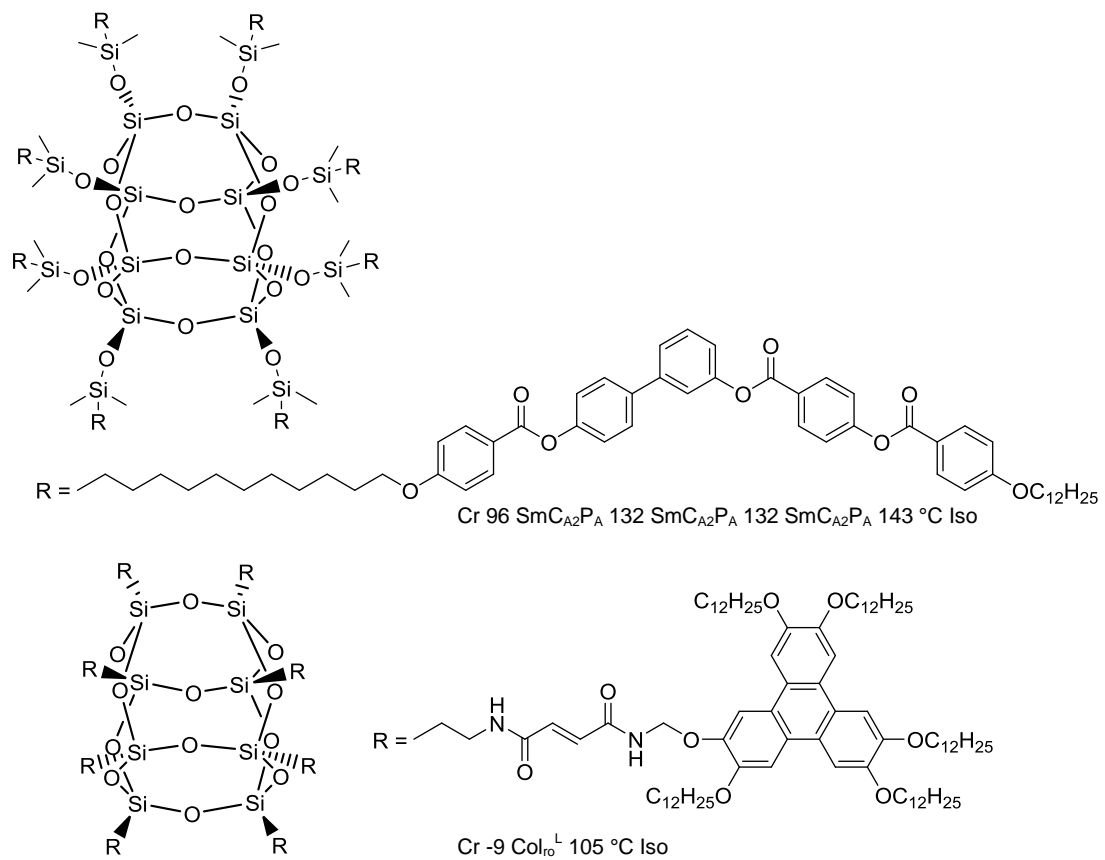
Figure 1.32: An example of a bent-core (top) and a discotic (bottom) silsesquioxane supermolecular liquid crystal, along with their thermal properties and phase classification.

When eight bent-core mesogens are attached to the silsesquioxane core depicted in Figure 1.32, two bilayer SmC_AP_A phases can be observed, this is where the silsesquioxane cores are sandwiched between the bilayers of the bent-core mesogenic units. If an ether oxygen is added to the alkyl chain spacer the stability of the mesophase goes down, this is due to the increase in flexibility due to the reduced rotational barriers around the CH_2-O bond.[66] Interestingly, if only one bent-core unit is incorporated into the structure, the addition of an ether oxygen has no effect on the stability of the mesophase. If the bent-core mesogenic unit to silicon atom is in a 1:1 ratio or less the molecules have antiferroelectric tendencies with birefringent textures, if the silicon atom to bent-core mesogen ratio is more than 1:1 the birefringent textures get replaced by dark textures and ferroelectric switching.[66] When discotic mesogenic units

are incorporated into a silsesquioxane core unit columnar phases are observed. These systems are distorted in a way that conforms to the general shape of the discotic monomer and so usually exhibit phases typical of the mesogenic monomer. When the alkyl chain length of the triphenylene arms are short in length, no mesophases are observed, when the alkyl chain length is increased to C_{12} hierarchical liquid crystal self-assembly is observed with the molecules arranged into columns.[67] When the alkyl spacer between the triphenylene and the silsesquioxane core is short *i.e.* C_2 a column within a column hexagonal columnar phase is obtained. This is where the smaller columns formed by the triphenylene derivatives, pack into larger columns due to the silsesquioxane core holding them in place. When the alkyl spacer length is increased the triphenylene arms decouple from the core. For example, a lamellar morphology with rectangular columnar symmetry is observed when the alkyl spacer is C_6, when the alkyl spacer is C_{10}, an inverted columnar morphology is observed where four triphenylene groups form a column in the silsesquioxane core matrix.[67]

Chapter Two:
Aims

2. Aims

The general aims of this work are to investigate the properties of novel liquid crystalline supermolecular architectures. These architectures should possess one or more different mesogenic units attached by covalent bonds to a silsesquioxane core.

The effect of the spacer length, the number of terminal alkyl chains and the effect of the core have all been studied and reviewed previously. However, what is still left unanswered is what effect the number of mesogenic groups has on the formation of mesophases, more precisely what is the miniumum number of mesogenic groups required to be able to get a rigid silsesquioxane core to self-assemble in a liquid crystalline phase. To be able to study this an incompletely condensed silsesquioxane must be used, as it is difficult to tailor a completely condensed silsesquioxane with fewer than eight mesogenic units. Two examples of incompletely condensed silsesquioxanes which can be used for this purpose are shown in Figure 2.1.

Trisilanol   Disilanol
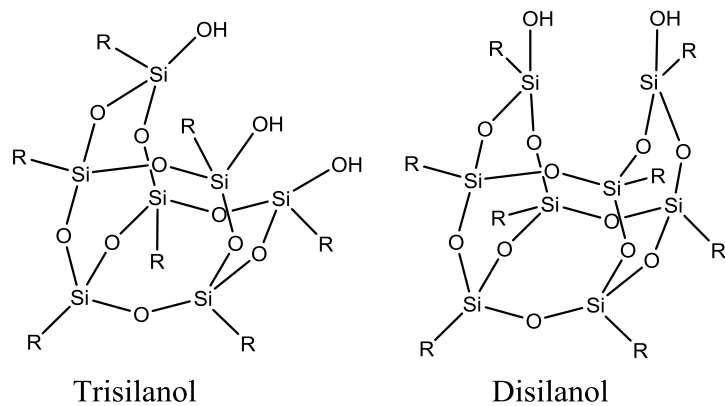
Figure 2.1. Examples of a trisilanol (left) and adisilanol (right).

Derivatives of silsesquioxane disilanol and trisilanol where R groups are iso-butyl, iso-octyl and cyclopentyl will be prepared to study the effect that a dichotomous structure with a degree of microsegregation has on the formation of liquid-crystalline phases in these systems. The compounds in Figure 2.1 makes it possible to attach two mesogens to the disilanol and three to the

trisilanol which allows the study of the effect the extra mesogen has on the system.

Different types of mesogens will be used in order to establish the effect of the nature of the mesogen on the LC properties of the materials. The topology of the attachment of the mesogens to the core will be explored (either end-on or side-on) to tailor the type of mesophase exhibited.

Previous research involving 'Janus' supermolecules has focused on a soft, flexible core unit, there has been very little research into what effect a hard, rigid core unit would have on these materials. In order to produce a 'Janus' liquid crystalline supermolecule using a hard, rigid silsesquioxane as the core unit it must be possible to attach two different moieties to the same core structure in a segregated fashion (as opposed to randomly distributed on the octafunctional core), a good core for this purpose would be the disilanol depicted in Figure 2.1. The core, such as the disilanol in Figure 2.1 will be bi-functionalised in order to study the effect of two distinct groups on the incompletely condensed silsesquioxane. In particular the formation of the chiral nematic phase of this type of material is targeted. The focus of this part of the work is to study materials that contain a chiral group together with mesogenic arms as substituents on the octasilsesquioxane core. The octavinyl octasilsesquioxane disilanol will be used as the starting material to produce Janus LC that exhibit the chiral nematic phase (the chiral group is needed to induce the N* phase). The materials properties will be compared to those of the uniformally substituted system in order to establish the effect of reduced symmetry of the cage and the presence of the chiral group on the mesomorphic behaviour.

Chapter Three:

Synthetic Methods

3.1. Preparation of Silsesquioxane Cyanobiphenyl Derivatives

The synthesis of the open-cage silsesquioxane derivatives was carried out by hydrosilylation of the mesogenic alkene with the appropriate silsesquioxanes carrying silane functional groups. The silanol groups in the commercially available, incompletely condensed silsesquioxanes are difficult to functionalise with mesogenic units. Additionally, in general alkoxysilanes tend to be hydrolytically sensitive. Therefore, the silanol groups were converted to the more versatile silanes by condensation with dimethylchlorosilane in the presence of triethylamine. This reaction proceeds without any rearrangement or further cleavage of the cage, usually observed in presence of stronger bases. Commercially available heptaisobutyl trisilanol POSS and heptaisooctyl trisilanol POSS were capped with dimethychlorosilane to yield the hydridosiloxanes **6** and **7** in good yields (>90%).
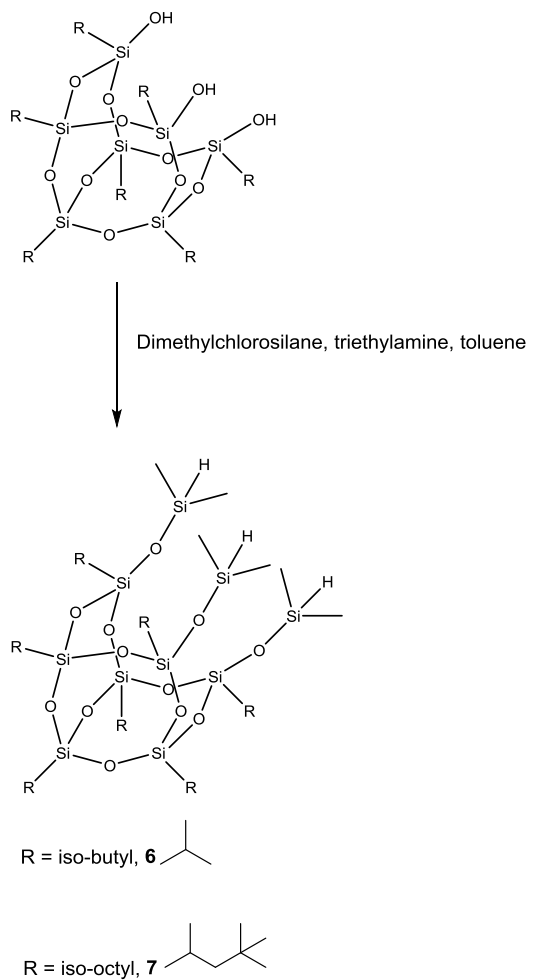
Scheme 1: Synthetic route used to prepare compounds **6** and **7**.

The structure of compounds **6** and **7** were confirmed by ^{1}H and ^{13}C{^{1}H} NMR spectroscopy; especially by the appearance of a septet resonance at 4.70 ppm due to the Si-H group and a doublet at around 0.15 ppm due to the CH$_3$-Si groups. Additionally, MALDI-ToF MS corroborated the molecular mass.

Once the core structures had been synthesised, the mesogens were attached to the core by hydrosilylation of the terminal C=C bond of the corresponding mesogenic alkenes catalysed by Karstedt's catalyst (tris-(divinyltetramethyldisiloxane)-bis-platinum (0), at room temperature. The generally accepted mechanism for the hydrosilylation reaction, using Karstedt's catalyst, is the Chalk-Harrod mechanism.[68]

The hydrosilylation reaction can proceed to yield either the α-addition or the β-addition products, resulting in the linear isomer (major product) or the branched isomer (minor product) respectively. Karstedt's catalyst at room temperature usually yields the linear isomer almost exclusively. The presence of the branched isomer is to be avoided at all costs, since it would be expected to show different liquid crystal properties and it is very difficult to separate from the linear isomer. Another undesired side-reaction is the isomerisation of the alkene to yield an internal olefin that is inactive towards Pt-catalysed hydrosilylation, which can reduce the yield of the reaction dramatically.

In order to ensure that as little as possible of the branched product and isomerised alkene were obtained, the reactions were carried out at room temperature. The catalyst was used until variance in the results was observed, in which case a new catalyst batch was used. Dry, low-sulfur toluene was used for all the hydrosilylation reactions in order to avoid poisoning the catalyst, glass instead of plastic syringes were used to stop contamination from siloxane-based plasticisers and no grease was used on any glassware.

Three families of incompletely condensed POSS were prepared, with iso-butyl, iso-octyl and cyclopentyl substituents on the cage. The first family is based on the cyanobiphenyl core as the behaviour of cyanobiphenyl LC dendrimers, multipedes and polypedes has been described and extensive structure-property correlations exist for CB-based side-chain liquid crystal polymers for comparison. In order to study the effect of increased anisotropy of the mesogens on the LC properties of the POSS derivatives, a cyanobiphenylbenzoate was used in the second family of POSS. As described in the introduction, the topology of the attachment of the mesogen to the core also affects the LC properties to a great extent. Lateral attachment of the mesogens to a scaffold usually results in the formation of the nematic phase. We targeted the nematic phase by introducing a laterally appended phenylenebis(benzoate) derivative. This mesogen was chosen because it has been used extensively to generate the nematic phase in side-chain liquid crystal polymers.[69] In all the cases, the spacer separating the mesogenic core from the POSS cage has been

kept to the same length (*i.e.* pentyl chain) so that the materials properties could be compared. This spacer length is relatively short, but this choice was deliberate since we wanted to allow the POSS core to express its influence on the mesogenic organization. Long spacer lengths usually result in full decoupling of the mesogenic motions from those of the scaffold, masking to some extent, the influence of the core on the mesomorphic behaviour.

The first mesogenic unit used was the cyanobiphenyl based 4'-(pent-4-enyloxy)-[1,1'-biphenyl]-4-carbonitrile. A number of cyanobiphenyl-based octasilsesquioxanes (including dendrimers) are described in the literature and the effect of the scaffold has been discussed.[62-63][70-71] The hydrosilylation of the mesogen with the POSS trisilanes **6-8** yields the corresponding tri-substituted open cage POSS **9**, **10** and **11** in moderate yields (~40%), (Scheme 2). The products were purified by column chromatography and recrystallisation and were characterised by multinuclear NMR spectroscopy, MALDI-ToF MS FT-IR and elemental analysis
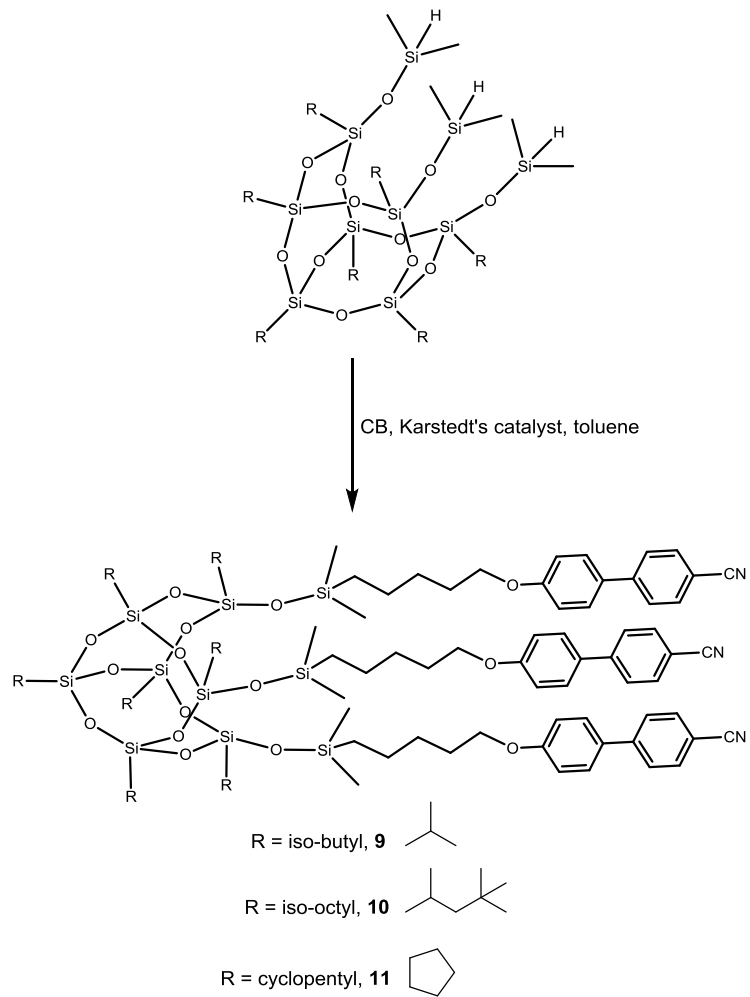
Scheme 2: Synthetic route used to prepare compounds **9**, **10** and **11**.

^{1}H NMR spectroscopy showed the disappearance of the Si-H moiety of the cage and the olefinic protons of the mesogen and the appearance of a new resonance at ~0.5 ppm due to the new CH_2-Si fragment, together with a singlet for the methyl-silicon resonance at ~0.0 ppm. Overall the resonances of the mesogen relative to the R groups on the cage were observed in a ratio of 3:7 respectively, indicating that hydrosilylation of the three arms took place.

However, the most appropriate technique to ascertain the full substitution of the cage is MALDI-ToF MS. This soft ionisation technique proved that the materials are monodisperse showing the molecular envelope, without any fragments due to the partially substituted cage. The MALDI-ToF MS spectrum of

9 is shown in Figure 3.1 together with the molecular envelope, showing the absence of molecular species due to missing mesogen arms on the cage (top) and the expanded molecular ions (bottom).

Meas. m/z	#	Formula	m/z	err [ppm]	err [mDa]	mSigma	Mean err [ppm]
1776.75780	1	C 88 H 135 N 3 Na O 15 Si 10	1776.74781	-5.63	-10.00	56.8	-4.37
1792.75014	1	C 88 H 135 K N 3 O 15 Si 10	1792.72174	-15.84	-28.40	58.3	-11.78

Meas. m/z	#	Formula	m/z	err [ppm]	err [mDa]	mSigma	Mean err [ppm]
1776.75780	1	C 88 H 135 N 3 Na O 15 Si 10	1776.74781	-5.63	-10.00	56.8	-4.37
1792.75014	1	C 88 H 135 K N 3 O 15 Si 10	1792.72174	-15.84	-28.40	58.3	-11.78
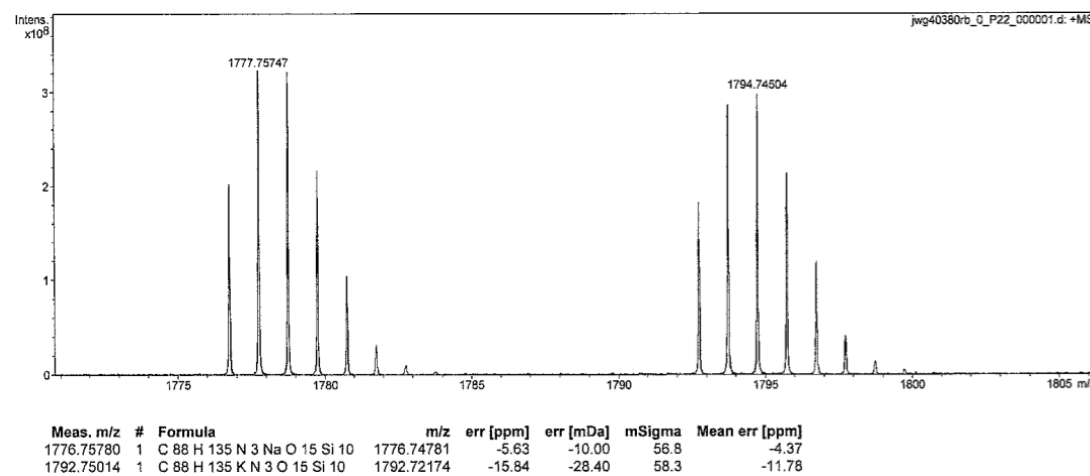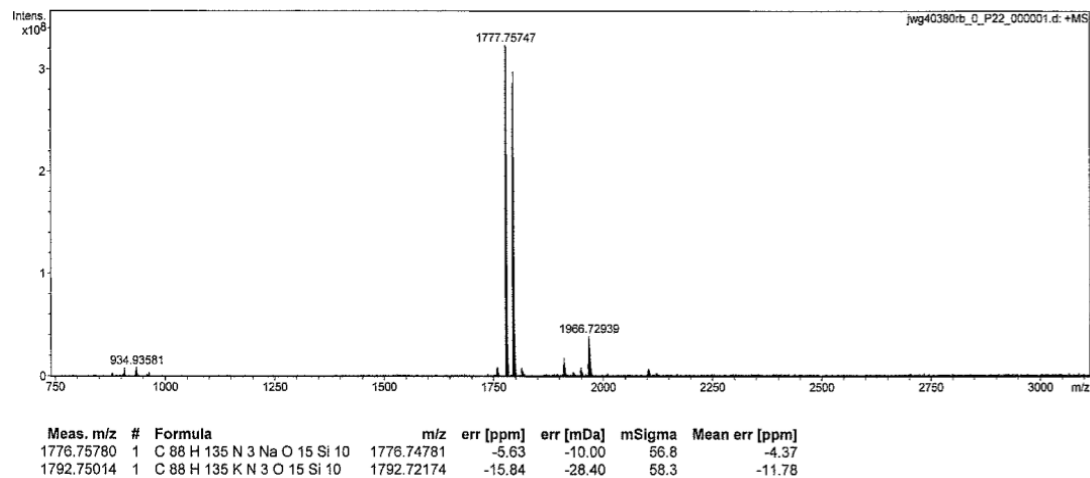
Figure 3.1: Mass Spectrum of compound **9**, showing the [M+Na]$^+$ and [M+K]$^+$ ions (top: full spectrum, bottom: expansion).

As well as ^{1}H NMR spectroscopy and MALDI-MS, these compounds were fully characterized by ^{13}C{^{1}H} NMR, ^{29}Si{^{1}H} NMR spectroscopy, IR and elemental analysis. Occasionally it was observed in some samples that the %C was very slightly lower than the calculated one. This fact has been previously observed in some silsesquioxane derivatives and has been attributed to the large proportion of silicon and oxygen in the sample leading to partial combustion. In all the cases described here a combustion enhancer (V_2O_5) was added to the samples to aid complete combustion.

The symmetry of the cage can be ascertained by ^{29}Si$\{^1$H$\}$ NMR spectroscopy because the various silicon atom environments show distinct resonances. The ^{29}Si$\{^1$H$\}$ NMR spectrum of these species shows three resonances in the T region of the spectrum (-60 ppm to 70 ppm) due to the three SiO$_3$ environments and a singlet at ~9 ppm due to the OSiMe$_2$ groups. However, due to the presence of at least four Si environments, the signals are usually weak and the spectra need long acquisition times.

^{13}C$\{^1$H$\}$ NMR spectroscopy is a more useful technique in this case because it allows the symmetry of the silsesquioxane cage in most cases to be established and it is less costly and quicker to implement than ^{29}Si NMR. Three different types of C$_R$-Si environments are present in these structures according to its C$_{3v}$ symmetry, in a 3:3:1 relative ratio (Figure 3.2).
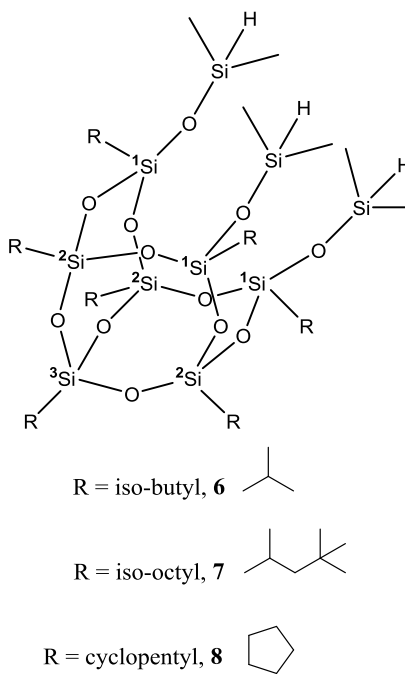
Figure 3.2: An illustration showing the different silicon environments in their 3:3:1 ratio of the three intermediates, compounds **6**, **7**, and **8**.

DEPT ^{13}C NMR was used to determine the phase and chemical shift of the C-Si environments (the first carbon atom of the R substituent, attached to silicon).

Figure 3.3 shows the portion of the DEPT ^{13}CNMR due to the isobutyl chains of compound **6**.
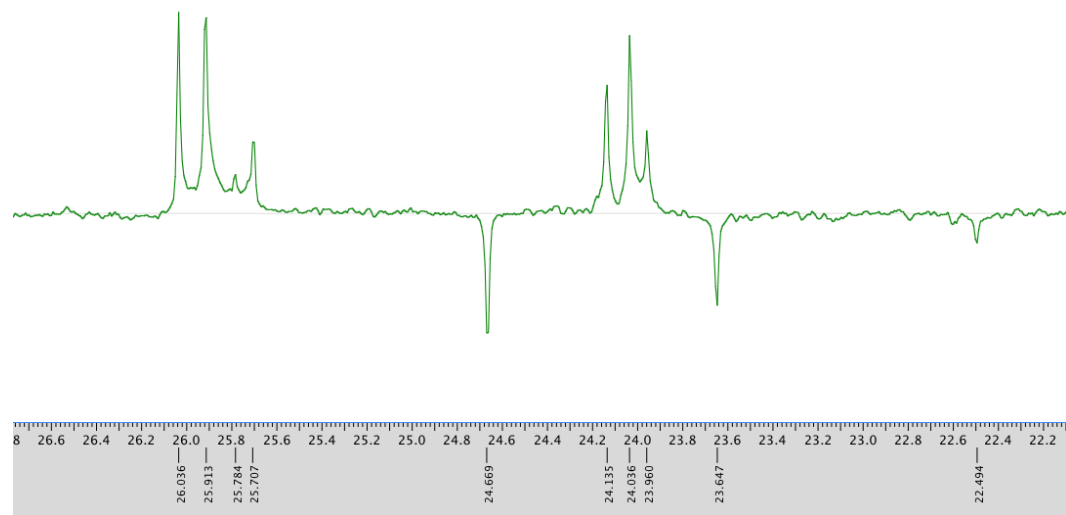
Figure 3.3: DEPT ^{13}C NMR spectrum of the intermediate compound **6**.

It can be seen from Figure 3.3 that the Si-CH$_2$ groups of the iso-butyl group are clearly in a 3:3:1 ratio (in terms of intensity) at 24.66, 23.64 and 22.50 ppm and are opposite in phase to the CH groups at 24.12, 24.02 and 23.95 ppm (also in a 3:3:1 ratio). The CH$_3$ group resonances at 26.03, 25.90 and 25.69 ppm are also clearly visible in a 3:3:1 ratio. Although it is not strictly accurate to determine intensities in ^{13}C NMR due to the different relaxation times of carbon atoms in different environments, at least it gives a fair indication of the relative ratios of the *same* C atom in different molecular environments. This type of pattern, showing the ratio 3:3:1 was also observed for the iso-octyl **7** and cyclopentyl **8**.

3.11. Preparation of Silsesquioxane Cyanobiphenylbenzoate Derivatives

The family comprising the cyanobiphenyl benzoate as mesogenic moiety were prepared through the same hydrosilylation reaction. The flexible spacer is pentyl as in the previous group. Materials **12**, **13** and **14** were prepared according to Scheme 3, and isolated in a similar yield.
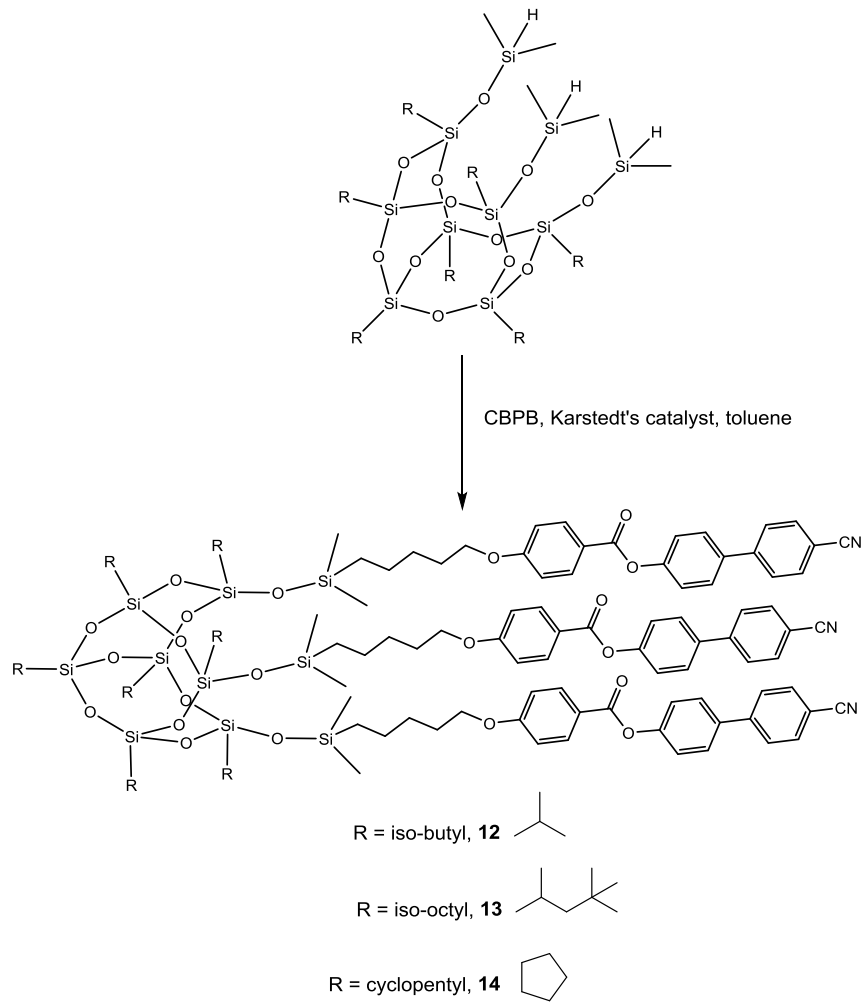
Scheme 3: Synthetic route used to prepare compounds **12**, **13** and **14**

The NMR spectral features are very similar to those for materials **9**, **10** and **11**. Again, MALDI-ToF MS was used to ascertain the monodispersity of the products (Figure 3.4).

Meas. m/z | # | Formula | m/z | err [ppm] | err [mDa] | mSigma | Mean err [ppm]
2136.80502 | 1 | C 109 H 147 N 3 Na O 21 Si 10 | 2136.81120 | 2.89 | 6.18 | 26.8 | 3.67
2152.79644 | 1 | C 109 H 147 K N 3 O 21 Si 10 | 2152.78513 | -5.25 | -11.31 | 26.6 | -2.13

Meas. m/z | # | Formula | m/z | err [ppm] | err [mDa] | mSigma | Mean err [ppm]
2136.80502 | 1 | C 109 H 147 N 3 Na O 21 Si 10 | 2136.81120 | 2.89 | 6.18 | 26.8 | 3.67
2152.79644 | 1 | C 109 H 147 K N 3 O 21 Si 10 | 2152.78513 | -5.25 | -11.31 | 26.6 | -2.13
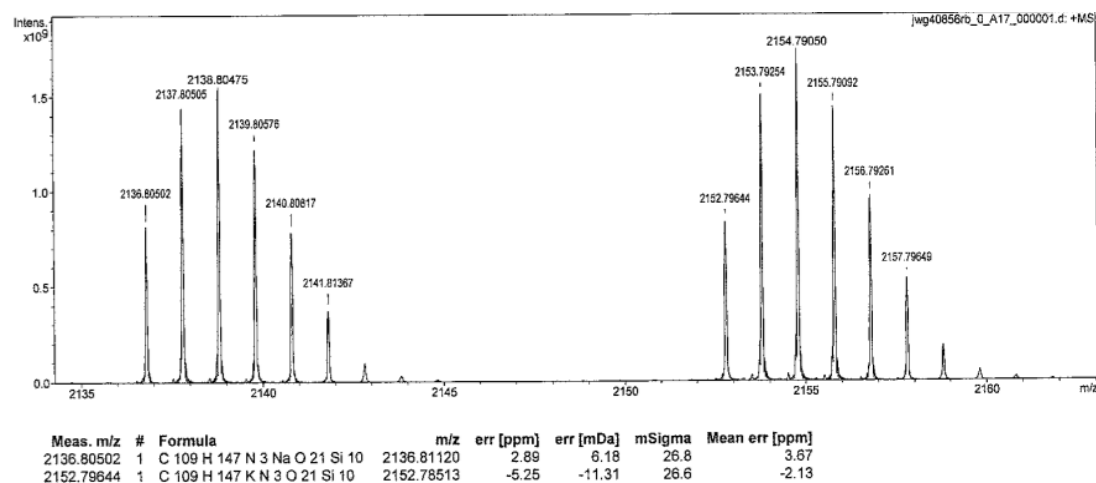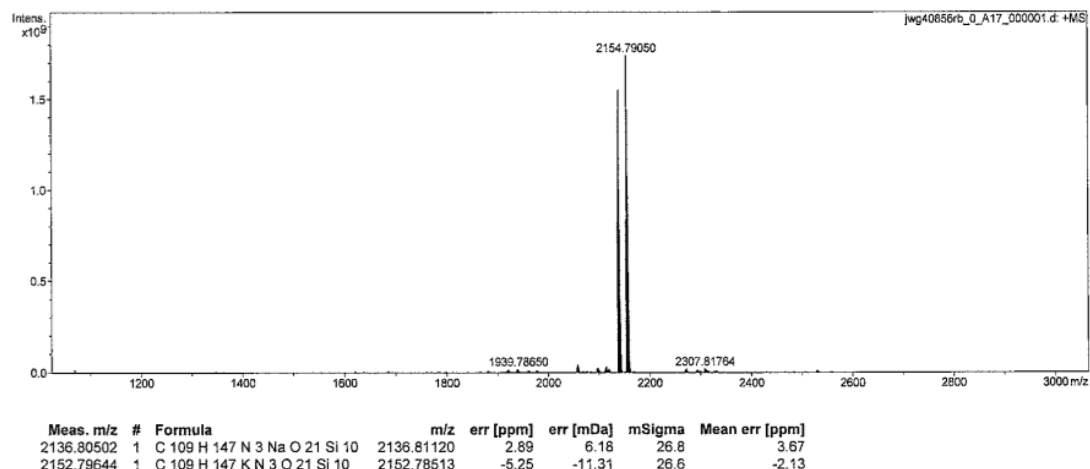
Figure 3.4: Mass Spectrum of compound **12**, showing the [M+Na]⁺ and [M+K]⁺ ions (top: full spectrum, bottom: expansion).

Once we established the requirements to obtain liquid crystallinity in the open cage silsesquioxanes, we endeavour to investigate the number of mesogens needed to achieve it. Therefore, incompletely condensed octasilsesquioxanes containing only two mesogenic arms were prepared. The synthesis of the octaisobutyl octasilsesquioxane disilane, **16**, was carried out by first capping the hydroxyl groups with dimethylchlorosilane, Scheme 4.
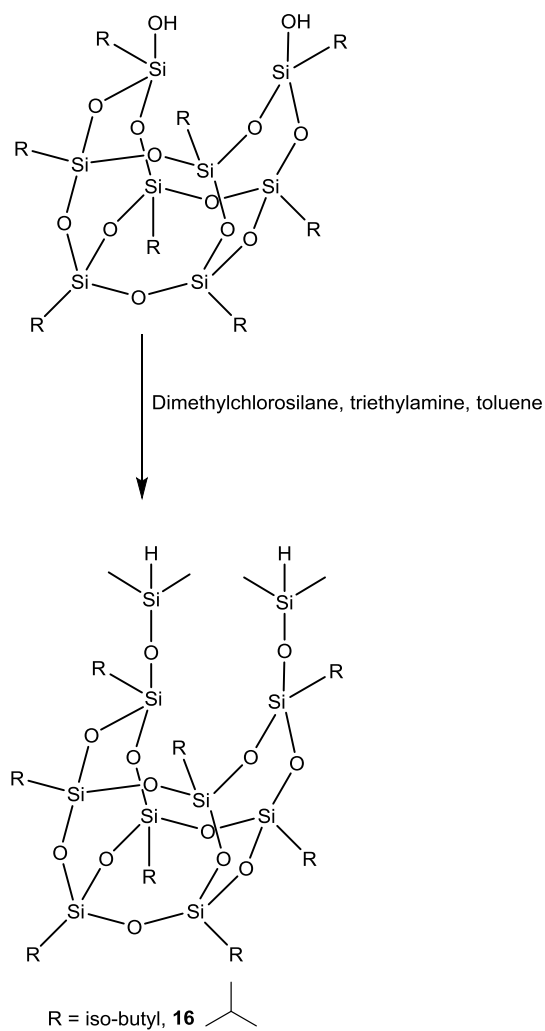
R = iso-butyl, **16**

Scheme 4: Synthetic route used to produce compound **16.**

Compound **16** was reacted with the cyanobiphenylbenzoate mesogen to yield the disubstituted octaisobutyl octasilsesquioxane, **17**, by platinum-catalysed hydrosilylation, as described in Scheme 5.
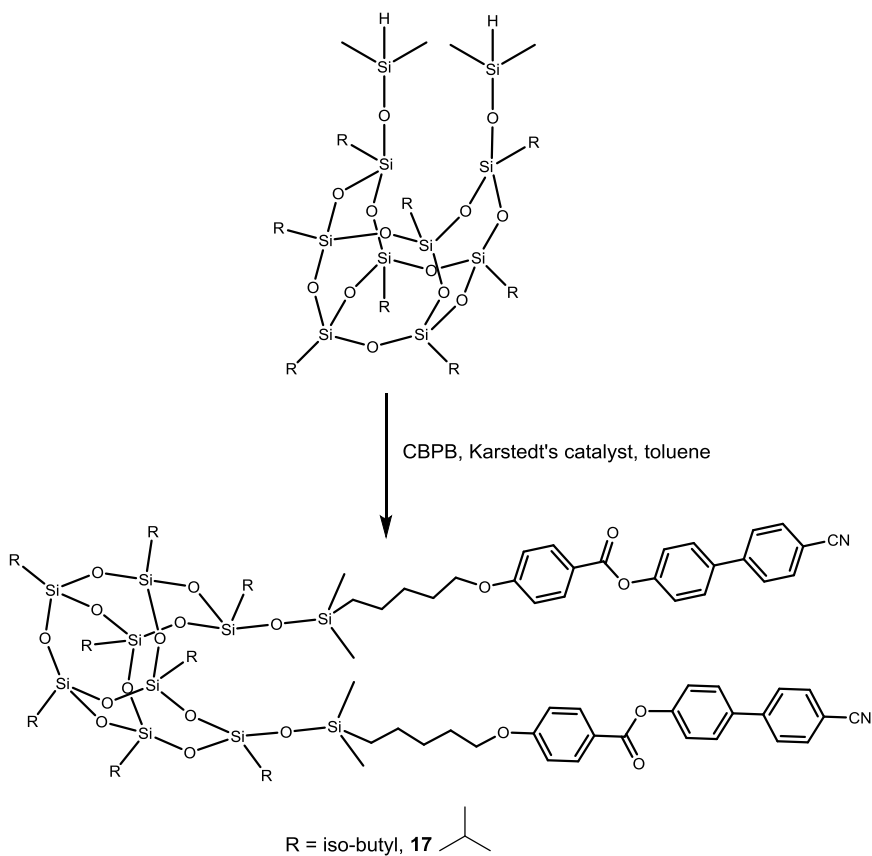
Scheme 5: Synthetic route used to prepare compound **17**.

As well as ^{1}H NMR spectroscopy and MALDI-ToF MS, these compounds were fully characterized by ^{13}C{^{1}H} NMR spectroscopy, ^{29}Si{^{1}H} NMR spectroscopy, IR and were found to be >99% pure by elemental analysis. Compound **17** was obtained in a yield of 40%.

3.12. Preparation of side-on Mesogen Derivatives

It has been found in earlier studies that monomeric octasilsesquioxanes and octasilsesquioxane dendrimers with laterally appended mesogens exhibit nematic mesophases.[23] It was therefore thought that appending a laterally attached mesogen to intermediate compounds **6**, **7** and **16** could produce the nematic mesophase. The mesogen chosen is 4-((pent-4-en-1-yloxy)carbonyl)-1,4-phenylene bis(4-butoxybenzoate), Figure 3.5. This mesogen was chosen

because of its ability to induce the nematic mesophase in side-chain liquid crystalline polysiloxane and polyacrylate polymers.[69]
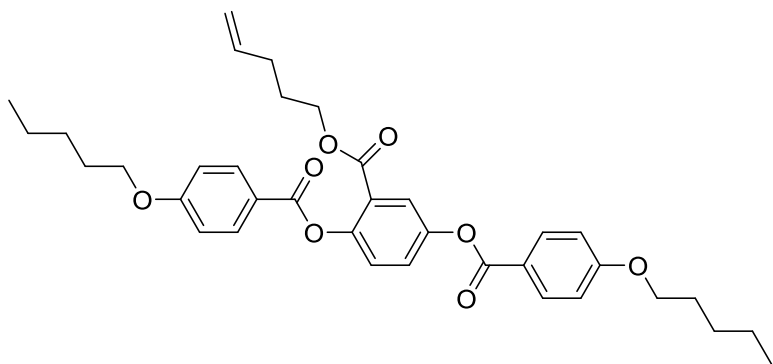
Figure 3.5: The laterally substituted mesogen used to synthesise **18**, **19**, **20** and **22**.

The synthesis of open cage silsesquioxanes with laterally appended mesogens is shown in Scheme 6. The hydrosilylation reaction was used as above to attach the mesogens to the cage, and despite the steric hindrance of the lateral attachment **18** and **19**, with isobutyl and isooctyl chains on the POSS cage respectively, were isolated in similar yields to the terminally substituted analogues. Their spectroscopic characterisation was similar to those described above; in particular MALDI-ToF MS was used to ascertain their monodispersity.
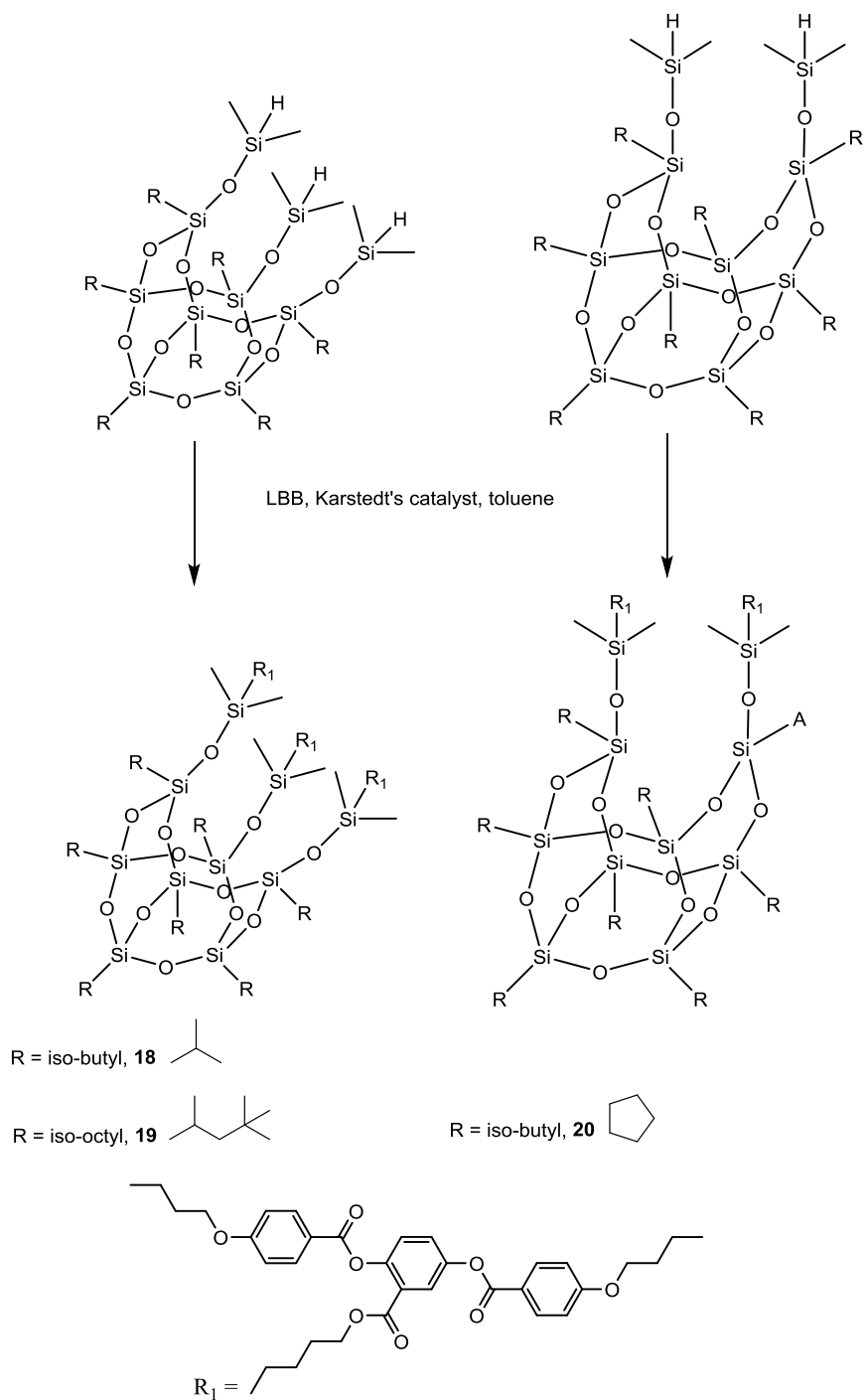
Scheme 6: Synthetic route used to make compound **18**, **19** and **20**.
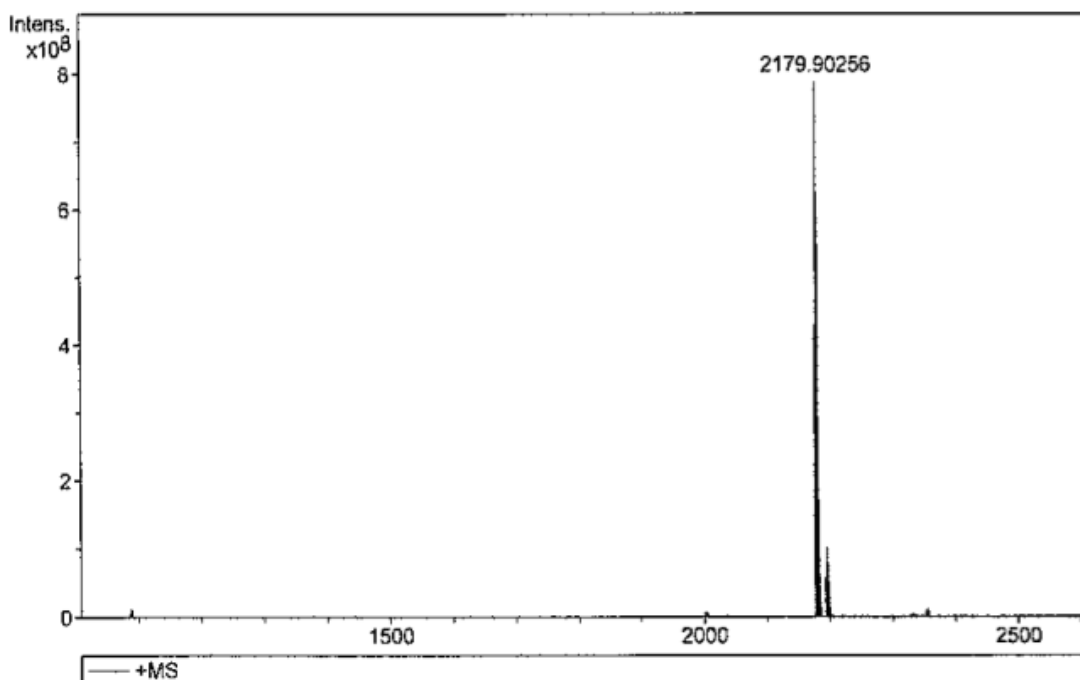
Meas. m/z	#	Formula	m/z	err [ppm]	err [mDa]
2177.90203	1	C 104 H 162 Na O 29 Si 10	2177.87867	-10.73	-23.36
2193.88924	1	C 104 H 162 K O 29 Si 10	2193.85260	-16.70	-36.64

Figure 3.6: Mass spectrum of compound **20**, showing the [M+Na]$^+$ and [M+K]$^+$ ion peak.

As can be seen from Figure 3.6, there are no residual peaks below the molecular peak in the spectrum that is on the contrary to the mass spectra of compounds **18** and **19**. The reason that this reaction has gone to completion and the other two have not is likely due to steric hindrance. The steric bulk of the mesogen, coupled with the steric bulk of the iso-butyl and iso-octyl R-groups on these compounds means it is not favourable to fit three of these mesogens around the silsesquioxane core. However, this steric effect diminishes when only two mesogens are used, hence the reaction to make compound **20** has gone to completion.
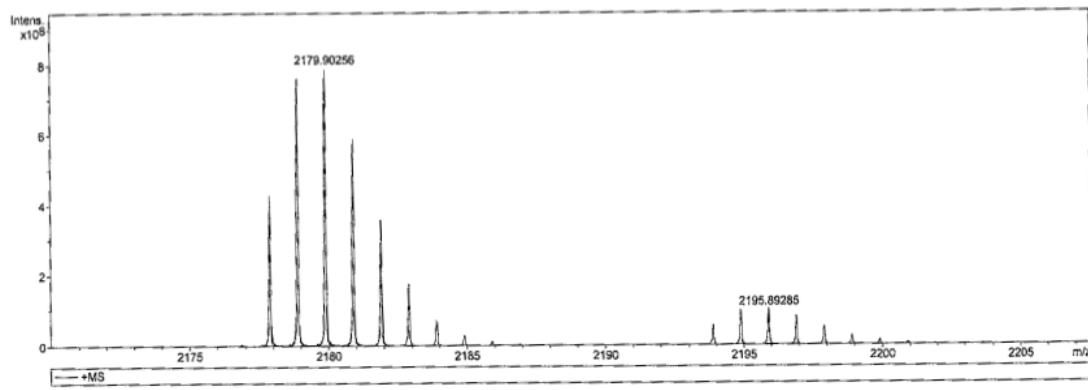
Meas. m/z	#	Formula	m/z	err [ppm]	err [mDa]	mSigma	Mean err [ppm]
2177.90203	1	C 104 H 162 Na O 29 Si 10	2177.87867	-10.73	-23.36	29.7	-10.40
2193.88924	1	C 104 H 162 K O 29 Si 10	2193.85260	-16.70	-36.64	26.9	-16.93

Figure 3.7: Mass spectrum of compund **20**, showing an expanded region of the [M+Na]+ and [M+K]+ ion peaks.

In order to obtain meaningful comparisons, the fully substituted closed cage with eight laterally appended mesogens **22** was also prepared by hydrosilylation of the octahydrido octasilsesquioxane **21** with the laterally substituted mesogenic alkene, Scheme 7. **22** was characterised as above and shown to be monodisperse by MALDI-ToF MS. The NMR spectra of **22** are in full agreement with the structure, showing spectra of simplified features in comparison with those of the incompletely condensed cages.
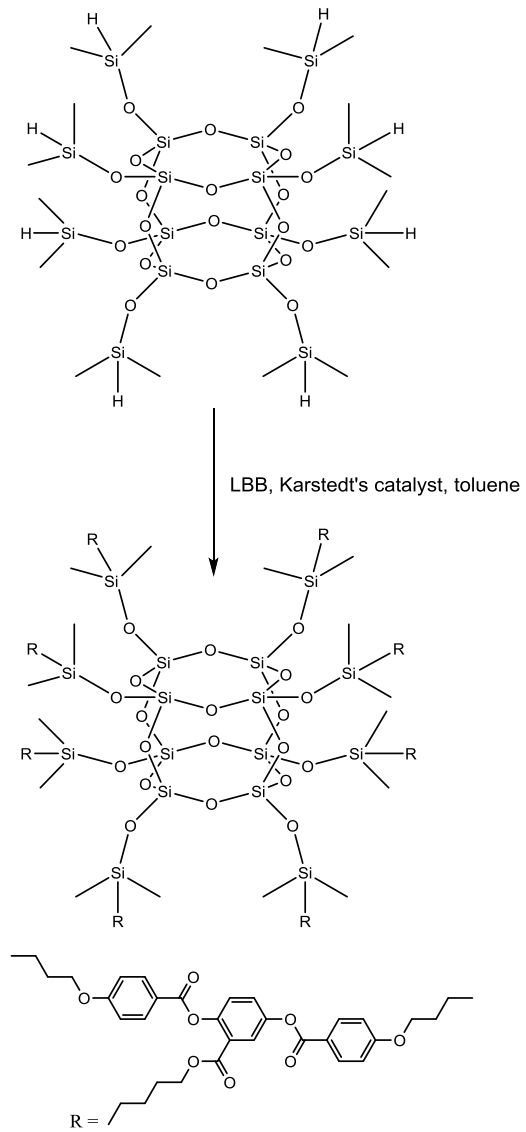
Scheme 7: The synthetic route used to make compound **22**.

3.13. "Janus" Silsesquioxanes

The overall design of the Janus silsesquioxanes is based on the segregated functionalisation of the cage so that two different entities are attached in opposite faces of the cube or at least in a segregated "patch" on the cube. These entities could be two different mesogens or a mesogen and a segregating unit. In this project we describe Janus silsesquioxanes comprising the combination of a mesogenic unit and a non-mesogenic chiral unit anchored on the cage in a segregated fashion.

In order to explore the segregated, or "Janus", functionalisation in this type of material, the precursors described above are not appropriate since the alkyl chains on the cage are unreactive. Therefore, we sought to develop a suitable functionalisation of octavinyl ocatsilsesquioxane, since the vinyl groups are amenable to a range of organic transformations.

There have been reported several methodologies for the synthesis of octavinyloctasilesquioxane in the literature, the most common for cubic silsesquioxanes is the hydrolysis/condensation reaction of a $RSiX_3$ species.[72] The likely reason for the preference for forming the cubic T_8 structure as opposed to the T_{10} and T_{12} is due to the stability of the SiO_4 ring structure and its smaller discrete size. After a number of methods were tried, the variation reported here was chosen due to its better reproducibility and limited by-products. The hydrolysis of vinyltriethoxysilane (VTS) in acetonitrile/water to yield octavinyltriethoxysilane (Scheme 8) reported by Hu was followed.[73]
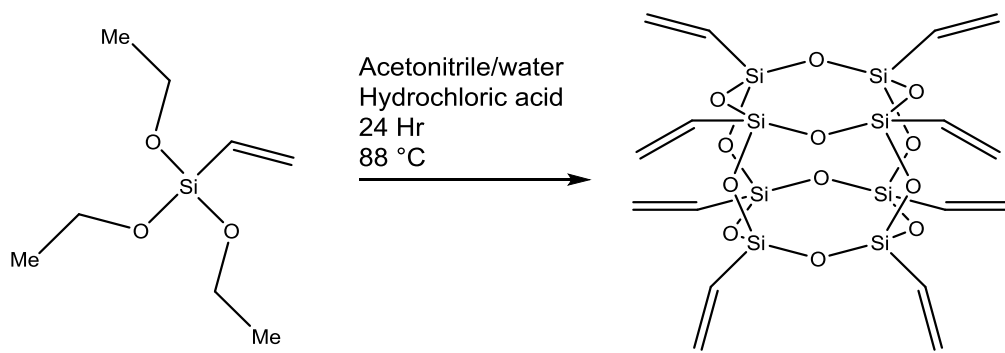
Scheme 8: Synthetic route used to make compound **23**.

The yield obtained, 7.02%, was much lower than that reported by Hu (49%) The hydrolysis reaction produces T_6, T_8, T_{10}, T_{12} and T_{14} cages as well as other various polymers and hydrolysis products with the T_8 cage being the most abundant. ESI-MS was used to characterise the product and confirmed, after purification, pure T_8 octavinylsilsesquioxane had been obtained $^{13}C\{^1H\}$ NMR spectroscopy showed two resonances for the vinyl group, 128.76 ppm for the CH=CH$_2$ carbon and 137.08 ppm for the CH$_2$=CH carbon , Figure 3.8.
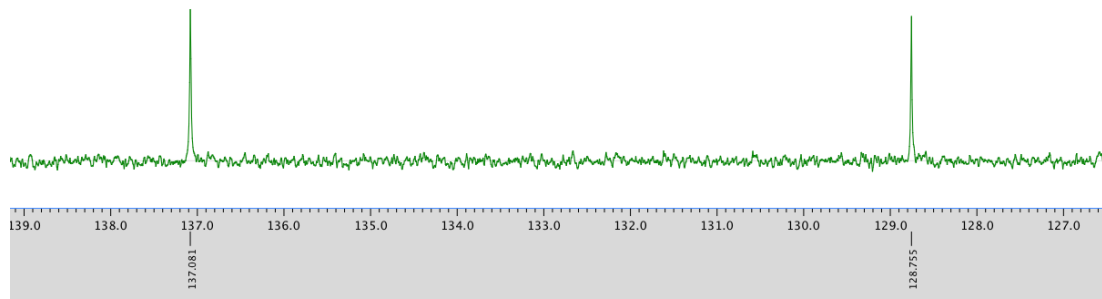
Figure 3.8: ^{13}C{^{1}H} NMR showing the characteristic vinyl peaks of compound **23**.

In an effort to achieve the yield reported by Hu *et al.* the reaction was completed under various conditions, the conditions tried and their respective yields are reported in Table 1.[73]

Table 1: Reaction conditions and yields for the synthesis of **23**.

Reflux Temp/°C	HCl$_{(aq)}$ Added Dropwise	HCl$_{(aq)}$ Added before VTS	Yield/%
80	Yes	No	3.27
84	Yes	No	4.13
88	Yes	No	7.12
88	No	No	5.08
88	No	Yes	4.98

The maximum yield achieved was 7.12%, which was done by adding the hydrochloric acid dropwise over a period of 45 minutes and then refluxing at 88 °C.

The controlled functionalisation of the octavinyl cage is virtually impossible beyond monosubstitution because a range of multifunctionalised materials are produced. Therefore, the introduction of different reactive functional groups is needed. This was achieved by the controlled cage opening by hydrolysis

reactions, to yield an endo-disilanol ocatavinyl POSS. The presence of the silanol and vinyl groups with different reactivites allows the direct functionalisation of the cage.

The base hydrolysis cage opening reaction of a silsesquioxane T_8 cage was first reported by Feher *et al* in 1999.[59] The reaction involves the base hydrolysis of a silicon-oxygen bond along one edge of the silsesquioxane cage using tetraethylammonium hydroxide solution as the base. However, when octavinyl POSS is subjected to hydrolysis under the reaction conditions given, total decomposition occurs.

Schmid reported the controlled hydrolysis of octavinyl POSS to yield the endo-disilanol POSS.[74-75] This is a very sensitive reaction and so is done at -35°C to prevent the hydrolysis of more than one silicon-oxygen bond of the cage. Nevertheless it also forms, among other things the tetrasilanol as a by-product (Scheme 9). However, even under this conditions, the cage opening was unsuccessful. Reiss and Saez have reported the successful cage opening by hydrolysis of octavinyl POSS with tetraethylammonium hydroxide, based on a modification of Schmid's method.[76]. Compound **25** was obtained in a yield of 78% (Scheme 9).
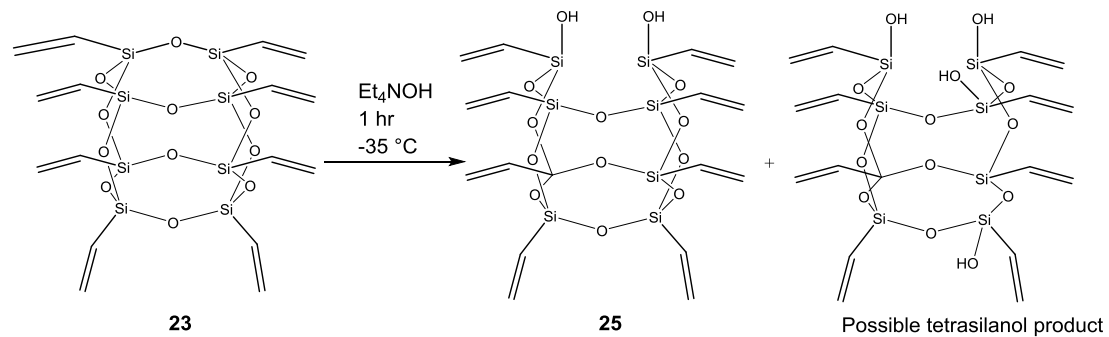
Scheme 9: Synthetic route to compound **25**.

The confirmation of the structure and its symmetry is accopmplished by $^{13}C\{^1H\}$ NMR spectroscopy, which shows two sets of three resonances in the olefinic carbon region, corresponding to CH and CH_2. Each set of resonances consist of three signals in a 2:4:2 ratio, confirming the C_{2v} symmetry of the cage, Figure 3.9.
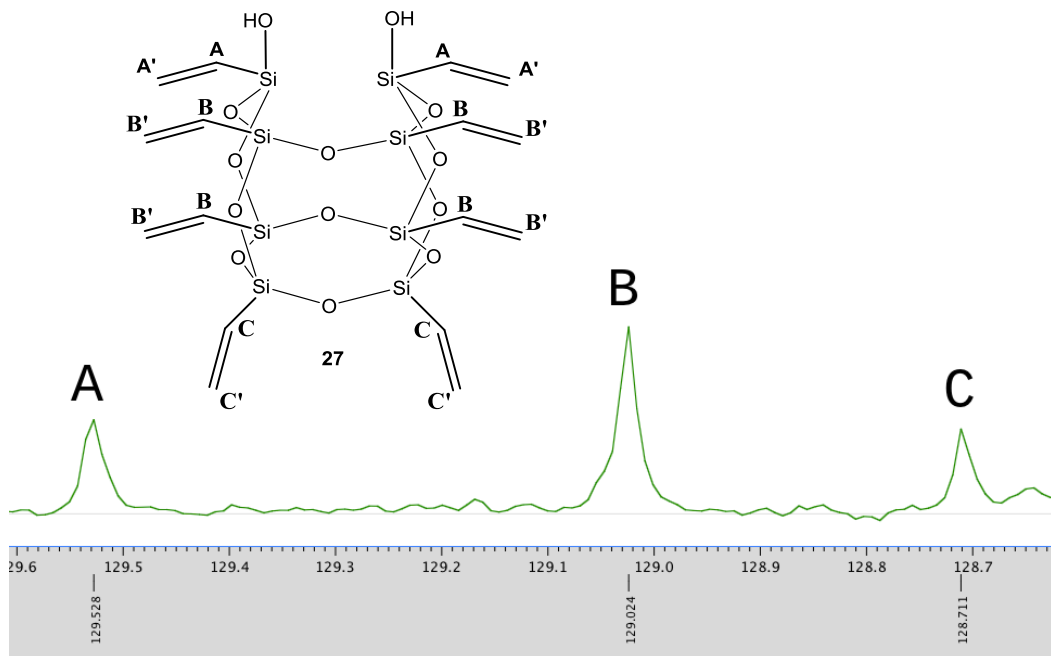
Figure 3.9: $^{13}C\{^1H\}$ NMR spectrum showing the three different environments in compound **25**.

The symmetry ideally can be determined by ^{29}Si NMR, however the long acquisition times needed makes ^{13}C NMR a lot more convenient technique.

The formation of the desired product is confirmed by MALDI-MS

63

Meas. m/z	#	Formula	m/z	err [ppm]	err [mDa]	mSigma	Mean err [ppm]
672.9403	1	C 16 H 26 Na O 13 Si 8	672.9420	2.4	1.6	92.3	1.3
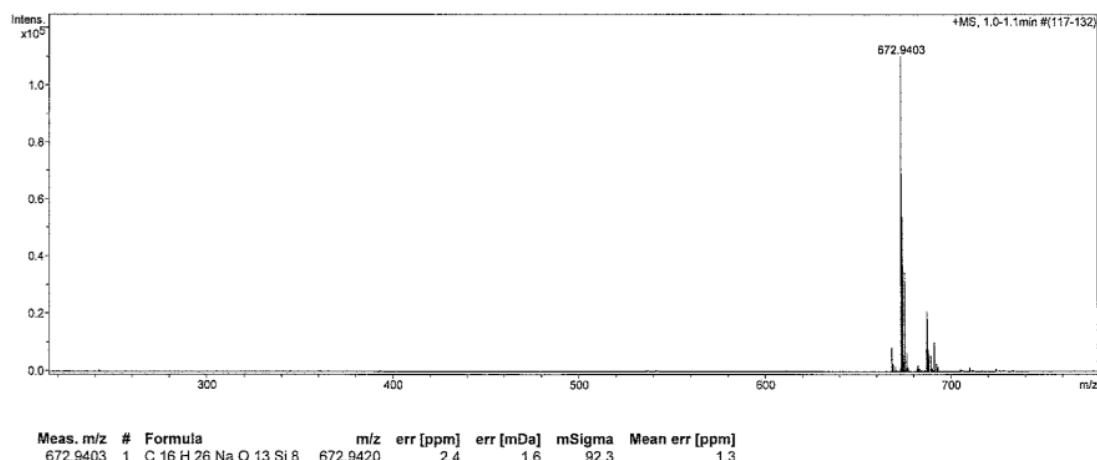
Figure 3.10: Mass spectrum of compound **25**, showing the peak at 672.94 Daltons for the [M+Na]$^+$ ion peak.

In order to test the interplay between a non-mesogenic chiral moiety and a mesogen both attached to the same core, a non-mesogenic chiral compound first had to be made. The silanol groups were capped with a chiral chlorosilane, in a reaction parallel to that described above for the introduction of the silane group.

The chiral non-mesogenic chlorosilane **26** was prepared by hydrosilylation of *(S)*-2-methylbutyl-but-3-enoate, **24**, with dimethylchlorosilane and was used in situ in the following step, Scheme 10.

a...dimethylchlorosilane, toluene, Karstedt's castalyst
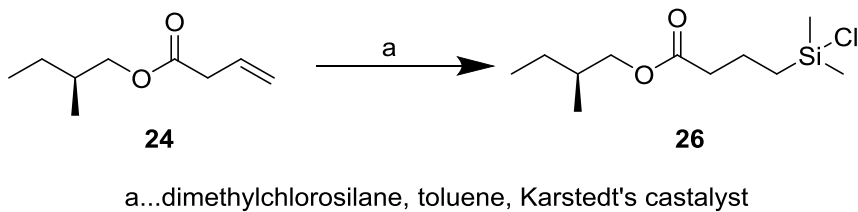
Scheme 10: Synthetic route used to make chlorosilane, compound **26**.

The condensation of **26** with the disilanol **25** in presence of triethylamine yields the endo-disubstituted octavinyl POSS **27** in a moderate yield, Scheme 11. **27** was characterized by a number of techniques, as described above for related materials.
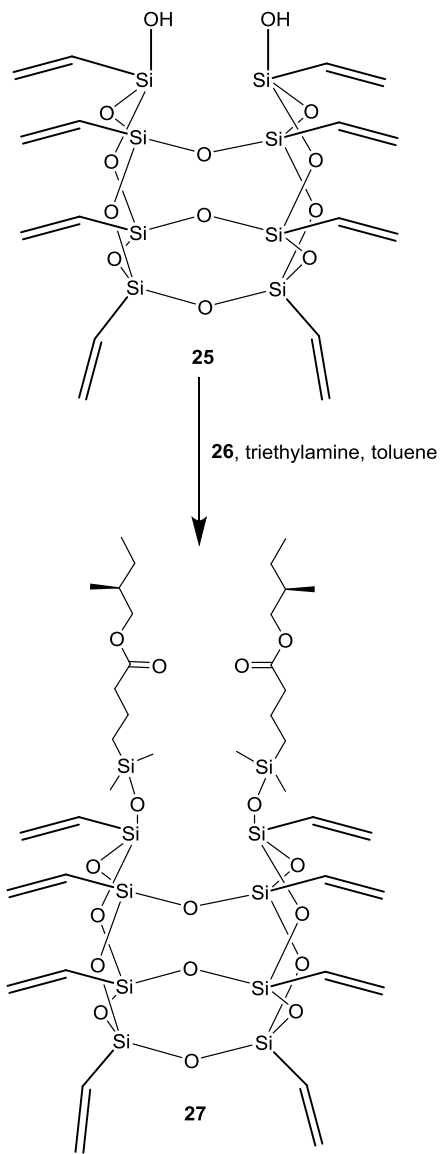
Scheme 11: Synthetic route used to make compound **27**.

The structure was confirmed by both ^{1}H NMR spectroscopy and MALDI-MS.

The most useful structural information was gleaned from the ^{13}C{^{1}H} NMR spectrum, which showed unequivocally the different vinyl resonances relative to their positions in the cube in a 2:4:2 ratio. The different environments of the vinyl resonances and the ^{13}C{^{1}H} NMR, showing the 2:4:2 ratio are shown in Figure 3.11 and the ^{13}C{^{1}H} NMR spectrum of the vinylic region in Figure 3.12 respectively.
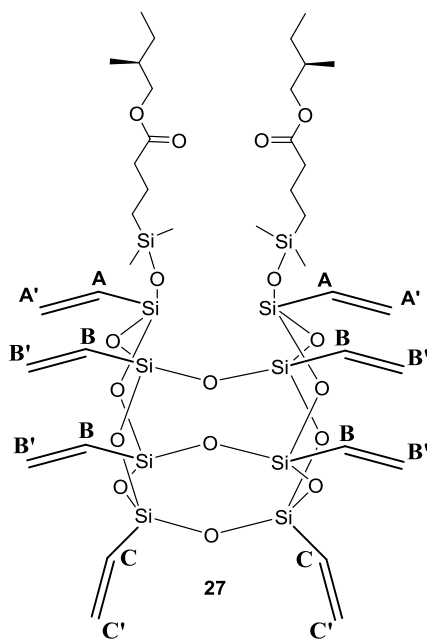
Figure 3.11: Vinyl environments of compound **27**.

As can be seen from Figure 3.11 and 3.12, the CH_2 resonances of the vinyl group appear higher in chemical shift than the CH resonances appearing at (A') 136.88 ppm, (B') 136.42 ppm and (C') 135.15 ppm respectively and can be clearly seen in a 2:4:2 ratio in terms of intensity. The CH resonances appear lower down in the spectrum at (A) 131.82, (B) 129.76 and (C) 128.84 ppm and are also clearly visible in a 2:4:2 configuration in regards to intensity. Compound **27** was obtained in a yield of 37%.
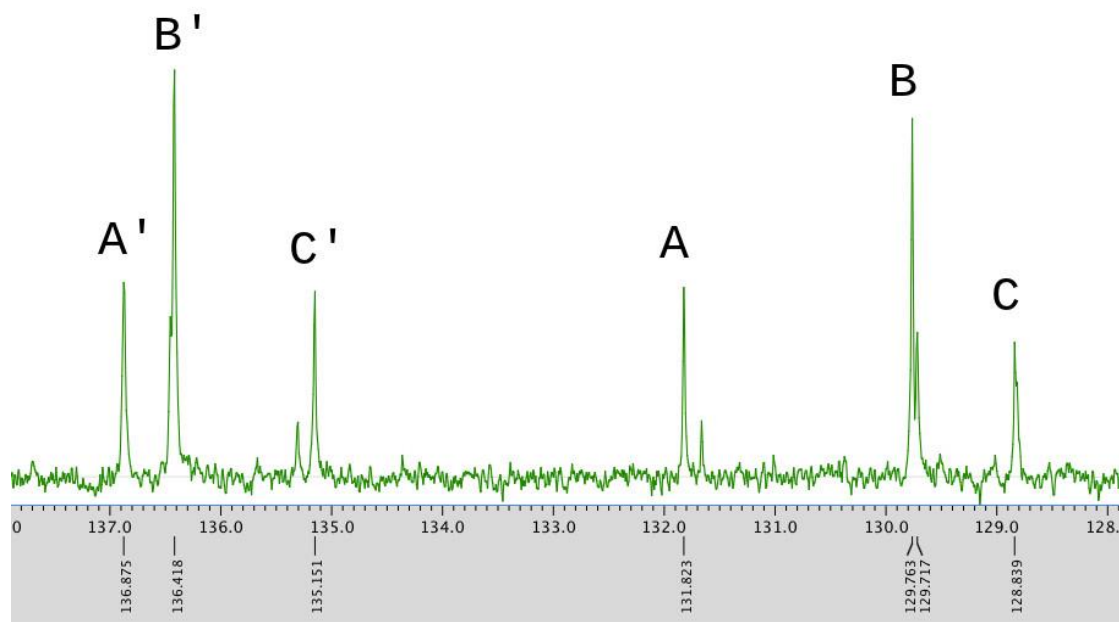
Figure 3.12: $^{13}C\{^1H\}$ NMR of compound **27** showing the vinyl resonances of the CH and CH$_2$ groups in a 2:4:2 ratio.

Once the silanol groups had been capped, the vinyl groups on the cage could be modified by hydrosilylation to attach the appropriate mesogen. In this case a mesogen with a Si-H functional group is needed. The cyanobiphenyl-based tetramethyldisiloxane CBDS (Figure 3.13) was used to finally produce the Janus silsesquioxane **28**, which has two chiral groups positioned next to each other on one side of the cube and eight cyanobiphenyl mesogens on the corners, Scheme 12.
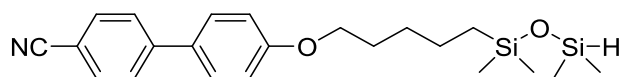
Figure 3.13: CBDS mesogen used to make compound **28**.
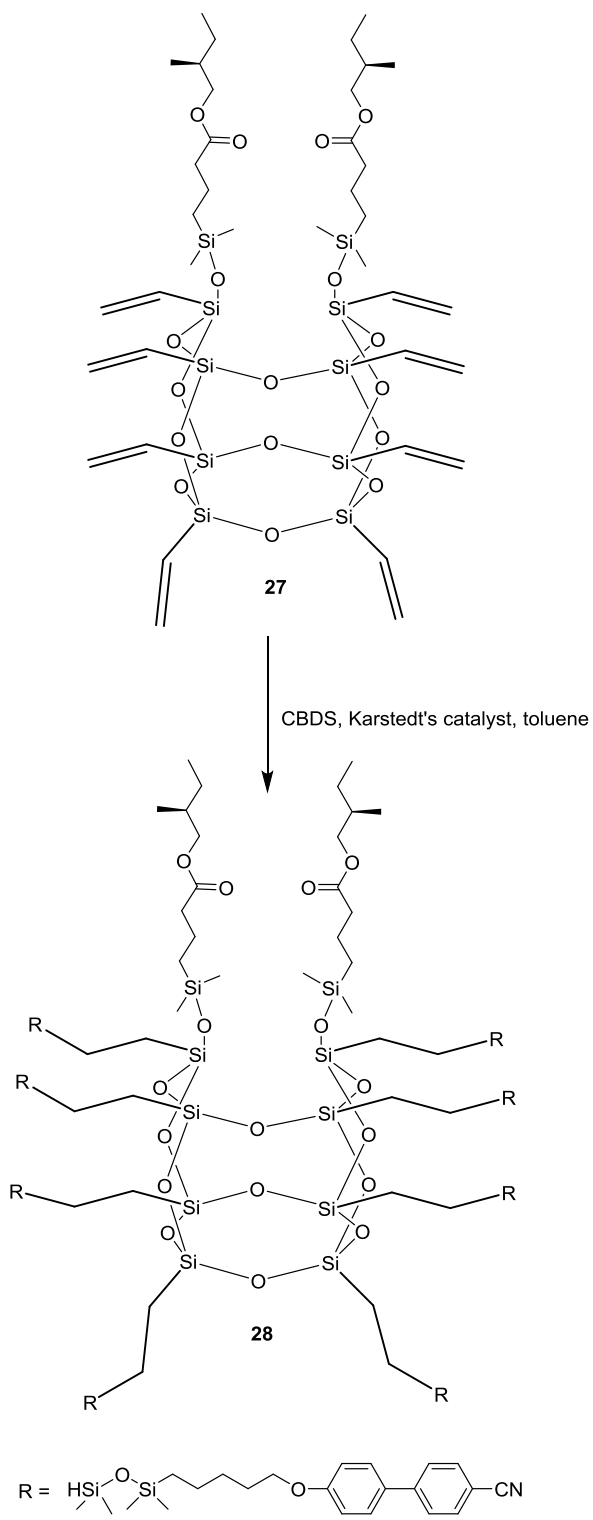
Scheme 12: Synthetic route used to prepare compound **28**.

28 was characterised by ^{1}H and ^{13}C{^{1}H} NMR spectroscopy and its purity established by elemental anaylsis, showing the correct structure. However,

MALDI-ToF MS could not be obtained so far. ^{1}H NMR showed the presence of all the different fragments of the molecule, especially the chiral arms, the cyanobiphenyl aromatic protons and the CH_2-Si resonaces in different environments in the molecule in the right ratio. After the structure was confirmed by ^{1}H NMR, it was further verified by ^{13}C NMR, IR and was found to be >99% pure by elemental analysis. Compound **28** was obtained in a yield of 59%.

Chapter Four:

Structure-property Relationships

4.1. Cyanobiphenyl derivatives

The incompletely condensed silsesquioxanes with three cyanobiphenyl mesogens (compounds **9**, **10** and **11**) were studied by differential scanning calorimetry (DSC) and polarized light optical microscopy (POM). The thermal behaviour of these compounds is shown in Table 1.
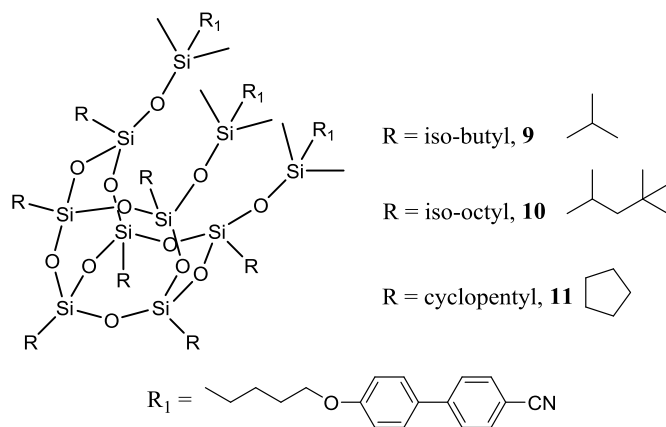
Table 1. Transition temperatures (°C) and enthalpies of transition (kJ mol^{-1}) for compounds **9**-**11**; **9** R = iso-butyl, **10** R = iso-octyl, **11** R = cyclopentyl. All temperatures and enthalpies determined by DSC except the SmA-Iso.Liq. transition of compound **10** which was determined by polarized optical microscopy.

No										Transition Temperatures /°C			
	Cr		Cr		Cr		Cr		SmA		Iso		
9	•	39.7 [9.2]	•	44.6 [10.9]	•	85.9 [9.9]	•	87.5 [7.2]			•		
10	•	-6.3 [0.9]	•	1.9 [0.5]					•	25.2 [N/A]	•		
11	•	7.9 [12.4]	•	69.3 [12.7]	•	82.0 [22.2]					•		

Compounds **9** (ᶦBut) and **11** (Cp) were found to be non-mesomorphic, although several crystal-crystal transitions were detected. The crystalline nature of the materials was corroborated by POM, Figure 4.1.
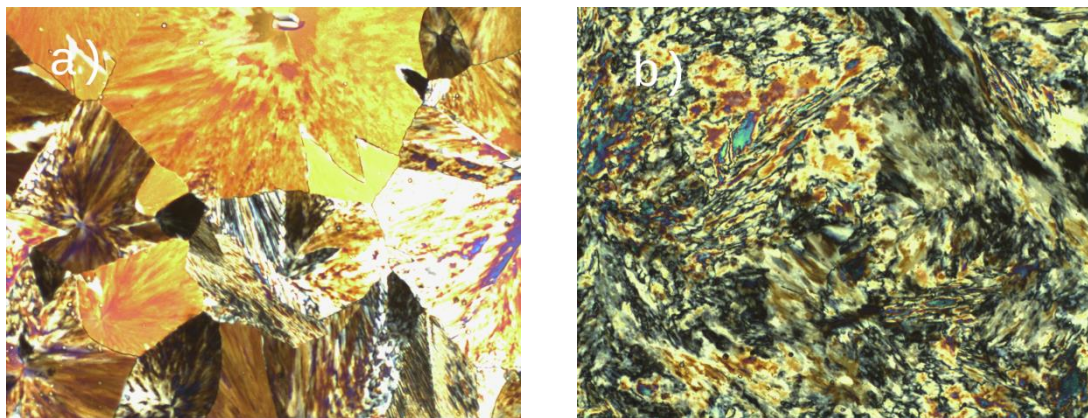
Figure 4.1: Photomicrographs (x200) of compound **9**; showing (a) the texture of the crystal at 85 °C and (b) the texture of the crystal-crystal at 50 °C.

Conversely, compound **10** (R = iso-octyl) did exhibit liquid-crystalline behaviour. The DSC of compound 10 is shown in Figure 4.2.
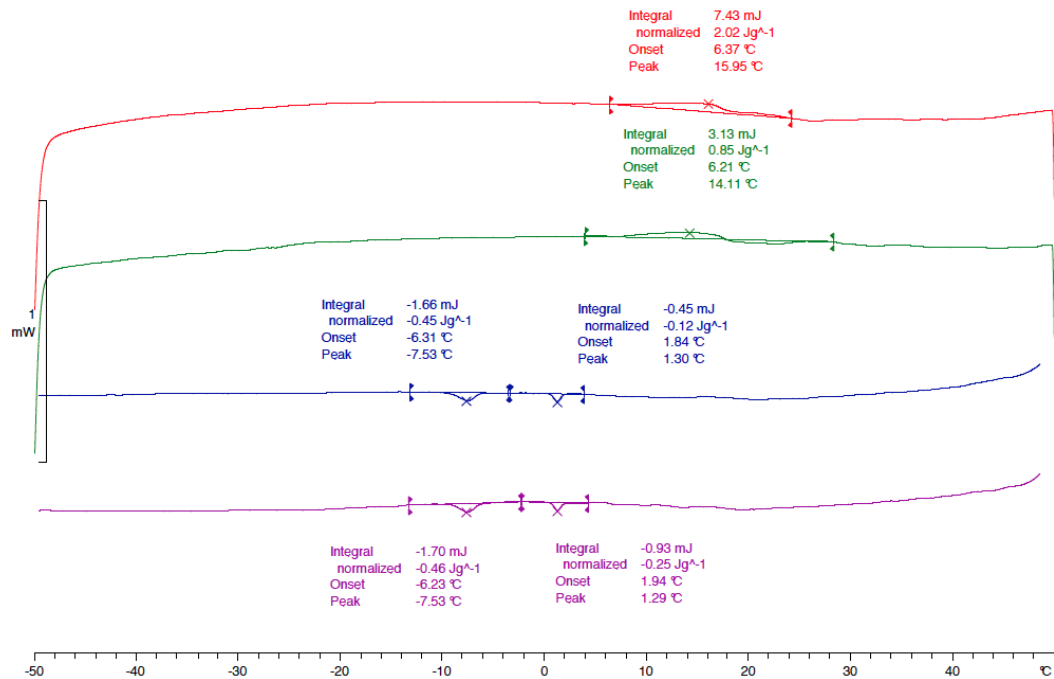
Figure 4.2: DSC thermogram of compound **10**.

The temperature of the SmA-Iso liq transition quoted in Table 1 of 25.2 °C was recorded by POM on cooling of the isotropic liquid. This transition cannot be seen in the DSC trace, indicating that the transition is very broad at a scan rate

of 10 °C per minute. However, the mesophase texture was observed by POM, although it proved difficult to obtain a well-developed defect texture due to the viscosity of the sample. The phase was identified as the SmA phase due to the presence of optically extinct homeotropic regions alongside a grainy fan-like texture, Figure 4.3.

Comparison of **10** with the fully condensed octasilsesquioxane functionalised with eight CB moieties (g 3.0 S_1 22.5 SmA 116.5 Iso Liq), Fig 1.31 in the introduction) shows that there is a dramatic decrease in mesophase stability when only three of the eight substituents are CB mesogens. This is expected, as there is a significant loss of anisotropy due to the non-mesogenic branched iso-butyl chains. At the same time, there is also a significant decrease in crystal stability if we compare compounds **9, 10, 11** with their respective symmetrical octaalkylsilsesquioxanes, in particular in relation to octacyclopentyl octasilsesquioxane (which does not melt but decomposes on heating at 343°C). Overall, this trend agrees with the idea that a reduction in the symmetry of the systems increases disorder and causes a marked drop in transition temperatures.

The difference in properties between compound **10** and compounds **9** and **11** can be rationalized *via* consideration of the steric bulk of the different R groups of the three materials. The iso-octyl group is more sterically demanding in comparison to the short R groups of compounds **9** and **11**. Thus, because of this increased steric bulk compound **10** has a far lower melting point than compounds **9** and **11** and, consequently, exhibits an enantiotropic smectic A phase.
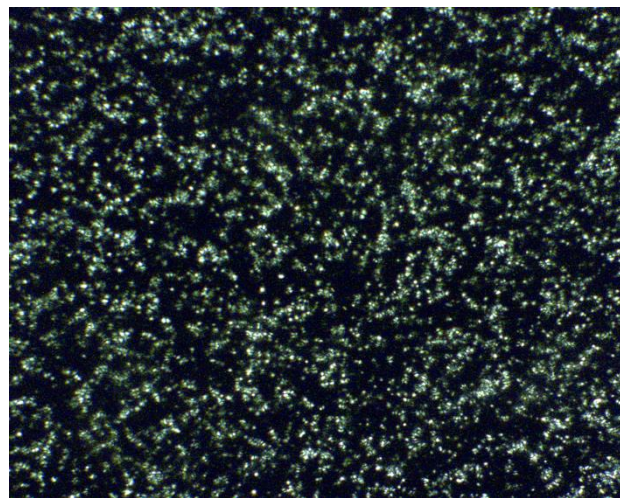
Figure 4.3: Photomicrograph (x200) of the SmA phase of compound **10** taken at 25 °C.

4.2. Single Crystal X-ray Diffraction

Single crystals of **9** of sufficient quality for X-ray structure determination were obtained by crystallisation from dichloromethane/ethanol. It is relatively unusual to obtain large single crystal of mesomorphic materials. Although there have been many reports in the literature of crystal structures of polyhedral oligomeric silsesquioxanes, these have centred almost exclusively around fully condensed silsesquioxane structures[60][77-78] and certainly there are no X-ray crystal structure determinations reported for any LC polyhedral silsesquioxanes. Herein we describe the single crystal X-ray structure of an incompletely condensed silsesquioxane, Figure 4.4. The main crystallographic parameters are collected in Table 2.
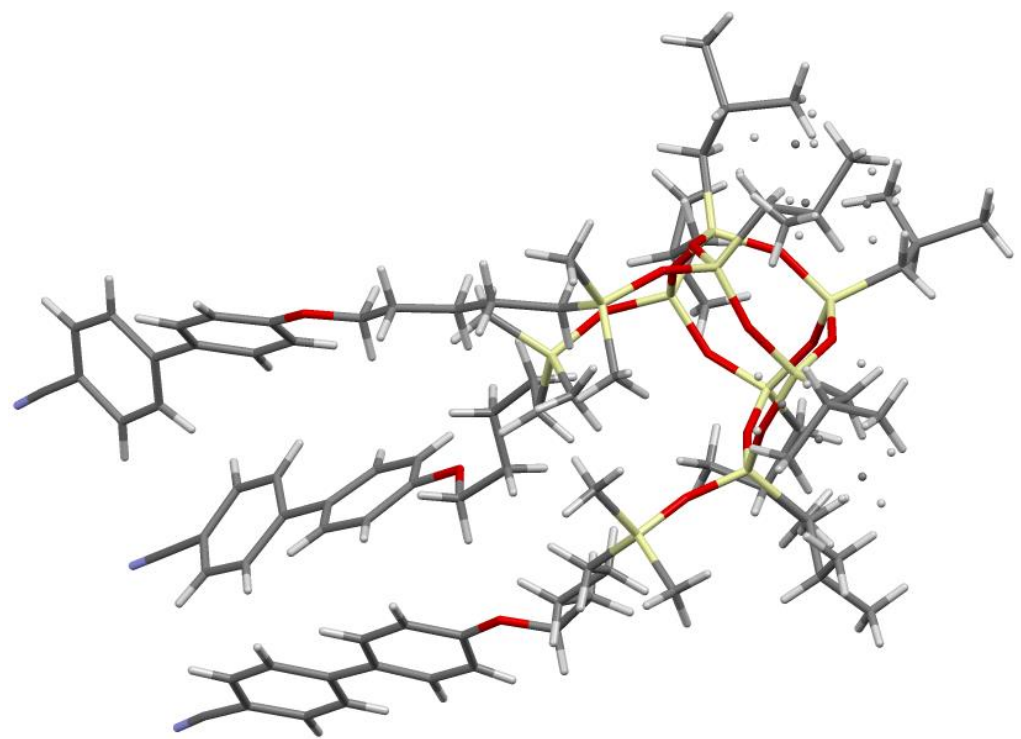
Figure 4.4: X-ray crystal structure of compound **9**

Table 2. Crystallographic data for compound **9**.

Parameter	Result
Empirical formula	$C_{88}H_{135}N_3O_{15}Si_{10}$
Formula weight	1755.89
Temperature/K	109.9(2)
Crystal system	triclinic
Space group	P-1
a/Å	13.4216(17)
b/Å	14.3443(20)
c/Å	28.982(4)
α/°	94.715(11)
β/°	91.342(11)
γ/°	117.528(13)
Volume/Å^3	4919.3(12)
Z	2
ρ_{calc}mg/mm^3	1.185
m/mm^{-1}	0.193
$F(000)$	1888.0
Crystal size/mm^3	0.4782 × 0.265 × 0.0406
2Θ range for data collection	6 to 41.64°
Index ranges	-13 ≤ h ≤ 10, -13 ≤ k ≤ 14, -28 ≤ l ≤ 28
Reflections collected	18848
Independent reflections	10244[R(int) = 0.0529]
Data/restraints/parameters	10244/146/1107
Goodness-of-fit on F^2	1.027
Final R indexes [I>=2σ (I)]	R_1 = 0.1652, wR_2 = 0.3613
Final R indexes [all data]	R_1 = 0.2359, wR_2 = 0.4166
Largest diff. peak/hole / e Å^{-3}	0.71/-0.33

The unit cell is triclinic and the space group is P-1. This has been found to be a common space group among silsesquioxanes as shown by Aziz *et al*.[60] The reported cell dimensions are a = 13.4216 Å, b = 14.3443 Å and c = 28.982 Å and the number of molecules per unit cell is 2; the unit cell lengths give the unit cell

a 2:1 aspect ratio with regards to length and breadth. The data quality for this crystal structure is poor due to packing disorder of the isobutyl groups, resulting in poor quality factors and a large ADP. Two of the iso-butyl groups were disordered with the iso-propyl portion modelled in two positions of equal occupancy, namely C7-C9 and C-26-C28. The ADP of many of the iso-butyl group carbons were restrained to be approximately isotropic. Similarly, the 1-2 and 1-3 C-C distances were restrained to be 1.52 and 2.48Å, respectively, in many of the iso-butyl groups.
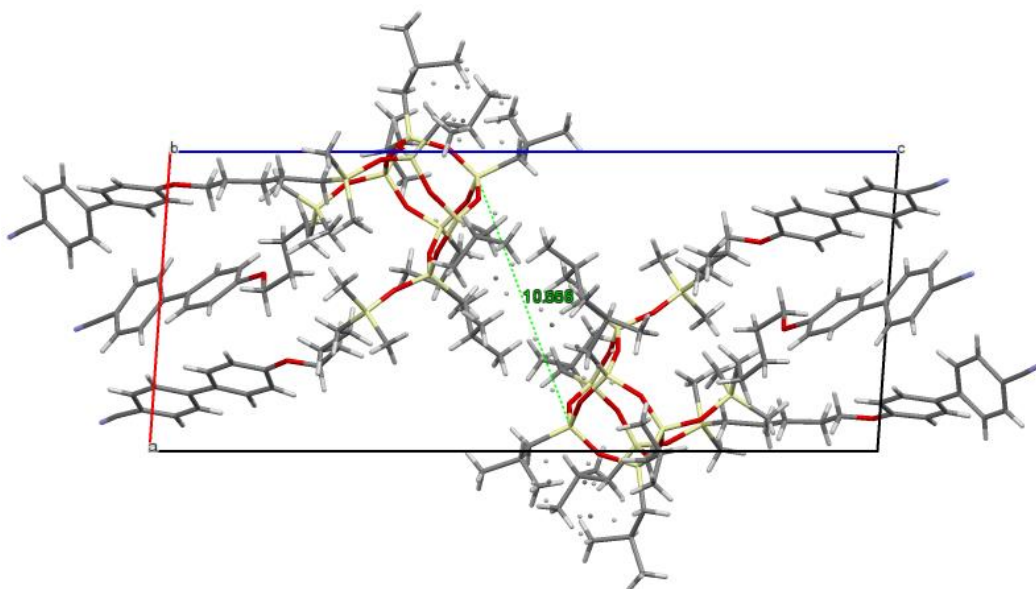
Figure 4.5: The packing of two molecules of compound **9** in the unit cell along the *b*-axis.

The unit cell consists of two molecules with the cage end of the molecules packing together, Figure 4.5. It has been demonstrated by Aziz *et al.* that alkyl-substituted polyhedral oligomeric silsesquioxanes (POSS) typically adopt a rod-like molecular shape and pack in a lamellar arrangement in the crystal even when they are not mesogenic, *i.e.* in a similar way to how calamitic mesogens pack together in a smectic liquid-crystalline phase.[60]
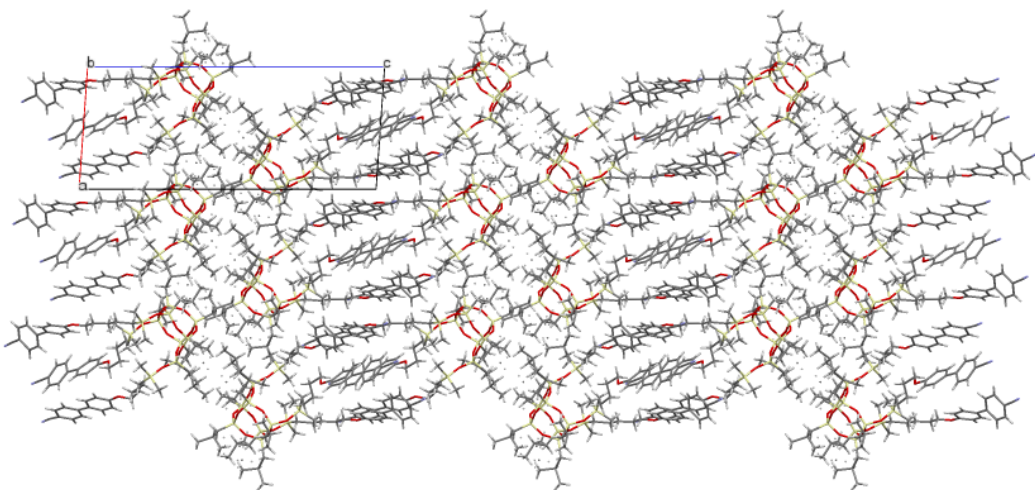
Figure 4.6: Crystal structure showing the packing of the molecules along the *b*-axis.

The molecular packing of **9** in the crystal consists of molecules packed together in layers, with the silsesquioxane cores packed together and segregated from the cyanobiphenyl moieties, which interdigitate and pack side by side in a lamellar-type arrangement. The molecules possess a slight tilt with respect to the layer normal, Figure 4.6. The smallest distance between the cage-centre of one molecule to the cage-centre of the next molecule is 10.588 Å and is labelled in Figure 4.7. Interestingly, this is slightly longer than the reported distance of 9.595 Å by Bassindale in a completely condensed closed silsesquioxane cage substituted with eight butyl chains, suggesting that the cyanobiphenyl groups push the incompletely condensed cage slightly apart in comparison with the completely condensed silsesquioxanes.
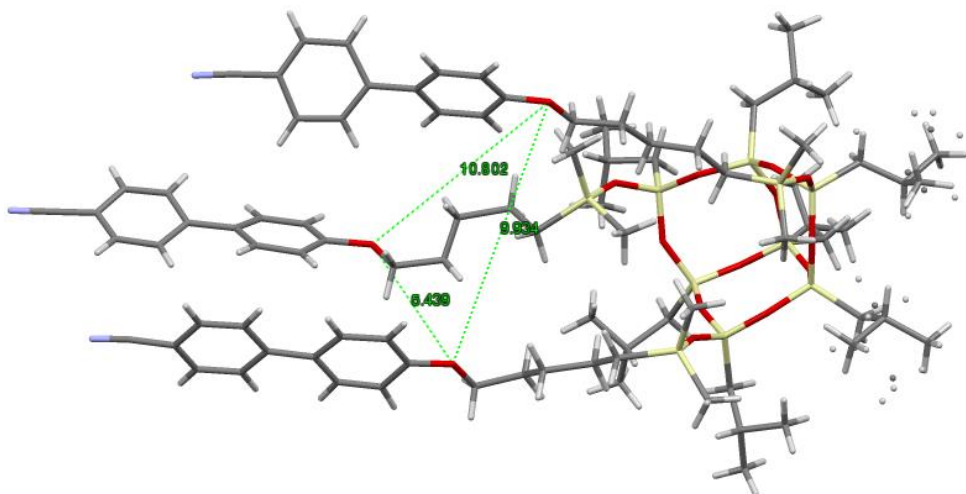
Figure 4.7: X-ray structure of compound **9**, showing the distances between the three alkyl chains on each mesogen.

The three distances between each alkyl chain on each mesogen are 10.802, 9.934 and 5.439 Å respectively, Figure 4.7. Interestingly these arms interdigitate in the unit cell with the Iso-butyl groups packing together and the cyanobiphenyl arms interdigitating. This result is interesting as it is reminiscent of the antiparallel interactions between cyanobiphenyl cores observed in liquid crystal mesophases. The results differ from those of Aziz *et al*, who found that the alkyl chains in alkyl-substituted POSS do not interdigitate and that instead the molecules pack together in a monolayer-like arrangement in the crystalline state.

4.3. Cyanobiphenylbenzoate Derivatives.

Since compounds **9** and **11** were found to be non-mesogenic, it was postulated that stabilization of the liquid-crystalline state could be achieved by using a mesogen with a wider temperature mesophase *via* elongation of the pro-mesogenic unit to increase its anisotropy. Materials **12**, **13** and **14** based on the cyanobiphenyl benzoate core were prepared and their properties evaluated. In contrast to the behaviour of compounds **9** and **11**, thermotropic mesophases were observed for all the materials with the cyanobiphenyl benzoate mesogenic unit (compounds **12**, **13** and **14**). The transition temperatures and associated enthalpies for these three materials are shown in Table 3.

R = iso-butyl, **12**

R = iso-octyl, **13**

R = cyclopentyl, **14**

R₁ = CBPB =

Table 3. Phase classification, transition temperatures (°C) and enthalpies of transition (kJ mol⁻¹) for compounds **12**-**14** and for the mesogen CBPB.

No	R	Cr		SmA		N		Iso
				Transition Temperatures /°C				
12	Isobutyl	•	96.7	•	231.6			•
			[25.9]		[20.9]			
13	Isooctyl	•	73.7	•	174.0			•
			[19.9]		[8.7]			
14	Cyclopentyl	•	152.5	•	196.4			•
			[37.0]		[11.8]			
CBPB [79]		•	108.0			•	264.0	•

Thus, all three materials presented in Table three were found to be mesogenic, with each exhibiting an enantiotropic smectic A phase. The identification of the smectic A phase was made *via* POM. Figure 4.8 shows the textures of all three compounds, that are typical of the smectic A phase, *i.e.* they show the focal-conic fan texture in conjunction with optically extinct hometropic regions.[13]
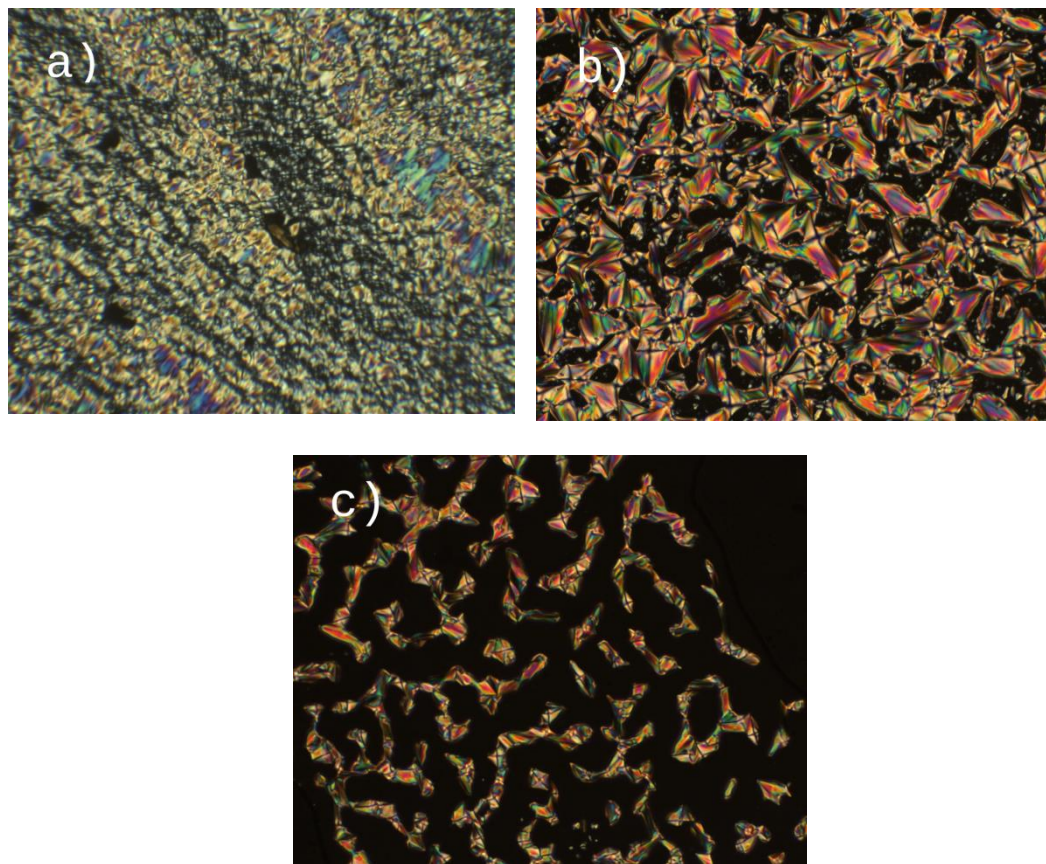
Figure 4.8: Photomicrographs (x200) showing (a) the fan-like texture and homeotropic regions and of the smectic A phase of compound **12** at 204 °C, (b) the fan-like texture and homeotropic regions of the smectic A phase of compound **13** at 190 °C and (c) the fan-like texture of compound **14** at the isotropisation point at 215 °C.

Differential scanning calorimetry shows that the SmA to isotropic liquid transition for **12**, **13** and **14** are all first-order and all are relatively broad in shape. This indicates that the molecules have a high degree of disorder and have slow rearrangement kinetics.

As expected, **12** and **13** have lower melting point and isotropisation temperature than the parent monomeric mesogen (Cr 108.0 SmA 264.0 °C Iso liq). However the melting point of **14** is higher than the melting point of the

parent mesogen. Comparisons of the thermal behaviour of compounds **12-14** in Table 3 reveal the effect of the R-group on the thermal properties of the cyanobiphenyl benzoate-based materials. Compound **13,** in which R is the iso-octyl group, has the lowest melting point within this series. Conversely, the melting point of the iso-butyl-substitued analogue, compound **12**, is ~23 °C higher. The cyclopentyl-substituted analogue, compound **14**, has the highest melting point within this series, consistent with the parent octa-alkyl substituted POSS having the highest melting point too.

However, owing to the difference in chemical structure, size and shape of the three R groups it is difficult to draw precise conclusions. It is, however, interesting to note that the trend with respect to the melting point is not reflected in the clearing points of the three materials. For example, although compound **13**, which has the lowest melting point, exhibits the lowest clearing point within the series, the clearing point of compound **14**, which has the highest melting point, is lower than that of compound **12**. Owing to the similarities in their chemical structures, a tentative comparison of the clearing points of compounds **12** and **13** can be made. Indeed, such a comparison may provide some insight into the effects of elongation of the R group. In this regard it seems likely that the increased steric bulk and flexibility associated with the longer group disrupts the molecular packing in the smectic A phase, thereby reducing the isotropization temperature.

Nevertheless, in reality this comparison is not straightforward as the elongation of the R group not only impacts on the molecular packing but also upon the relative balance between polar and non-polar and rigid and non-rigid sections of the molecular structure.

It is however, important to note that three cyanobiphenyl mesogens are not able to induce liquid crystallinity (compounds **9** and **11**) whereas three cyanobiphenylbenzoate mesogens with the same spacer length induce liquid crystal behaviour (compounds **12** and **13**). This difference can be attributed to the increase in anisotropy of the constituent mesogens. For the cyclopentyl

material **14**, intermediate values respect to iso-butyl and iso-octyl derivatives are observed for the melting and isotropisation temperatures.

In order to further investigate how many mesogens would be able to counteract the effect of the silsesquioxane core and induce LC behaviour, compound **17** was studied (isobutyl, with two cyanobiphenyl benzoate mesogens rather than three). Thus, this material allows the boundaries of the self-organization process in these systems with rigid silsesquioxane cores to be evaluated. The structure and the thermal behaviour of compound **17** are shown in Table 4. It shows monotropic behaviour.
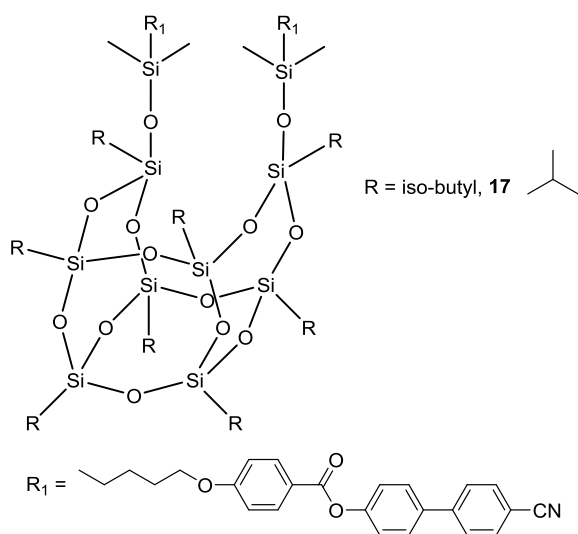
Table 4. The phase classification, transition temperatures (°C) and enthalpies of transition (kJ mol^{-1}) for compound **17,** values in parentheses indicate a monotropic transition.

No.	Transition Temperatures /°C						
	Cr		SmB		SmA		Iso
17	•	138.4	(•	145.2)	(•	165.5)	•
		[57.0]		[5.8]		[2.2]	

POM shows that the higher temperature phase separates from the isotropic liquid in the form of bâtonnets, which coalesce to form a fan-like texture, which contains focal-conic defects. Optically extinct regions were also observed within the preparation, thereby confirming that the phase is optically uniaxial and therefore consistent with the assignment of smectic A. Additionally, DSC showed an additional, first order, transition at 145.2 °C with an associated enthalpy of 5.8 kJ mol^{-1}. However, there was little change observable by POM (going from smectic A to smectic B) and so therefore not likely to be associated with a large structural change. Optically extinct regions were still observed and no breaking of the fans were observed in the texture and so therefore cannot be tilted or biaxial which is consistent with the assignment of SmB mesophase, Figure 4.9 (b).[80] Thus, it can be concluded that compound **17** exhibits monotropic SmA and SmB phases on cooling before finally crystallizing.
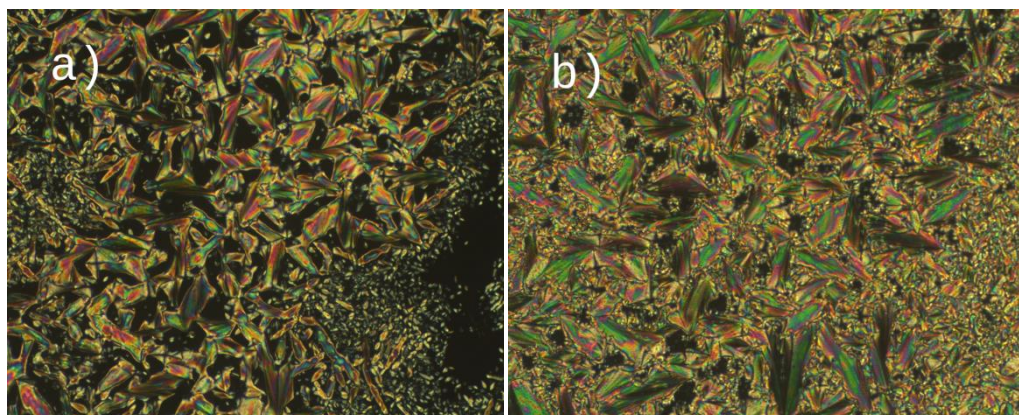
Figure 4.9: Photomicrographs of compound **17** (x100) showing (a) the fan-like texture and homeotropic regions of the SmA phase at 165 °C and (b) the fan-like texture of the SmB phase at 145 °C.

This is in contrast to compound **12,** which exhibits an enantiotropic SmA phase. The DSC trace of this compound, showing the monotropic nature of both the smectic A and smectic B phases of compound **17** is shown in Figure 4.10.
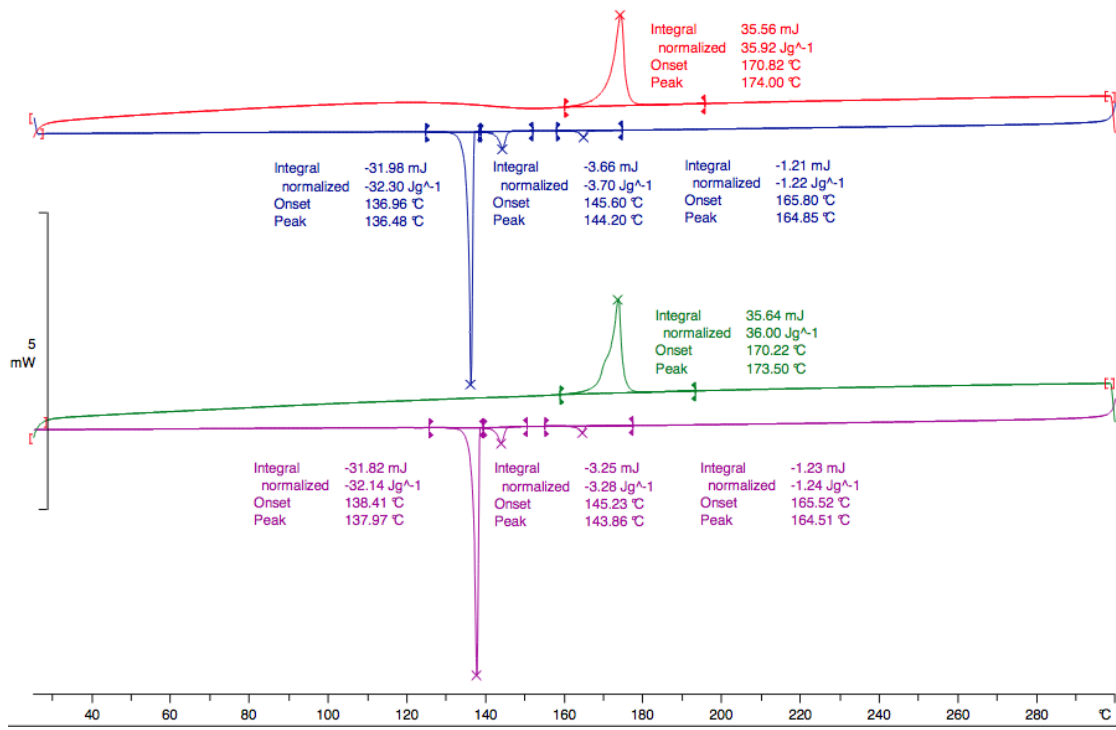
Figure 4.10: DSC thermogram of compound **17**.

Comparison of **17** (two mesogens) with **12** (three mesogens) shows that the melting point and the Iso-SmA transitions are higher for **12** than for **17** and the mesophase range is wider. This is a common trend found in supermolecular liquid crystals, where it has been established that increasing the number of mesogens on a scaffold increases the phase stability and mesomorphic range.[70] It is also interesting to note the appearance of a SmB mesophase in compound **17**, this could be due to the change to a more rod-like shape. It is however difficult to draw strong conclusions due to the large structural differences between the two moieties.

4.4. Materials with Side-on Mesogens

It was postulated that a laterally appended mesogen would induce the formation of the nematic mesophase as seen in other studies.[62] Therefore four compounds were made with the mesogen depicted in Figure 4.11.
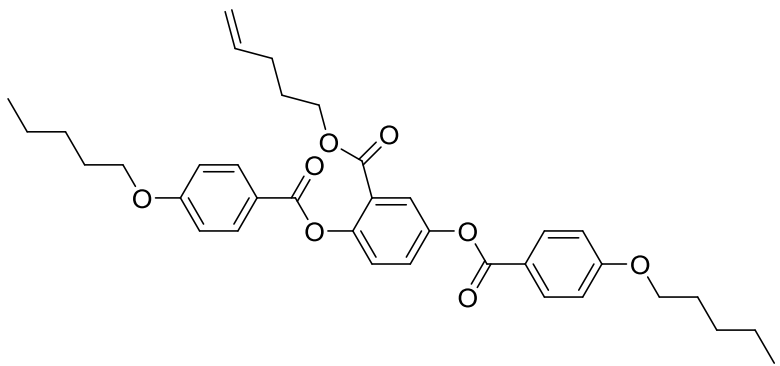
Figure 4.11: Mesogen with a lateral alkene chain used to make compounds **18**, **19**, **20** and **22**.

The transition temperatures and associated enthalpies for materials **18**, **19**, **20**, **22** and **LBB** are collected in Table 5.

R = iso-butyl, **18**

R = iso-octyl, **19**

R = iso-butyl, **20**

R₁ =

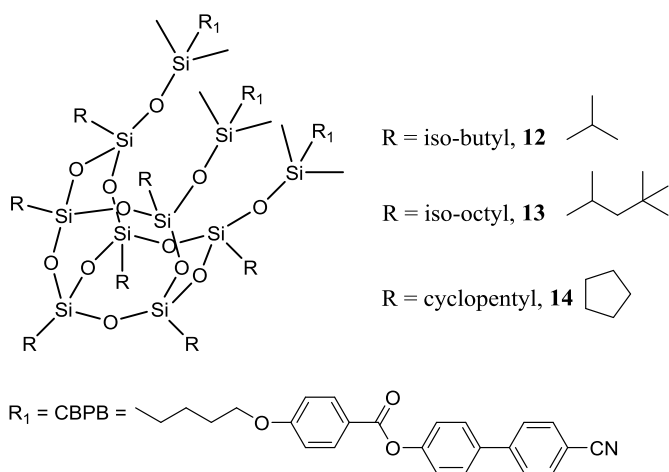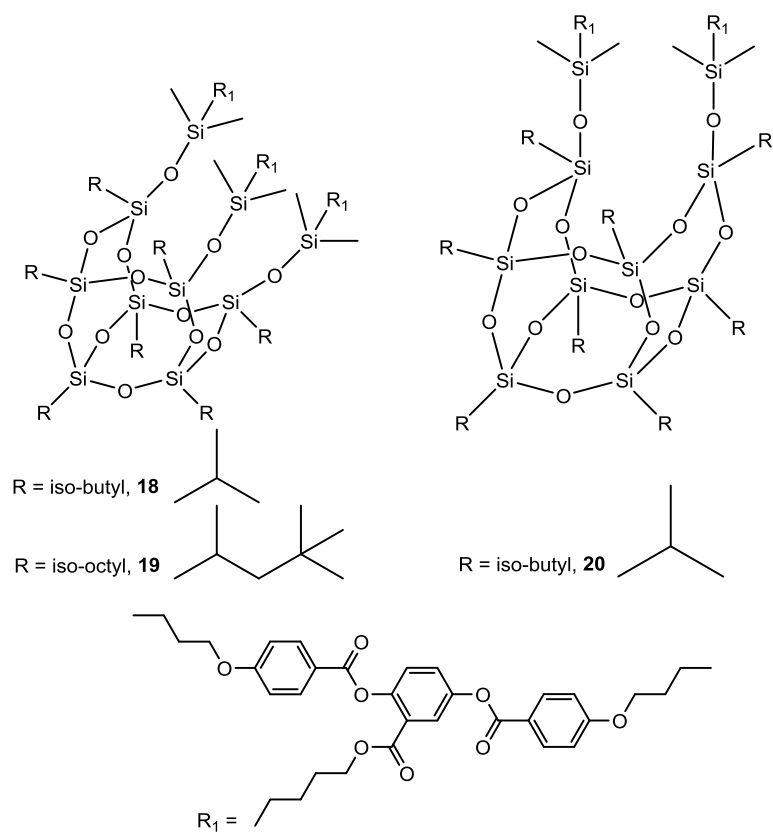**Table 5**. Phase classification, transition temperatures (°C) and enthalpies of transition (kJ mol⁻¹) for compounds **18-22** and **LBB.**

No	Transition Temperatures /°C		
	Cr	**N**	**Iso**
18	• 45.3 [44.8]		•
19	• 33.8 [50.7]		•
20	• 57.4 [7.6]		•
22	• 52.5 [0.6]		•
LBB	• 85.5 [38.9]	• 108.8 [1.5]	•

Surprisingly, all these compounds were found to be non mesomorphic. Furthermore, the melting point does not vary greatly across the series. The lack of mesogenic behaviour in the incompletely condensed silsesquioxanes **18**, **19** and **20** could result from two related factors. Firstly, the spacer chain between the mesogen and the cage is short and therefore the pro-mesogenic units have very little rotational and translational freedom. Furthermore, as a consequence of this short spacer length and the steric bulk of the pro-mesogenic unit, there is a large amount of steric interference between the mesogens, which is detrimental to the formation of a mesophase. Also, the overall shape of the molecule has likely changed to a more wedge-like shape, thereby making packing more difficult.

In order to establish whether the lack of mesomorphic behaviour in **18**, **19** and **20** was simply due to there not being enough mesogenic moieties around the core to be able to 'bury' it among the mesogenic cloud, as it has been demonstrated in fullerene derivatives.[81]

Therefore material **22**, the fully substituted octasilsequioxane with eight mesogens, was studied. Surprisingly too, **22** did not show mesomorphic behaviour either. This fact suggests that the probable reasons that none of the materials with this mesogen being liquid crystalline is a combination of the spacer being too short in the case of side-on attachment and the mesogen not having enough anisotropy, since it is known that octasilsesquioxanes substituted with a four-ring mesogen with the same spacer length are mesomorphic [81] and only four of such mesogens are able to induce the chiral nematic phase in the much more sterically demanding fullerene.[3]

4.5. Incompletely Condensed Janus Octasilsesquioxanes

In order to further investigate the properties of incompletely condensed silsesquioxanes, material **28** was studied, with a 'Janus' structure comprising

eight cyanobiphenyl mesogens and two chiral groups attached to a rigid silsesquioxane core in a segregated manner (the two chiral chains next to each other as opposed to randomly distributed on the eight corners of the cube). The transition temperatures and associated enthalpies are presented in Table 6.

Table 6. Phase classification, transition temperatures (°C) and enthalpies of transition (kJ mol⁻¹) for compounds **28** and **29**.

No	g		SmC/SmC*		SmA		N*		Iso
			Transition Temperatures /°C						
28	•	-24.9 [0.3]	•	18.7 [0.5]			•	22.8 [0.4]	•
29	•	-15.9 [0.5]	•	41.8 [11.4]	•	85.8 [22.5]			•

DSC revealed that **28** exhibits two phase transitions, one occurring at 22.8 °C and one at 18.7 °C. Furthermore, a glass transition was observed at -24.9 °C (measured at a cooling rate of 10 °C per minute). Both of the transitions present in compound **28** were found to be weakly first order with small associated enthalpies. The DSC thermograms of successive heating and cooling cycles for compound **28** are shown in Figure 4.12.
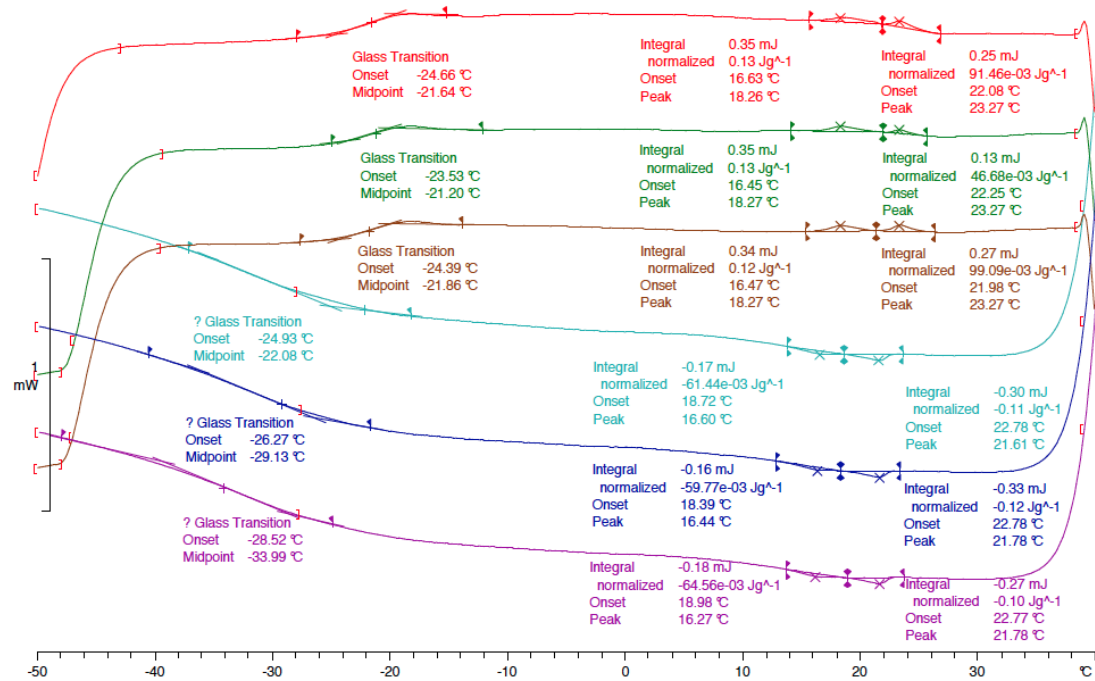
Figure 4.12: Dfferential scanning thermograms of compound **28**.

Analysis of compound **28** by POM revealed a transition from the isotropic liquid to a liquid-crystalline phase. The texture, shown in Figure 4.13, was weakly birefringent and poorly defined. However, what appear to be focal-conic defects are visible (Figure 4.13a), thereby suggesting that the phase has a periodic structure, *e.g.* a helical structure or a lamellar molecular arrangement. Shearing the sample resulted in an increase in the birefringence, giving a poorly defined streaky texture (Figure 4.13b). No optically extinct regions or schlieren texture was observed in either sheared or unsheared samples. Another feature of this texture is that optical activity was observed upon rotation of the analyser, thereby confirming that the phase exhibits a helical macrostructure with a left-handed helix. Based on these observations, the phase is tentatively assigned as the chiral nematic phase.
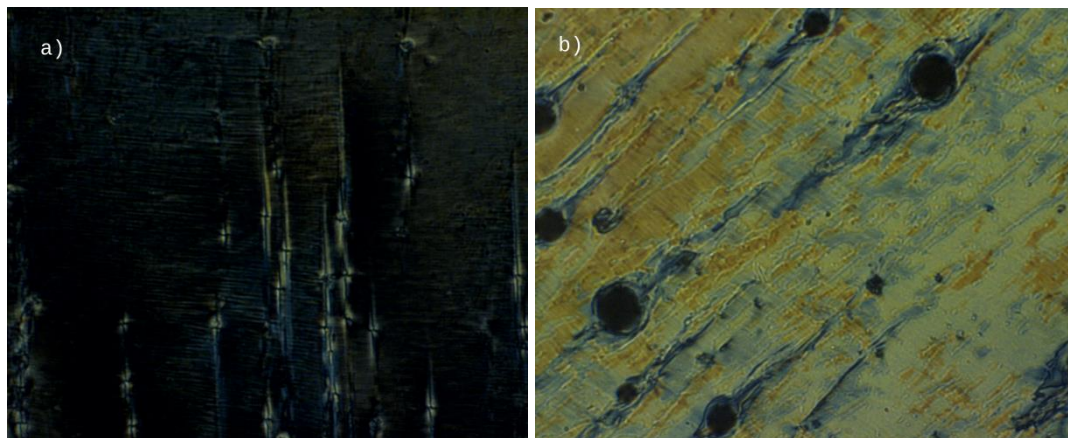
Figure 4.13: Photomicrographs (x200) of (a) focal-conic defects of compound **28** at 22 °C and (b) sheared sample of compound **28** at 22 °C.

As expected from DSC studies, once compound **28** was cooled down from to 18.72 °C it began to undergo a phase transition, which was accompanied by a slight change in birefringence and the appearance of very small domains. However, the overall texture observed for this lower-temperature phase was very similar to that observed for what is believed to be the chiral nematic phase, as can be seen in Figure 4.14 (a, natural; b) sheared).
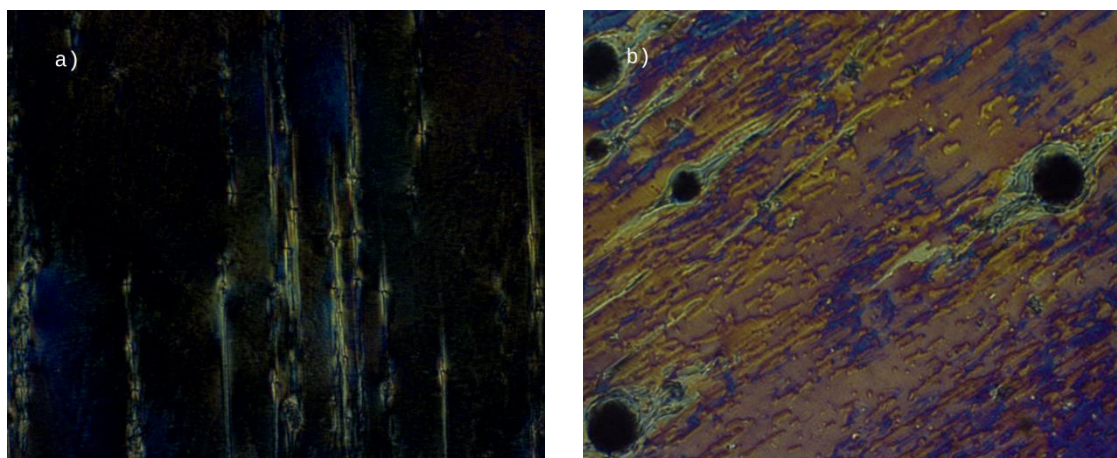
Figure 4.14: Photomicrographs (x200) of (a) the focal-conic defects of compound **28** at 11 °C and (b) the change in birefringence of compound **28** at 17 °C.

The very slight change in birefringence is indicative that the molecular reorganization at the phase transition is kinetically hindered, which is often the case for high molecular weight materials. This is in agreement with the observed broad transition peak in the DSC thermogram shown in Figure 4.12. Thus, identification of this lower-temperature mesophase is difficult, although it should be noted that rotation of the analyser indicated that the phase exhibits a helical structure, thereby suggesting that the phase is a helical smectic phase. Based on this evidence, it is plausible that the lower-temperature phase is either a smectic C*, smectic I* or smectic F* phases, although the low enthalpy of transition and the lack of textural change at the phase transition lend weight to the assignment of this phase as smectic C*. However, to fully assign the structure of this phase further studies such as X-ray diffraction studies need to be undertaken.

The related symmetrical ocatsilsesquioxane **29** with eight cyanobiphenyl mesogens around the silsesquioxane core, exhibited smectic C and smectic A phases.[71] Thus, assuming that compound **28** does exhibit a chiral nematic to smectic C* phase transition, the thermal behaviour of this material differs from other octa-substituted silsesquoxanes in that it exhibits a nematic phase, in this case the chiral nematic phase, and lacks the smectic A phase between the N* and the SmC*.
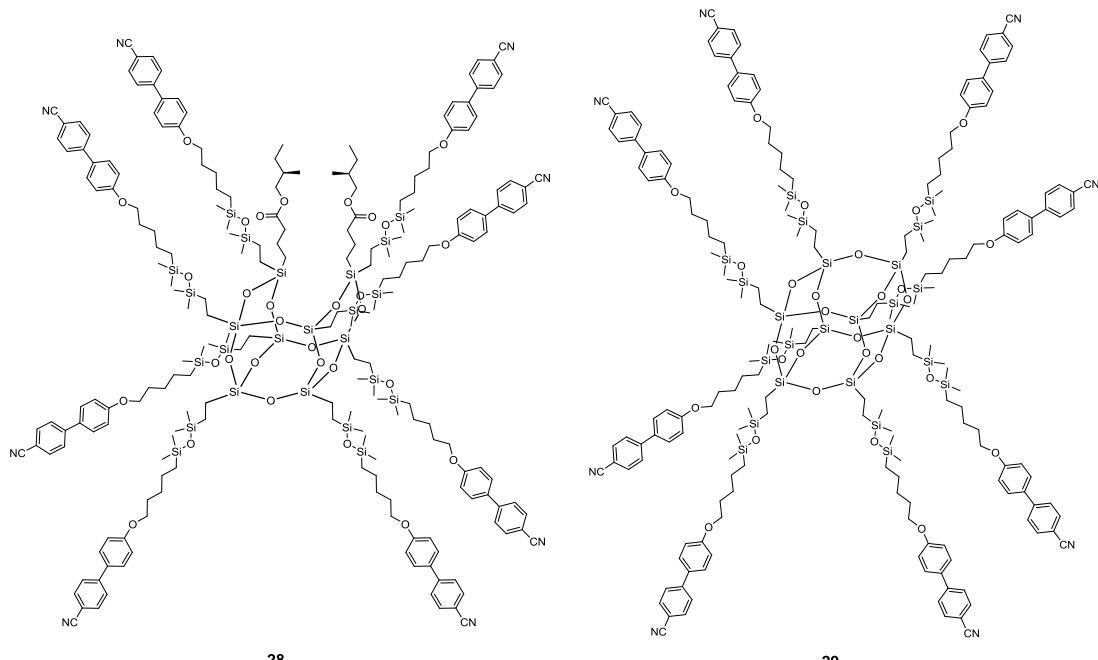
Figure 4.15: Illustration showing the structures of compound **28** and a similar compound for comparison, compound **29.**

The major differences between the structures of these two compounds are the chiral ester group present and the cage is open in compound **28** *i.e.* one edge Si-O-Si bond has been broken. The lower symmetry of the cage and the presence of the chiral chains act to introduce considerable disorder in the structure. These two factors likely have the effect of disrupting the packing efficiency of the molecules (in comparison with compound **29**) and thus a sharp decrease in all the transition temperatures of the various phases is observed. Furthermore, this reduced packing efficiency of compound **28** results in the breakdown of the cyanobiphenyl interlayer interdigitation present in these type of materials (**29** is purely smectogenic) and only the nematic arrangement is present. It follows then that the chirality transfer from the chiral groups in the two open arms of the cage to the nematic arrangement results in the chiral nematic phase. This type of behaviour has also been observed beautifully in the chirality transfer from the fulleropyrrolidine core to the mesogenic arms imparted by chiral core in the dendrimers studied by Deschenaux *et al.*[82-83]

Chapter Five:

Conclusions

5.1. Conclusions

The general aims of this work were to investigate the properties of novel liquid-crystalline supermolecular architectures. These architectures should include one or more different mesogenic units attached by covalent bonds to a silsesquioxane core.
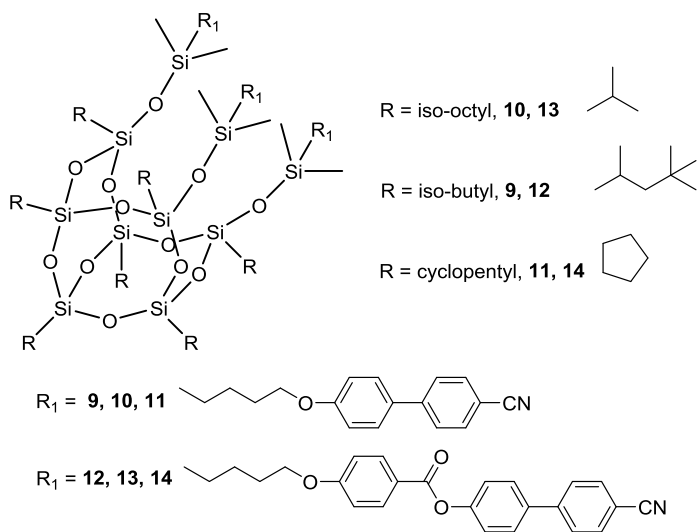
Figure 5.1: Chemical structures of compounds **9-14**.

Several incompletely condensed silsesquioxanes were prepared that contained a number of different mesogenic units and a number of different non-mesogenic R-groups, enabling the study of the self-organisation of a silsesquioxane core in the liquid-crystalline phase. It was found that materials prepared with three cyanobiphenyl-based mesogenic units (CB, compounds **9**, **10** and **11**) did not possess liquid-crystalline properties. This was an expected result and was attributed to the aspect ratio of the final structures being too small to induce liquid crystallinity into the system. For example, it has been shown in previous studies by Deschenaux *et al.* that if the mesogenic unit is attached solely to one end of the core, it does not provide a large enough aspect ratio to induce liquid crystallinity.[40] These materials did, however, crystallise which suggests that they do at least have the ability to form ordered structures in the solid state. Thus, the crystal structure obtained for compound **9** showed the molecules arranged in a lamellar-like fashion with a slight tilt, similar to that seen in a

smectic C phase. This lamellar arrangement seen in compound **9** has been seen previously in studies by El Aziz *et al.* in non-mesophorphic materials based on completely condensed silsesquioxane cores.[60] This is not, however, comparable directly to the crystal structure of compound **9** due to the different structural nature of an incompletely condensed silsesquioxane as opposed to a completely condensed silsesquioxane structure. However, if three CBPB mesogens are used, the materials prepared exhibit smectic A mesophases at temperatures above 200 °C (compounds **12**, **13** and **14**), suggesting that three CBPB mesogens produce enough anisotropy into the system to induce liquid crystallinity. The smectic A phases formed also suggests that the molecules conform to an overall rod-like shape as has been shown in other studies of more symmetrical, octasubstituted silsesquioxanes.[64] This is a surprising result considering the structural differences between the unsymmetrical incompletely condensed silsesquioxane structures and the completely condensed, symmetrical octasubstituted architecture. The rod-like shape also suggests that the mesogenic units must all be pointing roughly in the same direction, in a way comparable to the crystal structure of compound **9**. The phase stability of these materials is, however, remarkable. In previous studies it has been shown that as the number of mesogenic units appended to the scaffold is increased the phase stability increases. Compounds **12**, **13** and **14**, however, possess much greater phase stability *i.e.* clearing point, than their octasubstituted equivalents.
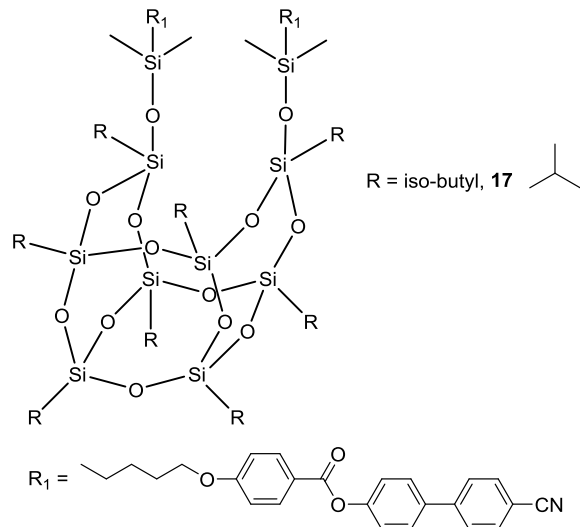
Figure 5.2: Chemical structure of compound **17**.

A material has also been prepared which contains two CBPB mesogenic units, which was also found to possess the smectic A mesophase in addition to the more ordered smectic B mesophase. The phase stability of this material conforms to the notion that phase stability decreases when the number of molecules appended to the scaffold decreases. That is, compound **17** (two mesogens) has a clearing point of 165.5 °C in comparison with compound **12** (three mesogens) which has a clearing point of 231.6 °C. This large difference in clearing point can be attributed to the stronger intermolecular forces in the three-mesogen system due to the presence of the extra mesogenic unit. The appearance of the smectic B phase in the three-mesogen system can be attributed to the structure being able to conform to a more rod-like shape. It is however very difficult to draw strong conclusions due to the large structural differences between the two moieties.
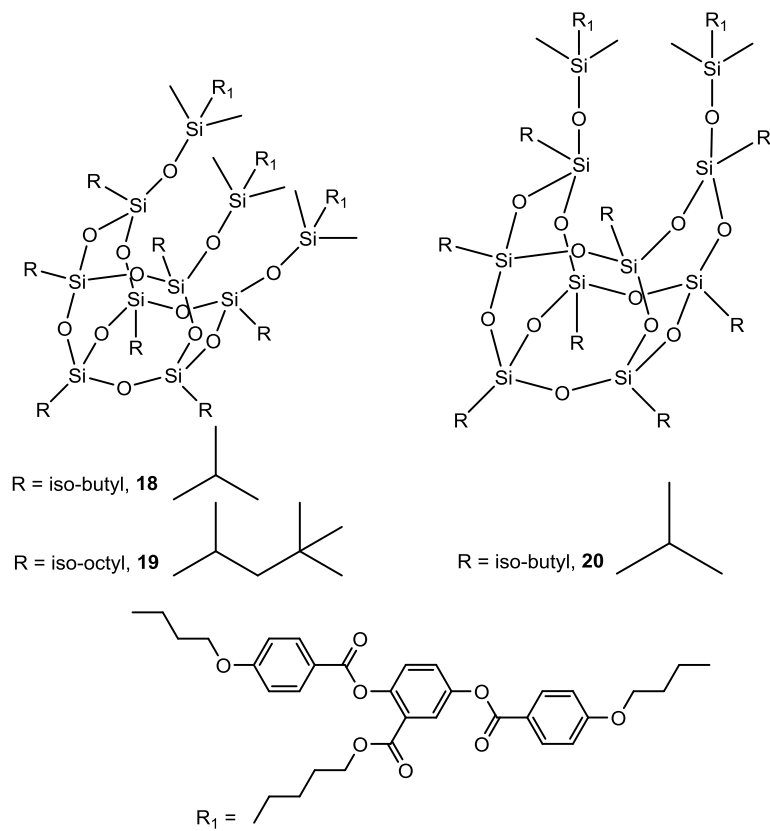
Figure 5.3: Chemical structures of compounds **18-20**.

Several materials were also prepared containing both two and three laterally attached mesogens (compounds **18**, **19**, **20** and **22**); none of these materials was found to be mesomorphic. It was postulated that appending laterally attached mesogenic units to the silsesquioxane scaffold would induce the nematic phase in this materials, as has been found in similar studies involving both silsesquioxane and fullerene derivatives.[23, 84] This was, however, not the case and the laterally attached mesogenic units decreased the order in the system beyond the point where liquid-crystalline phases could form.
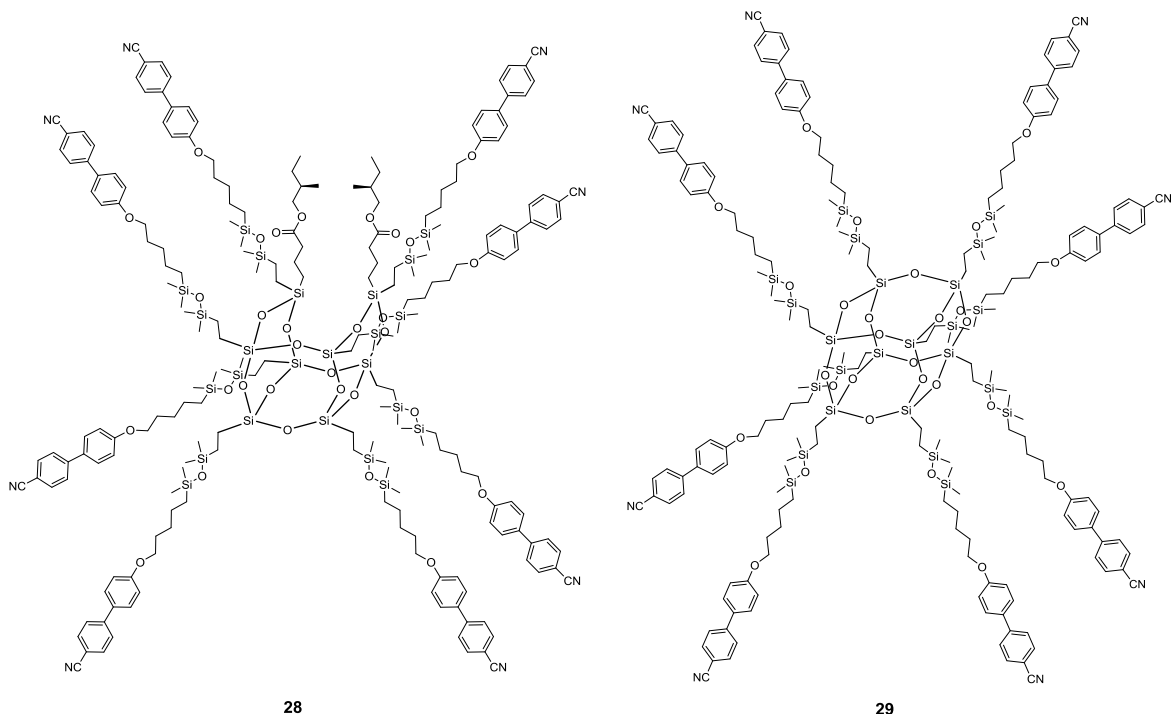
Figure 5.4: Chemical structures of compounds **28** and **29**.

Previous studies involving 'Janus' supermolecular liquid crystals have focused on using more flexible, 'soft-core' entities such as pentaerythritol derivatives.[39] These more flexible cores are able to deform more easily in order to conform to an anisotropic shape required to induce liquid crystallinity. The 'hard' cores in this work, however, are significantly less flexible and have greater bulk, and so provide a good contrast to these more flexible materials. Thus, compound **28** possesses eight cyanobiphenyl based mesogenic units and two chiral non-mesogenic entities and provides an example of how a chiral centre on a non-mesogenic portion of the molecule can induce chiral mesophases. The material was found to exhibit a room-temperature chiral nematic phase as well as an unidentified phase (M) at just below room temperature ($T_{\text{N*–M}}$ = 17 °C). The phase stability of this compound has decreased markedly in comparison with the octasubstituted completely condensed equivalent (compound **29**), signifying that the two chiral groups have decreased the order in the system significantly. The phase stability of the chiral nematic phase has also shown a marked decreased in comparison to its fulleropyrrolidine equivalent studied by Deschenaux *et al.*, but shows that two

chiral centres on different arms of a dendritic molecule can transfer chirality to the nematic arrangement of the molecules, resulting in the chiral nematic mesophase.[82]

In summary, a number of novel liquid-crystalline supermolecular architectures have been investigated involving silsesquioxane cores substituted with different types of mesogen in order to study the self-assembly of liquid-crystalline phases in silsesquioxane architectures. An additional silsesquioxane architecture was also investigated involving two distinct moieties appended to the same silsesquioxane core in order to study nanosegregation in liquid-crystalline silsesquioxane systems, specifically the transfer of chirality from a non-mesogenic portion of the molecule into the formation of chiral liquid-crystalline phases.

Chapter Six:

Experimental

6.1. Starting Materials, Reagents and Solvents

Unless otherwise stated, all starting materials and reagents were obtained from Sigma-Aldrich, Apollo Scientific or Alfa Aesar and used without further purification. All solvents were obtained from either Fisher or VWR Chemicals, with the exception of anhydrous solvents, which were purchased from Sigma-Aldrich and used without further purification. Sulfur-free dry toluene was purchased from Sigma-Aldrich. Karstedt's catalyst (platinum(0)-1,3-divinyl-1,1,3,3-tetramethyldisiloxane) was purchased from Sigma-Aldrich and each batch used until variable results obtained, after which a new batch was purchased. Isobutyl POSS diol, Isooctyl POSS diol, Cyclopentyl POSS triol, Isobutyl POSS triol and Isooctyl POSS triol were purchased from Hybrid Plastics. LBB and CPBP were kindly prepared by David Stewart. **26** was kindly prepared by Claire Bouwer.

6.2. Thin Layer Chromatography and Column Chromatography

Where appropriate, the progress of reactions was monitored by thin layer chromatography using a suitable solvent system. Silica coated aluminium plates (Kieselgel 60 F-254) were purchased from Merck and were visualized by UV light (254 nm or 365 nm) or by oxidation with potassium permanganate solution. In all cases, separations achieved via column chromatography were carried out using flash grade silica gel (Fluka, 70-230 mesh, 63 μm – 200 μm particle size).

6.3. Nuclear Magnetic Resonance (NMR) Spectroscopy

^{1}H, ^{13}C$\{^1$H$\}$ and ^{29}Si$\{^1$H$\}$ NMR spectra were recorded on either a JEOL EXS or a JEOL ECS spectrometer operating at a frequency of 400 MHz (^{1}H), 100.5 MHz (^{13}C) or 79 MHz (^{29}Si). In all cases, the residual protic solvent was used as an internal standard. Chemical shifts are quoted in ppm (δ). Abbreviations used to describe the multiplicity of the peaks observed are defined below.

s – singlet	t – triplet
d – doublet	sept – septet
dd – doublet of doublets	dt – doublet of triplets
ddt – doublet of double triplets	

6.4. Mass Spectrometry (MS)

Mass spectra were recoreded using a Bruker Solarix FT-ICR MS with 9.4 Tesla superconducting magnet (MALDI) or a Bruker micrOTOF MS-Agilent series 1200LC spectrometer (ESI).

6.5. Infrared Spectroscopy (FT-IR)

Infrared spectroscopy was performed using a Shimadzu IR prestige-21 equipped with a Specac diamond ATR IR insert.

6.6. Polarised Optical Microscopy (POM)

Polarized optical microscopy (x200 magnification) was performed on a Zeiss Axioskop 40 Pol microscope using a Metter FP82HT furnace, which was controlled by a Mettler FP90 control unit or on a Olympus BX50 polarizing microscope equipped with a Linkam scientific LTS350 heating stage, Linkam LNP2 cooling pump and a Linkam TMS92 controller. An Infinity X-21 digital camera was used to record photomicrographs.

6.7. Differential Scanning Calorimetry (DSC)

Melting points, cystallisation temperatures, enthalpies of transition and transition temperatures, were determined by differential scanning calorimetry. Thermograms were obtained using a Mettler DSC822^e unit operating in with Star^e software. In each case the scan rate was 10 °C min^{-1}. The results obtained were normalized relative to an indium standard (onset = 156.5 ± 0.2 °C, ΔH = 28.4 ± 0.40 J g^{-1}).

6.8. Elemental Analysis

Elemental analysis was recorded on a CE-440 elemental analyzer from Exeter Analytical Inc using a Sartorius SE2 analytical balance. Vanadium pentoxide was added to the samples as a combustion enhancer.

6.9. Single Crystal X-ray Diffraction

X-ray data was obtained using a Bruker Smart Apex X-ray diffractometer equipped with a 3-circle goniometer with an Oxford cryostream cooling system and a 180 litre nitrogen transport and storage dewar. Sample preparation was done with an Olympus binocular microscope.

6.10. 4'-(Pent-4-enyloxy)-[1,1'-biphenyl]-4-carbonitrile (2)

5-bromo-1-pentene (3.82g, 0.0256 mol) was added to 4'-cyano-4-hydroxy biphenyl (5g, 0.0256 mol) dissolved in butanone (75 mL). Potassium iodide (0.55g, 3.31 mmol) and potassium carbonate (14.15, 0.102 mol) were added and the mixture was heated at reflux temperature for 24 hr to yield a yellow solution. The inorganic materials were removed by vacuum filtration, the solvent was removed under reduced pressure and the solid was recrystallised twice from methanol to yield white crystals (4.87g, 72% yield).

^{1}H NMR (400 MHz, CDCl$_3$) δ_H (ppm): 7.67 (m, AA'XX' (J = 8.8 Hz), 2H, ArH), 7.62, (m, AA'XX' (J = 8.8 Hz), 2H, ArH), 7.51 (m, AA'XX' (J = 8.8 Hz), 2H, ArH) 6.97 (m, AA'XX' (J = 8.8 Hz), 2H, ArH), 5.84 (d (J$_{trans}$ = 16.84 Hz) d (J$_{cis}$ = 10.25 Hz) t (J = 6.59), 1H, CH$_2$=CH), 5.08 (d (J$_{trans}$ = 16.8 Hz) m, 1H, CH_2=CH), 4.99 (d (J$_{cis}$ = 10.2 Hz) m, 1H, CH_2=CH), 4.01 (t(J = 6.4 Hz), 2H, CH_2O), 2.24 (t (J = 6.95 Hz), 2H, CH_2CH$_2$), 1.90 (m, 2H, CH_2CH$_2$).

^{13}C{^{1}H} NMR (100 MHz, CDCl$_3$) δ_C (ppm): 159.67 (C$_{Ar}$), 145.23 (C$_{Ar}$), 137.65 (CH=CH$_2$), 132.53 (C$_{ArH}$), 131.31 (C$_{Ar}$), 128.30 (C$_{ArH}$), 127.05 (C$_{ArH}$), 119.10 (CN),

115.30 (CH_2=CH), 115.06 (C_{ArH}), 110.01 (C_{Ar}), 67.27 (CH_2O), 30.04 (CH_2), 28.31 (CH_2O).

IR υ_{max} cm^{-1} 3071 (CH stretch, alkene), 2932 (CH stretch, aromatic) 2222 (CN stretch).

ESI-MS: (m/z) – Calculated 286.12 [M+Na]$^+$; Found 286.11 [M+Na]$^+$

6.11. Heptaisobutylsilsesquioxane-*endo*-1, 3, 7-tris-(dimethylhydrido)silane (6)

Iso-butyl trisilanol POSS (100 mg, 0.126 mmol) was placed in a dry Schlenk tube under nitrogen, dissolved in dry dichloromethane (5 mL) and dimethlychlorosilane (0.085 mL, 0.76 mmol) was added via syringe. Triethylamine (0.140 mL, 1.01 mmol) was added and the solution was stirred overnight. The solvent was removed *in vacuo* to leave a brown solid that was extracted with petroleum ether, the solution filtered through celite and evaporated to dryness to yield a colourless oil (106 mg, 81% yield).

^{1}H NMR (400 MHz, CDCl$_3$) δ_H (ppm): 4.67 (sept, (J = 2.8 Hz), 3H, Si*H*), 1.76 (m, 7H, C*H*(CH$_3$)$_2$), 0.89 (m, 42H, (C*H$_3$*)$_2$CH), 0.49 (m, 14H, C*H$_2$*), 0.15 (m, (J = 2.8 Hz), 18H, (C*H$_3$*)$_2$Si).

^{13}C{^{1}H} NMR (100 MHz, CDCl$_3$) δ_C (ppm): 26.03, 25.90, 25.69 (*CH$_3$*)$_2$CH, 3:3:1 ratio), 24.12, 24.02, 23.95, (*C*H(CH$_3$)$_2$ 3:3:1 ratio), 24.66, 23.64, 22.50 (*CH$_2$*CH(CH$_3$)$_2$ 3:3:1 ratio), 0.707 (Si*C*H$_3$).

MALDI-MS: (m/z) – Calculated: 987.35 [M+Na]$^+$; Found: 987.34 [M+Na]$^+$.

6.12. Heptaisooctyllsilsesquioxane-*endo*-1, 3, 7, tris-(dimethylhydrido)silane (7)

Iso-octyl trisilanol POSS (200mg, 0.169 mmol) was placed in a dry Schlenk tube under nitrogen, dissolved in dry dichloromethane (5 ml) and dimethlychlorosilane (0.110 mL, 1.013 mmol) was added *via* syringe. Triethylamine (0.188 mL, 1.352 mmol) was added and the solution was left to stir overnight. The solvent was removed *in vacuo* to leave a brown solid that was extracted with petroleum ether, the solution filtered through celite and evaporated to dryness to yield a colourless oil (193 mg, 83% yield).

^{1}H NMR (400 MHz, CDCl$_3$) δ_H (ppm): 4.69 (sept, 3H, Si*H*), 1.74 (m, 7H, C*H*CH$_2$), 1.306-1.026 (m, 14H, C*H$_2$*CH(CH$_3$)$_3$), 0.932 (m, 21H, C*H$_3$*CH), 0.824 (m, 63H, (C*H$_3$*)$_3$CCH$_2$), 0.722-0.427 (m, 14H, C*H$_2$*CHCH$_2$), 0.155 (m, 18H, (C*H$_3$*)$_2$Si).

^{13}C{^{1}H} NMR (100 MHz, CDCl$_3$) δ_C (ppm): 54.59 (*C*H$_2$C(CH)$_3$), 31.16, (*C*(CH$_3$)$_3$), 30.32 (*C*H$_3$)$_2$CCH$_2$), 25.90-24.86, (*C*HCH$_2$), 25.90-24.86 (*C*H$_3$CH), 25.90-24.86 (*C*H$_2$CHCH$_3$), 0.693 (*C*H$_3$)$_2$Si).

MALDI-MS: (m/z) – Calculated: 1379.79 [M+Na]$^+$; Found: 1379.80 [M+Na]$^+$.

6.13. Heptaisobutylsilsesquioxane-*endo*-tris-[4'-pentyloxydimetylsiloxy)-(1,1'-biphenyl)-4-carbonitrile] (9)

6 (100 mg, 0.103 mmol) was placed in a dry Schlenk tube under nitrogen and dissolved in dry, sulphur-free toluene (5 ml). Karstedt's catalyst (15 μL) was added and the solution stirred for 15 minutes. **2** (109 mg, 0.414 mmol) in dry, sulphur-free toluene (5 mL) added dropwise under nitrogen and the solution stirred for 48hr. The solvent was removed *in vacuo* and the solid was purified by column chromatography (Dichloromethane, flash grade silica gel, R_f = 0.34) to yield a white solid that was recrystallised from dichloromethane/ethanol to yield **9** as colourless crystals (49 mg, 27% yield).

^{1}H NMR (400 MHz, CDCl$_3$) δ_H (ppm): 7.60 (m, AA'XX' (J = 8.4 Hz), 6H, Ar*H*), 7.54 (m, AA'XX' (J = 8.4 Hz), 6H, Ar*H*), 7.43 (m, AA'XX' (J = 8.4 Hz), 6H, Ar*H*), 6.89 (m, AA'XX' (J = 8.4 Hz), 6H, Ar*H*), 3.90 (t, (J = 6.8 Hz), 6H, C*H*$_2$O), 1.74 (m, 7H, C*H*(CH$_3$)$_2$), 1.74 (m, 6H, C*H*$_2$CH$_2$O), 1.37 (m, 6H, C*H*$_2$), 1.37 (m, 6H, C*H*$_2$), 0.89 (m, 42H, (C*H*$_3$)$_2$CH), 0.49 (m, 14H, C*H*$_2$CH(CH$_3$)$_2$) 0.49 (m, 6H, C*H*$_2$Si), 0.065 (m, (J = 2.8 Hz), 18H, (C*H*$_3$)$_2$Si).

^{13}C{^{1}H} NMR (100 MHz, CDCl$_3$) δ_C (ppm): 159.88 (C$_{Ar}$), 145.30 (C$_{Ar}$), 132.65 (C$_{ArH}$), 131.04 (C$_{Ar}$), 128.37 (C$_{ArH}$), 127.12 (C$_{ArH}$), 119.18 (CN), 115.11 (C$_{ArH}$), 110.14 (C$_{Ar}$), 68.24 (*C*H$_2$O), 29.87 (*C*H$_2$), 29.79 (*C*H$_2$), 29.13 (*C*H$_2$), 23.84 (*C*H$_2$), 26.14, 25.96, 25.71 (*C*H$_3$)$_2$CH, 3:3:1 ratio), 24.18, 24.08, 23.93 (*C*H(CH$_3$)$_2$, 3:3:1 ratio), 25.12, 23.18, 22.50 (*C*H$_2$CH(CH$_3$)$_2$, 3:3:1 ratio), 18.19 ((*C*H$_2$Si), 0.432 (*C*H$_3$)$_2$Si.

^{29}Si{^{1}H} NMR (79 MHz, CDCl$_3$) δ_{Si} (ppm): 9.41 (*Si*(CH$_3$)$_2$, -67.18 (*Si*O$_3$), -67.54 (SiO$_3$).

IR υ_{max} cm^{-1} 2947 (CH stretch, aromatic), 2222 (CN stretch), 1049 (CO stretch).

MALDI-MS (m/z) – Calculated: 1776.74 [M+Na]$^+$; Found: 1776.74 [M+Na]$^+$.

Elemental Analysis (%) – Calculated for C$_{88}$H$_{135}$N$_3$O$_{15}$Si$_{10}$: C 60.19, H 7.75, N 2.39; Found: C 60.23, H 7.69, N 2.34.

6.14. Heptaisooctylsilsesquioxane-*endo*-tris-[4'-pentyloxydimethylsiloxy)-(1,1'-biphenyl)-4-carbonitrile] (10)

7 (84 mg, 0.0618 mmol) was placed in a dry Schlenk tube under nitrogen and dissolved in dry, sulfur-free toluene (5 ml). Karstedt's catalyst (15 µL) was added, the solution stirred for 15 minutes. **2** (98 mg, 0.371 mmol) in toluene (5 mL) added dropwise under nitrogen and the solution stirred for 48hr. The

solvent was removed in vacuo and the solid was purified by column chromatography (Dichloromethane, flash grade silica gel, R_f = 0.34) to yield a white solid, that was recrystalised from dichloromethane/ethanol to yield **10** as colourless crystals (31 mg, 23% yield).

^{1}H NMR (400 MHz, CDCl$_3$) δ_H (ppm): 7.60 (m, AA'XX' (J = 8.4 Hz), 6H, Ar*H*), 7.54 (m, AA'XX' (J = 8.4 Hz), 6H, Ar*H*), 7.42 (m, AA'XX' (J = 8.4 Hz), 6H, Ar*H*), 6.89 (m, AA'XX' (J = 8.4 Hz), 6H, Ar*H*), 3.89 (t, (J = 6.4 Hz), 6H, C*H$_2$*O), 1.72 (m, 7H C*H*CH$_2$), 1.72 (m, 6H, C*H$_2$*), 1.37 (m, 6H, C*H$_2$*), 1.37 (m, 6H, C*H$_2$*), 1.26-1.00 (m, 14H, C*H$_2$*CH(CH$_3$)$_3$, 0.94 (m, 24H, C*H$_3$*CH), 0.82 (m, 63H, (C*H$_3$*)$_3$CHCH$_2$), 0.74-0.42 (m, 14H, C*H$_2$*CHCH$_2$), 0.74-0.42 (m, 6H, C*H$_2$*Si), 0.07 (s, 18H, (C*H$_3$*)$_2$Si).

^{13}C{^{1}H} NMR (100 MHz, CDCl$_3$) δ_C (ppm): 159.87 (C$_{Ar}$), 145.29 (C$_{Ar}$), 132.63 (C$_{ArH}$), 131.29 (C$_{Ar}$), 128.35 (C$_{ArH}$), 127.14 (C$_{ArH}$), 119.14 (CN), 115.12 (C$_{ArH}$), 110.13 (C$_{Ar}$), 68.23 (*C*H$_2$O), 31.26, 30.23, 29.91 (*C*HCH$_2$, 3:3:1 ratio), 30.38 (*C*H$_3$)$_3$CCH$_2$, 29.80 (*C*H$_2$), 29.53 (*C*H$_2$), 26.48 (*C*H$_2$), 25.78-24.95 (*C*H$_3$CH), 25.78-24.95 (*C*(CH$_3$)$_3$), 26.48-24.95 (*C*H$_2$), 23.22 (*C*H$_2$CH), 18.26 (*C*H$_2$Si), 0.504 (*C*H$_3$)$_2$Si).

^{29}Si{^{1}H} NMR (79 MHz, CDCl$_3$) δ_{Si} (ppm): 9.27 (*Si*(CH$_3$)$_2$, -67.68 (broad) (*Si*O$_3$).

IR υ_{max} cm^{-1} 2947 (CH stretch, aromatic), 2222 (CN stretch), 1049 (CO stretch).

MALDI-MS (m/z) – Calculated: 2169.1866 [M+Na]$^+$; Found: 2169.1732 [M+Na]$^+$.

Elemental Analysis (%) – Calculated for C$_{119}$H$_{197}$N$_3$O$_{15}$Si$_{10}$: C 64.78, H 9.05, N 1.68; Found: C 64.78, H 9.05, N 1.95.

6.15. Heptacyclopentylsilsesquioxane-*endo*-tris-[4'-(pentyloxydimethylsiloxy)-(1,1'-biphenyl)-4-carbonitrile] (11)

1 (115 mg, 0.437 mmol) was placed in a dry Schlenk tube under nitrogen and dissolved in toluene (5 mL). Karstedt's catalyst (15 μL) was added, the reaction was stirred for 15 minutes. Endo-3,7,14-tris(dimethylsilyoxy)-1, 3, 5, 7, 9, 11, 14 – heptacyclopentyltricyclo[7.3.1$5,11$]-heptasiloxane (115 mg, 0.109 mmol) was dissolved in toluene (2 mL) and added dropwise. The solution was stirred for 48 hrs, the solvent removed *in vacuo* and the solid was purified by column chromatography (Dichloromethane, flash grade silica gel, R_f = 0.37) to yield a white solid, that was recrystallised from dichloromethane/ethanol to yield **11** as colourless crystals (57 mg, 29% yield).

^{1}H NMR (400 MHz, CDCl$_3$) δ_H (ppm): 7.61 (m, AA'XX' (J = 8.4 Hz), 6H, ArH), 7.55 (m, AA'XX' (J = 8.4 Hz), 6H, ArH), 7.44 (m, AA'XX' (J = 8.4 Hz), 6H, ArH), 6.90 (m, AA'XX' (J = 8.4 Hz), 6H, ArH), 3.91 (t, (J = 6.4 Hz), 6H, C*H*$_2$O), 1.68 (m, 7H, C*H*Si), 1.68 (m, 6H, C*H*$_2$), 1.68 (m, 6H, C*H*$_2$), 1.68 (m, 6H, C*H*$_2$), 1.43 (m, 56H, C*H*$_2$), 0.56 (m, 6H, C*H*$_2$Si), 0.07 (s, 18H, (C*H*$_3$)$_2$Si).

^{13}C{^{1}H} NMR (100 MHz, CDCl$_3$) δ_C (ppm): 159.85 (C$_{Ar}$), 145.32 (C$_{Ar}$), 132.61 (C$_{ArH}$), 131.32 (C$_{Ar}$), 128.37 (C$_{ArH}$), 127.11 (C$_{ArH}$), 119.12 (CN), 115.11 (C$_{ArH}$), 110.14 (C$_{Ar}$), 68.25 (*C*H$_2$O), 29.85 (*C*H$_2$), 29.12 (*C*H$_2$), 27.78, 27.37 (*C*H$_2$), 27.13, 27.04 (*C*H$_2$), 24.72, 23.88, 22.55 (*C*H, 3:3:1 ratio), 23.21 (*C*H$_2$), 18.26 (*C*H$_2$Si), 0.55 ((*C*H$_3$)$_2$Si).

IR υ_{max} cm^{-1} 2947.23 (CH stretch, aromatic), 2222.00 (CN stretch), 1049 (CO stretch).

MALDI-MS (m/z): Calculated: 2221 [M+Na]$^+$; Found: 2221 [M+Na]$^+$.

Elemental Analysis (%) – Calculated for $C_{95}H_{135}N_3O_{15}Si_{10}$: C 62.01, H 7.40, N 2.28; Found: C 61.14, H 7.34, N 2.10.

6.16. Heptaisobutylsilsesquioxane-*endo*-tris-[4'-{pentyloxy-5-dimethylsiloxy}-(1-(cyanobiphenylbenzoate)] (12)

CBPB (80 mg, 0.207 mmol) was placed in a dry Schlenk tube under nitrogen and dissolved in toluene (5 mL). Karstedt's catalyst (15 μL) was added, the solution stirred for 15 minutes. **6** (50 mg, 0.0518 mmol) dissolved in toluene added dropwise, the solution stirred for 48hr. The solvent was removed *in vacuo* to yield a solid, that was purified by column chromatography (dichloromethane, flash grade silica gel, R_f = 0.12) to yield a white solid, that was recrystallised from dichloromethane/ethanol to yield **12** as a white solid (49 mg, 45% yield).

^{1}H NMR (400 MHz, CDCl$_3$) δ_H (ppm): 8.08 (m, AA'XX' (J = 8.4 Hz), 6H, Ar*H*), 7.67 (m, AA'XX' (J = 8.4 Hz), 6H, Ar*H*), 7.61 (m, AA'XX' (J = 8.4 Hz), 6H, Ar*H*), 7.55 (m, AA'XX' (J = 8.4 Hz), 6H, ArH), 7.24 (m, AA'XX' (J = 8.4 Hz), 6H, Ar*H*), 6.90 (m, AA'XX' (J = 8.4 Hz), 6H, ArH), 3.96 (t, (J = 6.8 Hz), 6H, C*H$_2$*O), 1.76 (m, 6H, C*H$_2$*), 1.76 (m, 7H, C*H*(CH$_3$)$_2$), 1.40 (m, 6H, C*H$_2$*), 1.40 (m, 6H, C*H$_2$*), 0.90 (m, 38H, (C*H$_3$*)$_2$CH), 0.52 (m, 14H, C*H$_2$*CH(CH$_3$)$_2$), 0.52 (m, 6H, C*H$_2$*), 0.08 (s, 18H, (C*H$_3$*)$_2$Si).

^{13}C{^{1}H} NMR (100 MHz, CDCl$_3$) δ_C (ppm): 164.87 (COO), 163.78 (C$_{Ar}$), 151.63 (C$_{Ar}$), 144.90 (C$_{Ar}$), 136.78 (C$_{Ar}$), 132.43 (C$_{ArH}$), 128.41 (C$_{ArH}$), 127.76 (C$_{ArH}$), 122.62 (C$_{ArH}$), 121.32 (C$_{Ar}$), 118.93 (CN), 114.41 (C$_{ArH}$), 111.09 (C$_{Ar}$), 68.44 (*C*H$_2$O), 29.81 (*C*H$_2$), 29.01 (*C*H$_2$), 26.13, 25.96, 25.71 ((CH$_3$)$_2$*C*H, 3:3:1 ratio), 25.13, 23.85, 23.17 (*C*H$_2$CH, 3:3:1 ratio), 24.19, 24.09, 23.94 (*C*H(CH$_3$)$_2$, 3:3:1 ratio), 18.18 (*C*H$_2$Si), 0.44 ((*C*H$_3$)$_2$Si).

^{29}Si{^{1}H} NMR (79 MHz, CDCl$_3$) δ_{Si} (ppm): 9.09 (*Si*(CH$_3$)$_2$, -67.25 (broad) (*Si*O$_3$).

IR υ_{max} cm^{-1} 2947 (CH stretch, aromatic), 2222 (CN stretch), 1728 (C=O stretch), 1057 (CO stretch).

MALDI-MS: (m/z) – Calculated: 2136.81 [M+Na]$^+$; Found: 2136.80 [M+Na]$^+$.

Elemental Analysis (%) – Calculated for $C_{109}H_{147}N_3O_{21}Si_{10}$: C 61.86, H 7.00, N 1.83; Found: C 61.30, H 7.01, N 1.83.

6.17. Heptaisooctylsilsesquioxane-*endo*-tris-[4'-{pentyloxy-5-dimethylsiloxy}-(1-(cyanobiphenylbenzoate)] (13)

CBPB (113 mg, 0.294 mmol) was placed in a dry Schlenk tube under nitrogen and dissolved in toluene (5 mL). Karstedt's catalyst (15 µL) was added, the solution stirred for 15 minutes. **7** (100 mg, 0.294 mmol) dissolved in added dropwise, the solution stirred for 48hr. The solvent was removed *in vacuo* to yield a solid, that was purified by column chromatography (Dichloromethane, flash grade silica gel, R_f = 0.11) to yield a white solid, that was recrystallised from dichloromethane/ethanol to yield **13** as a white solid (70 mg, 38% yield).

^{1}H NMR (400 MHz, CDCl$_3$) δ_H (ppm): 8.08 (m, AA'XX' (J = 8.4 Hz), 6H, Ar*H*), 7.67 (m, AA'XX' (J = 8.4 Hz), 6H, Ar*H*)), 7.61 (m, AA'XX' (J = 8.4 Hz), 6H, Ar*H*), 7.56 (m, AA'XX' (J = 8.4 Hz), 6H, Ar*H*), 7.24 (m, AA'XX' (J = 8.4 Hz), 6H, Ar*H*), 6.90 (m, AA'XX' (J = 8.4 Hz), 6H, Ar*H*), 3.96 (t, (J = 6.4 Hz), 6H, C*H*$_2$O), 1.76 (m, 7H, C*H*CH$_2$), 1.76 (m, 6H, C*H*$_2$), 1.41 (m, 6H, C*H*$_2$), 1.41 (m, 7H, C*H*$_2$), 1.14 (m, 14H, C*H*$_2$CH(CH$_3$)$_3$, 0.95 (m, 21H, C*H*$_3$CH), 0.84 (m, 63H, ((C*H*$_3$)$_3$CCH$_2$), 0.76-0.42 (m, 14H, CH$_2$CH), 0.76-0.42 (m, 6H, C*H*$_2$Si), 0.10 (s, 18H, (C*H*$_3$)$_2$Si).

^{13}C{^{1}H} NMR (100 MHz, CDCl$_3$) δ_C (ppm): 164.90 (COO), 163.78 (C$_{Ar}$), 151.65 (C$_{Ar}$), 144.90 (C$_{Ar}$), 136.78 (C$_{Ar}$), 132.74 (C$_{ArH}$), 132.43 (C$_{ArH}$), 128.42 (C$_{ArH}$), 127.76 (C$_{ArH}$), 122.64 (C$_{ArH}$), 121.28 (C$_{Ar}$), 118.92 (CN), 114.42 (C$_{ArH}$), 110.09 (C$_{Ar}$), 68.44 (*C*H$_2$O), 54.80 (*C*H$_2$C(CH$_3$)$_3$), 31.29, 30.23, 29.02 (*C*HCH$_2$, 3:3:1 ratio), 30.36 ((*C*H$_3$)$_3$CCH$_2$), 26.48-24.98 (*C*H$_3$CH), 26.48-24.98 (*C*(CH$_3$)$_3$), 29.89 (*C*H$_2$), 29.55 (*C*H$_2$), 26.48 (*C*H$_2$), 23.20 (*C*H$_2$CH), 18.28 (*C*H$_2$Si), 0.539 (*C*H$_3$)$_2$Si).

IR υ_{max} cm^{-1} 2947 (CH stretch, aromatic), 2222 (CN stretch), 1728 (C=O stretch), 1057 (CO stretch).

MALDI-MS: (m/z) – Calculated: 2529.25 [M+Na]$^+$; Found: 2529.24 [M+Na]$^+$.

Elemental Analysis (%) – Calculated for $C_{137}H_{203}N_3O_{21}Si_{10}$: C 65.58, H 8.16, N 1.56; Found: C 65.26, H 8.16, N 1.56

6.18. Heptaisooctylsilsesquioxane-*endo*-tris-[4'-{pentyloxy-5-dimethylsiloxy}-(1-(cyanobiphenylbenzoate)] (14)

CBPB (146 mg, 0.381 mmol) was placed in a dry Schlenk tube under nitrogen and dissolved in (5 mL). Karstedt's catalyst (15 μL) was added, the solution stirred for 15 minutes. *Endo*-3,7,14-Tris(dimethylsilyoxy)-1, 3, 5, 7, 9, 11, 14 – heptacyclopentyltricyclo[7.3.3.1^{5,11}]-heptasiloxane (100 mg, 0.0952 mmol) dissolved in added dropwise, the solution stirred for 48hr. The solvent was removed *in vacuo* to yield a solid, that was purified by column chromatography (Dichloromethane, flash grade silica gel, R_f = 0.12) to yield a white solid, that was recrystalised from dichloromethane/ethanol to yield **14** as a white solid (94 mg, 45% yield).

^{1}H NMR (400 MHz, CDCl$_3$) δ_H (ppm): 8.07 (m, AA'XX' (J = 8.4 Hz), 6H, Ar*H*), 7.66 (m, AA'XX' (J = 8.4 Hz), 6H, Ar*H*), 7.60 (m, AA'XX' (J = 8.4 Hz), 6H, Ar*H*), 7.55 (m, AA'XX' (J = 8.4 Hz), 6H, Ar*H*), 7.23 (m, AA'XX' (J = 8.4 Hz), 6H, Ar*H*), 6.89 (m, AA'XX' (J = 8.4 Hz), 6H, Ar*H*), 3.95 (t, (J = 6.4 Hz), 6H, C*H$_2$*O), 1.70 (m, 7H, C*H*Si), 1.70 (m, 6H, C*H$_2$*), 1.44 (m, 56H, C*H$_2$*), 1.44 (m, 6H, C*H$_2$*), 1.44 (m, 6H, C*H$_2$*), 0.56 (m, 6H C*H$_2$*Si), 0.084 (s, 18H, (C*H$_3$*)$_2$Si).

^{13}C{^{1}H} NMR (100 MHz, CDCl$_3$) δ_C (ppm): 164.91 (COO), 163.79 (C$_{Ar}$), 151.64 (C$_{Ar}$), 144.90 (C$_{Ar}$), 136.78 (C$_{Ar}$), 132.74 (C$_{ArH}$), 132.43 (C$_{ArH}$), 128.42 (C$_{ArH}$), 127.76 (C$_{ArH}$), 122.64 (C$_{ArH}$), 121.26 (C$_{Ar}$), 118.96 (C$_{Ar}$), 114.42 (C$_{ArH}$), 110.07 (C$_{Ar}$), 68.47 (*C*H$_2$O), 29.80 (*C*H$_2$), 29.00 (*C*H$_2$), 27.80, 27.77, 27.39 (*C*H$_2$, 3:3:1

ratio), 27.16, 27.00, 26.99 (CH_2, 3:3:1 ratio), 23.22 (CH_2), 18.26 (CH_2Si), 0.55 (CH_3)$_2$Si).

^{29}Si{^{1}H} NMR (79 MHz, CDCl$_3$) δ_{Si} (ppm): 9.14 (Si(CH$_3$)$_2$, -67.23 (broad) (SiO$_3$).

IR υ_{max} cm^{-1} 2947 (CH stretch, aromatic), 2222 (CN stretch), 1728 (C=O stretch), 1057 (CO stretch).

MALDI-MS: (m/z) – Calculated: 2220.81 [M+Na]$^+$; Found: 2220.80 [M+Na]$^+$.

Elemental Analysis (%) – Calculated for $C_{116}H_{147}N_3O_{21}Si_{10}$: C 63.32, H 6.73, N 1.91; Found: C 63.33, H 6.77, N 1.81

6.19. Octaisobutylsilsesquioxane-*endo*-bis-3, 7-(dimethylhydrido) silane (16)

Iso-butyl disilanol POSS, (100mg, 0.122 mmol) was placed in a dry Schlenk tube under nitrogen, dissolved in dry dichloromethane (5 ml) and dimethlychlorosilane (0.0733 mL, 0.673 mmol) was added via syringe. Triethylamine (0.125 mL, 0.896 mmol) was added and the solution was left to stir overnight. The solvent was removed *in vacuo* to leave a brown solid that was extracted with petroleum ether, the solution filtered through celite and evaporated to dryness to yield a colourless oil (107 mg, 95% yield).

^{1}H NMR (400 MHz, CDCl$_3$) δ_H (ppm): 4.62 (sept, (J = 2.8 Hz), 2H, SiH), 1.73 (m, 7H, CH(CH$_3$)$_2$, 0.84 (m, 42H, (CH_3)$_2$CH, 0.46 (m, 14H, CH_2), 0.10 (d, (J = 2.8 Hz), 12H, (CH_3)$_2$SiH).

^{13}C{^{1}H} NMR (100 MHz, CDCl$_3$) δ_C (ppm): 25.81 (CH(CH$_3$)$_2$), 24.59, 23.50, 22.42 (CH$_2$CH, 2:4:2 splitting), 23.96 (CH$_3$)$_2$CH), 0.601 (CH$_3$)$_2$Si).

MALDI-MS (m/z): Calculated: 1029.36 [M+H]$^+$; Found: 1029.36 [M+Na]$^+$.

6.20. Octaisobutylsilsesquioxane-*endo*-bis-[4'-{pentyloxy-5-dimethylsiloxy}-(1-(cyanobiphenylbenzoate)] (17)

CBPB (150 mg, 0.391 mmol) was placed in a dry Schlenk tube under nitrogen and dissolved in toluene (5 mL). Karstedt's catalyst (15 μL) was added, the solution stirred for 15 minutes. **16** (100 mg, 0.0992 mmol) dissolved in toluene added dropwise, the solution stirred for 48hr. The solvent was removed *in vacuo* to yield a solid, that was purified by column chromatography (Dichloromethane, flash grade silica gel, R_f = 0.31) to yield a white solid, that was recrystalised from dichloromethane/ethanol to yield **17** as a white solid (72 mg, 40% yield).

^{1}H NMR (400 MHz, CDCl$_3$) δ_H (ppm): 8.07 (m, AA'XX' (J = 8.4 Hz), 6H, Ar*H*), 7.66 (m, AA'XX' (J = 8.4 Hz), 6H, Ar*H*), 7.61 (m, AA'XX' (J = 8.4 Hz), 6H, Ar*H*), 7.56 (m, AA'XX' (J = 8.4 Hz), 6H, Ar*H*), 7.24 (m, AA'XX' (J = 8.4 Hz), 6H, Ar*H*), 6.90 (m, AA'XX' (J = 8.4 Hz), 6H, Ar*H*), 3.96 (t, (J = 6.4 Hz), 6H, C*H*$_2$O), 1.76 (m, 6H, C*H*$_2$), 1.76 (m, 8H, C*H*(CH$_3$)$_2$, 1.39 (m, 6H, C*H*$_2$), 1.39 (m, 6H, C*H*$_2$), 0.89 (m, 48H, (C*H*$_3$)$_2$CH), 0.51 (m, 16H, C*H*$_2$CH(CH$_3$)$_2$), 0.51 (m, 4H, C*H*$_2$Si), 0.07 (s, 12H, (C*H*$_3$)$_2$Si).

^{13}C{^{1}H} NMR (100MHz, CDCl$_3$) δ_C (ppm): 164.91 (COO), 163.81 (C$_{Ar}$), 151.66 (C$_{Ar}$), 144.93 (C$_{Ar}$), 136.78 (C$_{Ar}$), 132.73 (C$_{ArH}$), 132.43 (C$_{ArH}$), 128.42 (C$_{ArH}$), 127.76 (C$_{ArH}$), 122.65 (C$_{ArH}$), 121.28 (C$_{Ar}$), 118.96 (CN), 114.42 (C$_{ArH}$), 111.08 (C$_{Ar}$), 68.47 (*C*H$_2$O), 29.84 (*C*H$_2$), 28.99 (*C*H$_2$), 26.03 (*C*H$_3$)$_2$CH), 25.10, 23.16, 22.59 (*C*H$_2$CH, 2:2:4 ratio), 24.03 (*C*H(CH$_3$)$_2$), 18.22 (*C*H$_2$Si), 0.34 (*C*H$_3$)$_2$Si).

^{29}Si{^{1}H} NMR (79 MHz, CDCl$_3$) δ_{Si} (ppm): 9.77 (*Si*(CH$_3$)$_2$, -65.54 (*Si*O$_3$), -67.45 (*Si*O$_3$).

IR υ_{max} cm^{-1} 2955 (CH stretch, aromatic), 2222 (CN stretch), 1728 (C=O stretch), 1057 (CO stretch).

MALDI-MS (m/z): Calculated: 1795.67 [M+Na]$^+$; Found: 1795.66 [M+Na]$^+$.

Elemental Analysis (%) – Calculated for $C_{86}H_{128}N_2O_{19}Si_{10}$: C 58.20, H 7.27, N 1.58; Found: C 58.26, H 7.14, N 1.50.

6.21. Octaisobutylsilsesquioxane-endo-tris-4'-{pentyloxy-5-dimethylsiloxy}-(2 (pentyloxy)carbonyl)-1,4-phenylene-bis(4-butyloxybenzoate)] (18)

LBB (178 mg, 0.301 mmol) was placed in a dry Schlenk tube under nitrogen and dissolved in dry, sulphur-free toluene (5 mL). Karstedt's catalyst (15 μL) was added, the solution stirred for 15 minutes. **6** (50 mg, 0.0518 mmol) dissolved in toluene added dropwise, the solution stirred for 48hr. The solvent was removed *in vacuo* to yield a solid, that was purified by column chromatography (Dichloromethane, flash grade silica gel, R_f = 0.23) to yield a white solid, that was recrystalised from dichloromethane/ethanol to yield **18** as a white solid (51 mg, 37% yield).

^{1}H NMR (400 MHz, CDCl$_3$) δ_H (ppm): 8.07 (m, 12H, Ar*H*), 7.80 (m, 3H, Ar*H*), 7.37 (m, 3H, Ar*H*), 7.19 (m, 3H, Ar*H*), 6.89 (m, 12H, Ar*H*), 4.06 (m, 6H, C*H$_2$*OOCPh), 3.96 (m, 12H, C*H$_2$*O), 1.73 (m, 7H, C*H*(CH$_3$)$_2$), 1.73 (m, 12H, C*H$_2$*), 1.44 (m, 18H, C*H$_2$*), 1.18 (m, 6H, C*H$_2$*), 1.18 (m, 6H, C*H$_2$*), 0.87 (m, 42H, (C*H$_3$*)$_2$CH), 0.95-0.84 (m, 18H, C*H$_3$*CH$_2$), 0.45 (m, 14H, C*H$_2$*), 0.451 (m, 6H, C*H$_2$*Si), 0.01 (s, 18H, (C*H$_3$*)$_2$Si).

^{13}C{^{1}H} NMR (100 MHz, CDCl$_3$) δ_C (ppm): 165.00 (COO), 164.65 (COO), 164.00 (COO), 163.80 (C$_{Ar}$), 163.64 (C$_{Ar}$), 148.36 (C$_{Ar}$), 148.26 (C$_{Ar}$), 132.52 (C$_{ArH}$), 132.45 (C$_{ArH}$), 127.14 (C$_{Ar}$), 125.06 (C$_{ArH}$), 124.97 (C$_{ArH}$), 124.93 (C$_{ArH}$), 121.53 (C$_{Ar}$), 121.10 (C$_{Ar}$), 68.11 (*C*H$_2$O), 68.04 (*C*H$_2$O), 65.65 (*C*H$_2$OOCPh), 54.78 (*C*H$_2$C(CH$_3$)$_3$), 31.22, 30.20, 29.52 (*C*HCH$_2$, 3:3:1 ratio), 31.21-24.96 (*C*H$_2$), 31.21-24.96 (*C*H$_2$), 31.21-24.96 (*C*H$_2$), 31.21-24.96 (*C*H$_2$), 31.21-24.96 (*C*H$_2$), 31.21-24.96 (*C*H$_2$), 31.21-24.96 (*C*H$_2$), 25.75-24.95 (*C*H$_3$CH), 25.75-24.95

(C(CH$_3$)$_3$), 22.94 (CH_3CH), 19.28 (CH_3CH$_2$), 18.12 (CH_2Si), 13.93 (CH_3CH$_2$), 0.406 (CH_3CH$_2$).

IR υ_{max} cm^{-1} 2947 (CH stretch, aromatic), 1728 (C=O stretch), 1057 (CO stretch).

MALDI-MS: (m/z) – Calculated: 2710.12 [M+Na]$^+$; Found: 2712.27 [M+Na]$^+$.

Elemental Analysis (%) – Calculated for C$_{136}$H$_{198}$O$_{36}$Si$_{10}$: C 60.73, H 7.42,; Found: C 56.49, H 7.42.

6.22. Octaisooctylsilsesquioxane-*endo*-tris-4'-{pentyloxy-5-dimethylsiloxy}-(2 (pentyloxy) carbonyl)-1,4-phenylene bis(4-butoxybenzoate)] (19)

LBB (254 mg, 0.422 mmol) was placed in a dry Schlenk tube under nitrogen and dissolved in dry, sulphur-free toluene (5 mL). Karstedt's catalyst (15 μL) was added, the solution stirred for 15 minutes. **7** (100 mg, 0.0736 mmol) dissolved in toluene added dropwise, the solution stirred for 48hr. The solvent was removed *in vacuo* to yield a solid, that was purified by column chromatography (Dichloromethane, flash grade silica gel, R_f = 0.24) to yield a white solid, that was recrystalised from dichloromethane/ethanol to yield **19** as a white solid (81 mg, 36% yield).

^{1}H NMR (400 MHz, CDCl$_3$) δ_H (ppm): 8.06 (m, 12H, ArH), 7.79 (m, 3H, ArH), 7.36 (m, 3H, ArH), 7.16 (m, 3H, ArH), 6.88 (m, 12H, ArH), 4.04 (m, 6H, CH_2OOCPh), 3.96 (m, 12H, CH_2O), 1.72 (m, 12H, CH_2), 1.72 (m, 7H, CHCH$_2$), 1.43 (m, 18H, CH_2), 1.22-1.00 (m, 14H, CH_2CH), 1.22-1.00 (m, 6H, CH_2), 1.22-1.00 (m, 6H, CH_2), 0.945-0.765 (m, 18H, CH_3CH$_2$), 0.91 (m, 21H, CH_3CH), 0.80 (m, 63H, (CH$_3$)$_3$CCH$_2$), 0.69-0.36 (m, 14H, CH_2CH(CH$_3$)$_3$), 0.70-0.36 (m, 6H, CH_2Si), 0.00 (s, 18H, (CH_3)$_2$Si).

^{13}C{^{1}H} NMR (100 MHz, CDCl$_3$) δ_C (ppm): 164.99 (COO), 164.64 (COO), 164.00 (COO), 163.80 (C$_{Ar}$), 163.63 (C$_{Ar}$), 148.35 (C$_{Ar}$), 148.26 (C$_{Ar}$), 132.52 (C$_{ArH}$), 132.45 (C$_{ArH}$), 127.14 (C$_{Ar}$), 125.06 (C$_{ArH}$), 124.98 (C$_{ArH}$), 124.93 (C$_{Ar}$), 121.53 (C$_{Ar}$), 121.10 (C$_{Ar}$), 68.11 (*CH$_2$O*), 68.04 (*CH$_2$O*), 65.71 (*CH$_2$COO*), 54.80 (*CH$_2$C(CH$_3$)$_3$*), 31.22, 30.20, 29.51 (*CHCH$_2$*, 3:3:1 ratio), 30.33 ((*CH$_3$*)$_3$C), 25.75-24.98 (*CH$_2$CH*), 25.75-24.98 (*C(CH$_3$)$_3$*), 25.75-24.98 (*CH$_3$CH*), 29.76 (*CH$_2$*), 29.66 (*CH$_2$*), 29.32 (*CH$_2$*), 28.27 (*CH$_2$*), 25.74 (*CH$_2$*), 22.97 (*CH$_2$*), 22.94 (*CH$_2$*), 19.26 (*CH$_3$*), 18.14 (Si*CH$_2$*), 13.90 (*CH$_2$*), 0.40 (*CH$_3$*)$_2$Si).

IR υ_{max} cm^{-1} 2947 (CH stretch, aromatic), 1728 (C=O stretch), 1057 (CO stretch).

MALDI-MS: (m/z) – Calculated: 3102.56 [M+Na]$^+$; Found: 3102.60 [M+Na]$^+$.

Elemental Analysis (%) – Calculated for C$_{164}$H$_{254}$O$_{36}$Si$_{10}$: C 63.96, H 8.46,; Found: C 63.96, H 8.31.

6.23. Octaisobutylsilsesquioxane-*endo*-bis-4'-{pentyloxy-5-dimethylsiloxy}-(2-(pentyloxy)carbonyl)-1,4-phenylene bis(4-butoxybenzoate)] (20)

LBB (171 mg, 0.298 mmol) was placed in a dry Schlenk tube under nitrogen and dissolved in toluene (5 mL). Karstedt's catalyst (15 µL) was added, the solution stirred for 15 minutes. **16** (100 mg, 0.0992 mmol) dissolved in dry, sulphur-free toluene added dropwise, the solution stirred for 48hr. The solvent was removed *in vacuo* to yield a solid, that was purified by column chromatography (Dichloromethane, flash grade silica gel, R_f = 0.21) to yield a white solid, that was recrystalised from dichloromethane/ethanol to yield **20** as a white solid (61 mg, 29% yield).

^{1}H NMR (400 MHz, CDCl$_3$) δ_H (ppm): 8.06 (m, 12H, Ar*H*), 7.80 (m, 3H, Ar*H*), 7.38 (m, 3H, Ar*H*), 7.18 (m, 3H, Ar*H*), 6.90 (m, 12H, Ar*H*), 4.06 (t, (J = 6.8 Hz), 6H, C*H$_2$*OOCPh), 3.98 (m, 12H, C*H$_2$*O), 1.74 (m, 8H, C*H*(CH$_3$)$_2$), 1.74 (m, 12H, C*H$_2$*), 1.44 (m, 18H, C*H$_2$*), 1.17 (m, 6H, C*H$_2$*), 1.17 (m, 6H, C*H$_2$*), 0.95-0.84 (m, 18H, C*H$_3$*CH$_2$), 0.89 (m, 48H, (C*H$_3$*)$_2$CH), 0.47 (m, 16H, C*H$_2$*CH), 0.47 (m, 4H, C*H$_2$*Si), 0.00 (s, 12H, (C*H$_3$*)$_2$Si).

^{13}C{^{1}H} NMR (100 MHz, CDCl$_3$) δ_C (ppm): 165.01 (COO), 164.65 (COO), 164.05 (COO), 163.81 (C$_{Ar}$), 163.64 (C$_{Ar}$), 148.36 (C$_{Ar}$), 148.25 (C$_{Ar}$), 132.53 (C$_{ArH}$), 132.46 (C$_{ArH}$), 127.13 (C$_{Ar}$), 125.06 (C$_{ArH}$), 125.01 (C$_{ArH}$), 124.96 (C$_{ArH}$), 121.54 (C$_{Ar}$), 121.12 (C$_{Ar}$), 114.45 (C$_{ArH}$), 114.36 (C$_{ArH}$), 68.12 (*C*H$_2$O), 68.04 (*C*H$_2$O), 65.71 (*C*H$_2$COOPh), 31.21 (*C*H$_2$), 29.64 (*C*H$_2$), 28.26 (*C*H$_2$), 26.07-25.08 (*C*H$_2$), 26.05 (*C*H$_2$), 25.98 (*C*H$_2$), 25.85, 25.78 (*C*H(CH$_3$)$_2$), 25.05, 23.68, 22.93 (*C*H$_2$CH, 2:4:2 ratio), 24.07, 23.98, 23.85 ((*C*H$_3$)$_3$CH, 2:4:2 ratio), 22.58 (*C*H$_2$), 19.27 (*C*H$_3$), 18.08 (Si*C*H$_2$), 13.90 (*C*H$_3$), 0.23 ((*C*H$_3$)$_2$Si).

IR υ_{max} cm^{-1} 2947 (CH stretch, aromatic), 1728 (C=O stretch), 1057 (CO stretch).

MALDI-MS (m/z): Calculated: 2177.87 [M+Na]$^+$; Found: 2177.90 [M+Na]$^+$.

Elemental Analysis (%) – Calculated for C$_{104}$H$_{162}$O$_{29}$Si$_{10}$: C 57.90, H 7.58; Found: C 58.12, H 7.58.

6.24.   Octadimethylsilyoxy-octa[2-((pentyloxy)carbonyl)-1,4-phenylene-bis(4-butoxybenzoate)] silsesquioxane (22)

1, 3, 5, 7, 9, 11, 15, octakis-(dimethylsilyloxy)penta-cyclo[9.5.1.1^{3,9}-1$^{7, 13}$]octa-siloxane (30 mg, 0.0295 mmol) was placed in a dry Schlenk tube under nitrogen and dissolved in toluene (1 mL). LBB (339 mg, 0.590 mmol) was dissolved in toluene (4 mL) and added to the solution via syringe. Karstedt's catalyst (15 μL) was added and the solution stirred for 48 hrs. The solution was evaporated to

dryness *in vacuo* and purified by column chromatography (Dichloromethane, flash grade silica gel, R_f = 0.11) to yield a white solid, that was recrystallised from dichloromethane/ethanol to yield **22** as a white solid (yield = 151 mg, 92%).

^{1}H NMR (400 MHz, CDCl$_3$) δ_H (ppm): 8.08 (m, 32H, Ar*H*), 7.82 (d, (J = 3.05 Hz), 8H, Ar*H*), 7.39 (m, 8H, Ar*H*), 7.19 (m, 8H, Ar*H*), 6.91 (m, 32H, Ar*H*), 4.06 (t, (J = 6.71 Hz), 16H, C*H$_2$*OCO), 3.98 (m, 32H, C*H$_2$*O), 1.74 (m, 32H, C*H$_2$*CH$_2$O), 1.44 (m, 48H, C*H$_2$*), 1.16 (m, 32H, C*H$_2$*), 0.94 (m, 48H, C*H$_3$*), 0.417 (m, 16H, C*H$_2$*Si), 0.023 (m, 48H, (C*H$_3$*)$_2$Si).

^{13}C{^{1}H} NMR (100 MHz, CDCl$_3$) δ_C (ppm): 164.95 (COO), 164.59 (COO), 163.97 (COO), 163.78 (C$_{Ar}$), 163.62 (C$_{Ar}$), 148.34 (C$_{Ar}$), 148.23 (C$_{Ar}$), 132.50 (C$_{ArH}$), 132.43 (C$_{ArH}$), 127.24 (C$_{ArH}$), 125.11 (C$_{ArH}$), 125.08 (C$_{ArH}$), 121.49 (C$_{Ar}$), 121.07 (C$_{Ar}$), 114.43 (C$_{ArH}$), 114.36 (C$_{ArH}$), 68.09 (*C*H$_2$O), 68.02 (*C*H$_2$O), 65.60 (*C*H$_2$OCO), 31.19 (*C*H$_2$), 29.49 (*C*H$_2$), 28.17 (*C*H$_2$), 22.61 (*C*H$_2$), 19.27 (*C*H$_2$), 17.48 (*C*H$_2$Si), 13.92 (*C*H$_3$), -0.35 (*C*H$_3$)$_2$Si.

IR υ_{max} cm^{-1} 2955 (CH stretch, aromatic), 1728 (C=O stretch), 1057 (CO stretch).

MALDI-MS: (m/z) – Calculated: 5633.01 [M+Na]$^+$; Found: 5633.11 [M+Na]$^+$.

Elemental Analysis (%) – Calculated for C$_{288}$H$_{360}$O$_{84}$Si$_{16}$: C 61.60, H 6.46; Found: C 60.83, H 6.46.

6.25. Octavinyloctasilsesquioxane (23)

To a solution of acetonitrile/water (240 mL, 5:1) under nitrogen vinyltriethoxysilane (85 mL, 0.376 mmol) was added via syringe. Hydrochloric acid was added dropwise over a period of 45 mins via a dropping funnel and the solution heated to reflux at 88 °C for 24hr. The suspension was cooled down and the white precipitate collected by filtration, washed with methanol (100ml) and recrystallised from tetrahydrofuran (10 mL) and methanol (50 mL) several times to leave a white solid (2.24 g, 7.02%).

^{1}H NMR (400 MHz, CDCl$_3$) δ_H (ppm): 6.12-5.84 (m, 24H, CH=CH_2).

^{13}C{^{1}H} NMR (100 MHz, CDCl$_3$) δ_C (ppm): 137.08 (CH_2=CH), 128.76 (CH=CH$_2$).

MALDI-MS: (m/z) – Calculated: 633.03 [M]$^+$; Found: 632.94 [M]$^+$.

Elemental Analysis (%) – Calculated for C$_{16}$H$_{24}$O$_{12}$Si$_8$: C 30.36, H 3.82; Found: C 30.28, H 3.68.

6.26. *(S)*-2-methylbutyl-but-3-enoate (24)

3-Butenoic acid (2 g, 0.0232 mol) and *(S)*-2-methylbutanol were dissolved in dry dichloromethane (80 mL) under nitrogen. N,N'-dicyclohexylcarbodiimide (5.73 g, 0.286 mol) and 4-dimethylaminopyridine (0.57 g, 4.67 mmol) were added and the mixture was stirred overnight. The precipitate formed was filtered off and the solution was evaporated to dryness to leave a colourless liquid. Purification by column chromatography (dichloromethane, flash grade silica, R_f = 0.72) yielded a colourless liquid that was purified further via distillation at 22 mbar and at 80 °C to yield **24** as a colourless liquid (1.44 g, 40% yield).

^{1}H NMR (400 MHz, CDCl$_3$) δ_H (ppm): 5.96-5.83 (d (J$_{trans}$ = 17.89) d (J$_{cis}$ = 9.76), t (J = 7.02), 1H, CH=CH$_2$), 5.16-5.09 (m, 2H, CH_2=CH), 3.98-3.82 (d, (J = 6.10), 2H, CH_2O), 3.09-3.03 (d, (J = 7.02), d, (J = 1.53), d, (J = 1.53), 2H, CH_2COO), 1.74-1.59 (m, 1H, CHCH$_2$CH$_3$), 1.46-1.34 (m, 1H, CH_2CH$_3$), 1.22-1.09 (m, 1H, CH_2CH$_3$), 0.90-0.83 (m, 6H, CH_3CH$_2$, CH$_3$CH).

^{13}C{^{1}H} NMR (100 MHz, CDCl$_3$) δ_C (ppm): 171.66 (COO), 130.39 (CH=CH$_2$), 118.37 (CH$_2$=CH), 69.30 (CH$_2$O), 39.19 (CH$_2$COO), 34.07 (CHCH$_2$CH$_3$), 25.96 (CH$_2$CH$_3$), 16.31 (CH$_3$CH), 11.17 (CH$_3$CH$_2$).

IR υ_{max} cm^{-1} 2963 (CH stretch, alkene), 1754 (C=O stretch), 1173 (CO stretch).

MALDI-MS: (m/z) – Calculated: 179.10 [M+Na]$^+$; Found: 179.10 [M]$^+$.

Elemental Analysis (%) – Calculated for C$_9$H$_{16}$O$_2$: C 69.19, H 10.32; Found: C 69.16, H 10.32.

6.27. Octavinylsilsesquioxane-*endo*-disilanol (25)

23 (400mg, 0.632 mmol) was dissolved in a mixture of tetrahydrofuran, dichloromethane and isopropanol (30 mL, 1:1:1) under nitrogen. The solution was cooled to -35 °C using a methanol and liquid nitrogen bath and tetraethylammonium hydroxide solution (20 wt%, 367 µL, 0.00510 mmol) was added dropwise. The reaction was stirred and monitored by thin layer chromatography (in dichloromethane) and was stopped once the spot at R_f = 0.81 had disappeared (~1hr). The reaction was quenched with 1M hydrochloric acid (2 mL) and was left to warm up to room temperature. The mixture was washed with HCl 1M (2 x 10 mL), water (2 x 10 mL) and brine (2 x 10 mL), the organic layer was dried and the solvent removed *in vacuo* to leave a white tacky solid (321 mg, 78%).

^{1}H NMR (400 MHz, CDCl$_3$) δ_H (ppm): 6.32-5.78 (m, 24H, C*H*=C*H$_2$*), 4.95 (s, 2H, SiO*H*).

^{13}C{^{1}H} NMR (100 MHz, CDCl$_3$) δ_C (ppm) 136.95 (8 x CH=CH), 136.81 (8 x CH$_2$=CH$_2$), 129.53, 129.02, 128.71 (SiCH=, 2:4:2 relative ratio).

MALDI-MS: (m/z) – Calculated: 672.92 [M+Na]$^+$; Found: 672.94 [M+Na]$^+$.

6.28. Octavinylsilsesquioxane-*endo*-bis-((S)-2-methylbutylbutyrate) (27)

24 (144 mg, 0.922 mmol) was dissolved in dry, low sulphur toluene (5 mL). Dimethylchlorosilane (0.872 mg, 9.22 mmol) was added followed by Karstedt's catalyst (15 μL) and the reaction was left to stir overnight under nitrogen. The solvent and excess dimethylchlorosilane were then removed under reduced pressure to leave a colourless liquid, to which a solution of **25** (100 mg, 0.154 mmol) and triethylamine (373 mg, 3.69 mmol) in dry, sulphur-free toluene (1 mL) was added dropwise in situ. The solution was stirred overnight. The mixture was diluted with dichloromethane (5 mL) and washed with water (2 x 3 mL). The solvent was removed *in vacuo* to leave a colourless liquid. Purification by column chromatography (R_f = 0.21, 1:1 hexane:dichloromethane) yielded a colourless liquid (62 mg, 37% yield).

^{1}H NMR (400 MHz, CDCl$_3$) δ_H (ppm): 6.07-5.76 (m, 24H, C*H$_2$*=C*H*), 3.93-3.76 (m, 4H, C*H$_2$*O), 2.30-2.22 (m, 4H, C*H$_2$*COO), 1.70-1.54 (m, 4H, C*H$_2$*CH$_2$), 1.70-1.54 (m, 2H, C*H*CH$_2$), 1.43-1.31 (m, 2H, C*H$_2$*CH$_3$), 1.20-1.07 (m, 2H, C*H$_2$*CH$_3$), 0.931-0.792 (m, 12H, C*H$_3$*CH, CH$_3$CH$_2$), 0.594-0.459 (m, 4H, SiC*H$_2$*CH$_2$), 0.106-0.0334 (m, 12H, (C*H$_3$*)$_2$Si).

^{13}C{^{1}H} NMR (100 MHz, CDCl$_3$) δ_C (ppm): 173.77 (COO), 136.88, 136.42, 135.15 (*C*H=CH, 2:4:2 ratio), 131.84, 129.76, 128.84 (*C*H$_2$=CH$_2$, 2:4:2 ratio), 68.91

(CH_2O), 37.83 (CH_2COO), 34.21 ($CHCH_2CH_3$), 26.12 (CH_2CH_3), 19.08 (CH_2CH_2), 17.89 (SiCH_2), 16.49 (CH_3CH), 11.29 (CH_3CH_2), 0.0854 (CH_3)$_2$Si).

IR υ_{max} cm^{-1} 2963 (CH stretch, alkene), 1754 (C=O stretch), 1065 (CO stretch).

MALDI-MS: (m/z) – Calculated: 1101.2204 [M+Na]$^+$; Found: 1101.2205 [M+Na]$^+$.

Elemental Analysis (%) – Calculated for $C_{38}H_{70}O_{17}Si_{10}$: C 42.27, H 6.53; Found: C 41.94, H 6.73.

6.29. Octaethyl[4'-(pentyloxy-5-tetramethyldisiloxy)cyanobiphenylyl]-*endo*-bis-((S)-2-methylbutylbutyrate) octasilsesquioxane (28)

27 (38 mg, 0.0352 mmol) and 4'-(5-(1,1,3,3-tetramethyldisiloxy)pentyloxy)-[1,1'-biphenyl]-4-carbonitrile (270 mg, 0.704 mmol) were dissolved in dry, sulphur-free toluene (3 mL) and placed in a dry Schlenk tube under nitrogen. Karstedt's catalyst (15 μL) was added and stirred for 72 hr. The solvent was removed *in vacuo* to yield a colourless paste. Purification by column chromatography (R_f = 0.61, dichloromethane:ethyl acetate, 10:1) yielded a colourless tacky paste that was recrystallised from dichloromethane/ethanol to yield a colourless tacky solid (88 mg, 59% yield).

^{1}H NMR (400 MHz, CDCl$_3$) δ_H (ppm): 7.62 (m, AA'XX' (J = 8.4 Hz), 16H, ArH), 7.56 (m, AA'XX' (J = 8.4 Hz), 16H, ArH), 7.45 (m, AA'XX' (J = 8.4 Hz), 16H, ArH), 6.91 (m, AA'XX' (J = 8.4 Hz), 16H, ArH), 3.91 (m, 20H, CH_2OCO, CH_2OPh), 2.26 (t, (J = 7.2 Hz), 4H, CH_2COO), 1.70-1.54 (m, 2H, CHCH$_2$), 1.70-1.54 (m, 4H, CH_2CH$_2$), 1.70-1.54 (m, 16H, CH_2CH$_2$O), 1.48-1.27 (m, 32H, CH_2), 1.10-1.02 (m, 2H, CH_2CH$_3$), 1.10-1.02 (m, 4H, CH_2CH$_2$COO) 0.97-0.90 (m, 2H, CH_2CH$_3$), 0.86-0.81 (m, 12H, CH_3CH, CH$_3$CH$_2$), 0.60-0.39 (m, 52H, CH_2Si), 0.18-0.00 (m, 108H, (CH_3)$_2$Si).

^{13}C{^{1}H} NMR (100 MHz, CDCl$_3$) δ_C (ppm): 193.83 (COO), 159.85 (C$_{Ar}$), 145.28 (C$_{Ar}$), 132.65 (C$_{ArH}$), 131.33 (C$_{Ar}$), 128.39 (C$_{ArH}$), 127.11 (C$_{ArH}$), 119.16 (CN), 115.11 (C$_{ArH}$), 110.12 (C$_{Ar}$), 68.90 (*C*H$_2$OCO), 68.21 (*C*H$_2$OPh), 37.86 (*C*H$_2$COO), 24.21 (*C*HCH$_2$CH$_3$), 29.86 (*C*H$_2$), 29.10 (*C*H$_2$), 26.13 (*C*H$_2$CH$_3$), 23.26 (*C*H$_2$), 19.16 (*C*H$_2$), 18.48 (*C*H$_2$Si), 18.40 (*C*H$_2$Si), 16.52 (*C*H$_3$CH), 11.32 (*C*H$_3$CH$_2$), 1.11 (*C*H$_3$)$_2$Si), 0.562 (*C*H$_3$)$_2$Si), 0.413-0.181 (*C*H$_2$Si), 0.413-0.181 (*C*H$_2$Si), -0.217 (*C*H$_3$)$_2$Si).

IR υ_{max} cm^{-1} 2947 (CH stretch, aromatic), 2222 (CN stretch), 1753 (C=O stretch), 1041 (CO stretch).

Elemental Analysis (%) – Calculated for C$_{214}$H$_{318}$N$_8$O$_{33}$Si$_{26}$: C 60.32, H 7.52, N 2.63; Found: C 59.68, H 7.52, N 2.63.

Abbreviations

5CB	4′-pentyl-4-cyanobiphenyl
N	Nematic Phase
N*	Chiral Nematic Phase
SmA	Smectic A Phase
SmB	Hexatic Smectic B Phase
SmC	Smectic C Phase
SmC*	Chiral Smectic C Phase
SmI	Hexatic Smectic I Phase
SmF	Hexatic Smectic F Phase
LC	Liquid Crystal
Col$_h$	Columnar Hexagonal
Col$_r$	Columnar Rectangular
POSS	Polyhedral Oligomeric Silsesquioxane
NMR	Nuclear Magentic Resonance
ESI-MS	Electrospray Ionization Mass Spectrometry
MALDI-MS	Matrix-assisted Laser Desorption/ionization Mass Spectrometry
CB	4'-(pent-4-enyloxy)-[1,1'-biphenyl]-4-carbonitrile
CBPB	4-((pent-4-en-1-yloxy)carbonyl)-1,4-phenylene bis(4-butoxybenzoate)
LBB	4'-pentyloxy-5-dimethylsiloxy-2-pentyloxycarbonyl-1,4-phenylene-bis(4-butoxybenzoate**)**
Cr	Crystal Phase
DSC	Differential Scanning Calorimetry
POM	Polarized Optical Microscopy

References

1) P. J. Collings and M. Hird, *Introduction to Liquid Crystals*, Taylor and Francis, London, 1997.

2) G. W. Gray in *Thermotropic Liquid Crystals*, John Wiley & Sons, 1987.

3) J. W. Goodby, I. M. Saez, S. J. Cowling, J. S. Gasowska, R. A. MacDonald, S. Sia, P. Watson, K. J. Toyne, M. Hird, R. A. Lewis, S. Lee and V. Vaschenko, *Liq. Cryst.,* 2009, **36**, 567-605.

4) A. Skoulios and D. Guillon, Mol. Cryst. *Liq. Cryst.,* 1988, **165**, 317-332.

5) H. Takezoe and Y. Takanishi, *Jpn. J. Appl. Phys.,* 2006, **45**, 597-625

6) H. Takezoe, K. Kishikawa and E. Gorecka, *J. Mater. Chem.,* 2006, **16**, 2412-2416.

7) C. Tschierske, *J. Mater. Chem.,* 2001, **11**, 2647-2671.

8) D.W. Bruce, *The Chemical Record*, 2004, **4**, 10-22.

9) B. Donnio, S. Buathong, I. Bury and D. Guillon, *Chem. Soc. Rev.,* 2007, **36**, 1495–1513.

10) R. Pindak, D.E Moncton, S.C Davey and J. W. Goodby, *Phys. Rev. Lett.,* 1981, **46**, 1135-1138.

11) G. W. Gray and J. W. Goodby, *Smectic Liquid Crystals: Textures and Structures*, Leonard Hill, Glasgow, 1985.

12) A. Lösche, S. Grande and K. Eider, *1st Specialised Colloque Ampere,* 1973, Krakow, 103.

13) I. Direking, *Textures of Liquid Crystals,* Wiley-VCH, Weinheim, 2003.

14) J. W. Goodby *The Handbook of Liquid Crystals Vol. 1: Fundamentals*, Eds. D. Demus, J. W. Goodby, G. W. Gray, H. W. Spiess and V. Vill, Wiley-VCH, Weinheim, 1998, pp 115-132.

15) S. Singh, *Liquid Crystals: Fundamentals*, World Scientific, London, 2002.

16) P. G. De Gennes and J. Prost, *The Physics of Liquid Crystals 2nd Edition*, Clarendon Press, 1993.

17) R. B. Meyer, L. Liébert, L. Strzelecki and P. Keller, *J. Phys. Lett.*, **36**, 1975, L69.

18) J. A. Gonzalo in *The Handbook of Ferroelectrics*, Eds. J. A. Gonzalo and B. Jiménez, Wiley-VCH, Weinhein, 2005, pp 1-4.

19) C. T. Imrie, *Liq. Cryst.*, 2006, **33**, 1449-1454.

20) J. W. Goodby, I. M. Saez, S. J. Cowling, J. S. Gasowska, R. A. MacDonaold, S. Sia, P. Watson, K. J. Toyne, M. Hird, R. A. Lewis, S. Lee and V. Vaschenko., *Liq. Cryst.*, 2009, **36**, 567-605.

21) I. Nishiyama, T. Yamamoto, J. Yamamoto, H. Yokoyam and J. W. Goodby, *Mol. Cryst. Liq. Cryst.* 2005, **439**, 1921–1931.

22) C. T. Imrie, P. A. Henderson and A. Peter, *Chem. Soc. Rev.,* 2007, **36**, 2096-2124.

23) I. M. Saez and J. W. Goodby, *J. Mater. Chem.,* 2001, **11**, 2845–2851.

24) S. A. Ponomarenko, E. A. Rebrov, A. Y. Bobrovsky, N. I. Boiko, A. M. Muzafarov and V. P. Shivaev, *Liq. Cryst.,* 1996, **21**, 1-12.

25) J. W. Goodby, I.M. Saez and S. J. Cowling, *Supermolecular Chemistry: From Molecules to Nanomaterials,* Wiley, Hoboken, NJ, 2012.

26) G. S. Attard, R. W. Date, C. T. Imrie, G. R. Luckhurst, S. J. Roskilly, J. M. Seddon and L. Taylor., *Liq. Cryst.*, 1994, **16**, 529-581

27) C. V. Yelamaggad, S. A. Nagamani, U. S. Hiremath, D. S. S. Rao and S. K. Prasad, *Liq. Cryst.*, 2001, **28**, 1581-1583.

28) R. ElsaBer, G. H. Mehl, J. W. Goodby and M. Veith, *Angew. Chem. Int. Ed.*, 2001, **40**, 2688-2690.

29) I. M. Saez and J. W. Goodby, *J. Mater. Chem.,* 2005, **15**, 26-40.

30) I. M. Saez and J. W. Goodby, *J. Mater. Chem.,* 2003, **13**, 2727-2739.

31) J. W. Goodby, G. H. Mehl, I. M. Saez, R. P. Tuffin, G. Mackenzie, R. Auzely-Velty, T. Benvegnu and D. Plusquellec, *Chem. Commun.* 1998, 2057-2070.

32) I. M. Saez and J.W. Goodby, *"Supermolecular Liquid Crystals",* Struct. Bond., Springer-Verlag, Berlin, 2008.

33) J. M. Lehn, *Angew. Chem., Int. Ed. Engl.*, 1990, **29**, 1304-1319.

34) A. Perro, S. Reculusa, S. Ravaine, E. Vourgeat-Lami and E. Duguet, *J. Mater. Chem.,* **15**, 3745-3760.

35) R. Erhardt, M. Zhang, A. Boker, H. Zettl, C. Abetz, P. Frederick, G. Krausch, V. Abetz and A.H. Muller, *J. Am. Chem. Soc.,* 2003, **125**, 3260-3267.

36) S. M. Grayson and J. M. Frechet, *J. Am. Chem. Soc.,* 2000, **122,** 10335-10344.

37) D. J. Pesak and J. S. Moore, *Tetrahedron,* 1997, **53,** 15331-15347.

38) I. M. Saez and J. W. Goodby, *Chem. Commun.,* 2003, 1726-1727.

39) I. M. Saez and J. W. Goodby, *Chem. Eur. J.* 2003, **9**, 4869-4877.

40) R. Deschenaux, B. Donnio and D. Guillon, *New J. Chem.* 2007, **31**, 1064-1073.

41) B. Donnio and D. Guillon, *Adv. Polym. Sci.,* 2006, **201**, 45-155.

42) S. Campidelli, T. Brandmüller, A. Hirsch, I. M. Saez, J. W. Goodby, R. Deschenaux and *Chem. Commun.*, 2006, 4282-4284.

43) D. Cordes, P. D. Lickiss and F. Rataboul, *Chem. Rev.,* 2010, **110**, 2081-2173.

44) P. D. Lickiss and F. Rataboul, *Adv. Organomet. Chem.,* 2008, **57**, 1-116.

45) P. P. Pescarmona and T. Maschmeyer, *Aust. J. Chem.,* 2002, **54**, 583-596.

46) R. H. Baney, M. Itoh, A. Sakakibara and T. Suzuki, *Chem. Rev.,* 1995, *95*, 1409-1430.

47) M. G. Voronkov and V. I. Lavrent'yev, *Top. Curr. Chem.* 1982, **102**, 199-236.

48) P. G. Harrison, *J. Organomet. Chem.* 1997, **542**, 141-183.

49) F. J. Feher, D. A. Newman and J. F. Walzer, *J. Am. Chem. Soc.* **1989**, *111*, 1741-1748.

50) J. F. Brown and L. H. Vogt, *J. Am. Chem. Soc.* 1965, **87**, 4313.

51) H. Ishida and J. L. Koenig, *J. Polym. Sci., Polym. Phys. Ed.* 1979, *17*, 1807-1813.

52) S. S. Al-Juaid, N. H. Buttrus, R. I. Damja, Y. Derouiche, C. Eaborn, P. B. Hitchcock and P. D. Lickiss, *J. Organomet. Chem.* 1989, *371*, 287-295.

53) F. J. Feher, T. A. Budzichowski, R. L. Blanski, K. J. Weller and J. W. Ziller, *Organometallics* 1991, **10**, 2526-2528.

54) L. H. Vogt and J. F. Brown, *Inorg. Chem.* 1963, **2**, 189.

55) F. J. Feher, D. Soulivong and A. G. Eklund, *Chem. Commun.* 1998, 399-400.

56) F. J. Feher, D. Soulivong and F. Nguyen, *Chem. Commun.* 1998, 1279-1280.

57) F. J. Feher, F. Nguyen, D. Soulivong and J. W. Ziller, *Chem. Commun.* 1999, 1705-1706.

58) F. J. Feher, R. Terroba and J. W. Ziller, *Chem. Commun.* 1999, 2153-2154.

59) F. J. Feher, R. Terroba and J. W. Ziller, *Chem. Commun.* 1999, 2309-2310.

60) Y. El Aziz, A. R. Bassindale, P. G. Taylor, R. A. Stephenson, M. B. Hursthouse, R. W. Harrington and W. Clegg, *Macromolecules*, **46**, 2013, 988-1001.

61) G. Mehl, *Angew. Chem. Int. Ed. Engl.,* 1996, **35**, 2641-2643.

62) F. Kreuzer, R. Maurer, P. Spes, *Makromol. Chem. Macromol. Symp*. 1991, **50**, 215-228.

63) R. M. Laine, C. Zhang, A. Sellinger, L. Viculis, *Appl. Organomet. Chem.,* 1998, **12**, 715-722.

64) I. M. Saez and J. W. Goodby, Liq. Cryst., 1999, **26**, 1101-1105.

65) R. A. Lewthwaite, G. W. Gray and K. J. Toyne, J. Mater. Chem., 1992, **2**, 119-124.

66) C. Keith, G. Dantlgraber, R. A. Reddy, U. Baumeister, M. Prehm, H. Hahn, H. Lang, C. Tschierske, *J. Mater. Chem.,* 2007, **17**, 3796-3805.

67) J. Miao, L. Zhu, *J. Phys. Chem. B.,* 2010, **114**, 1879-1887.

68) A. J. Chalk and J. F. Harrod, *J. Am. Chem. Soc.*, 1965, **87**, 16-21.

69) P. Keller, D. L. Thomsen, M-H, Li, *Macromolecules,* 2002, **35**, 581-584.

70) G. Mehl, I. M. Saez, *Appl. Organomet. Chem.* 2009, **13**, 261-272.

71) B. Starkey, MChem Report, University of York, 2012.

72) P. D. Lickiss, F. Rataboul, *Advances in Organometallic Chemistry*, Volume 57, Eds A.F. Hill, M.J. Fink, 2008, Acadmic press inc, Waltham.

73) J. Hu, A. Gu, Z. Jiang, G. Liang, D. Zhuo, L. Yuan, B. Zhang, X. Chen, *Polym. Adv. Technol.*, 2012, **23**, 1219-1228.

74) G. Schmid, O. Vidonia, V. Torma, K. Pollmeier, H. Rehageb, A. Vassiliev, *Z. Anorg. Allg. Chem.* 2005, **631**, 2792-2799.

75) K. D. Wyndham, PhD Thesis, University of California, Irvine, 2000.

76) P. Reiss, MChem Report, University of York, 2010.

77) A. J. Waddon, E. B. Coughlin, *Chem. Mater*., 2003, **15**, 4555-4561.

78) K. Larsson, *K. Ark. Kemi,* 1960, **16**, 203.

79) Y. Z. Zhou, M. Jaromiec, G. L. Haun, R. K. Gilpin, *Anal. Chem.* 1994, 66, 1454.

80) D. Demus, L. Richter, *Textures of Liquid Crystals,* Verlag Chemie, Weinheim, 1978.

81) R. Deschenaux, B. Donnio, D. Guillon, *New J. Chem.*, 2007, 31, 1064–1073.

82) S. Campidelli, P. Bourgun, B. Guintchin, J. Furrer, H. Stoeckli-Evans, I. M. Saez, J. W. Goodby, R. Deschenaux, *J. Am. Chem. Soc.,* 2010, **132**, 3574-3581.

83) F. Lincker, P. Bourgun, H. Stoeckli-Evans, I. M. Saez, J. W. Goodby, R. Deschenaux, *Chem. Commun.,* 2010, **46**, 7522-7524.

84) S. Campidelli, C. Eng, I. M. Saez, J. W. Goodby and R. Deschenaux, *Chem. Commun.,* 2003, 1520-1521.